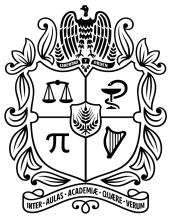

UNIVERSIDAD
NACIONAL
DE COLOMBIA

Location of Power Quality Stationary Disturbances Sources in Distribution Power Grids

Camilo Andrés Garzón

Universidad Nacional de Colombia
Facultad de Ingeniería
Departamento de Ingeniería Eléctrica y Electrónica
Bogotá, Colombia
September of 2023

Location of Power Quality Stationary Disturbances Sources in Distribution Power Grids

Camilo Andrés Garzón

Submitted as a partial requirement for the degree of:
Doctor of Philosophy in Engineering - Electrical Engineering

Advised by:
Ph.D. Fabio Andrés Pavas Martínez
Universidad Nacional de Colombia
Co-advised by:
Dr-Eng. Ana María Blanco Castañeda
Technische Universität Dresden

Research Area:
Power Quality
Research Group:
Program on Acquisition and Analysis of Electromagnetic Signals - PAAS-UN

Universidad Nacional de Colombia
Facultad de Ingeniería
Departamento de Ingeniería Eléctrica y Electrónica
Bogotá, Colombia
September of 2023

"So the universe is not quite as you thought it was. You'd better rearrange your beliefs, then. Because you certainly can't rearrange the universe."

Isaac Asimov, Nightfall

Acknowledgements

El autor agradece al Programa de Adquisición y Análisis de Señales electromagnéticas de la Universidad Nacional de Colombia PAAS-UN, así como a los colegas que con sus críticas y comentarios ayudaron a encaminar esta investigación. A Andrés Pavas, que siempre creyó en las capacidades de este servidor.

El autor también agradece al Institute of Electric Power Systems and High Voltage Engineering (IEEH) of the TUD Dresden University of Technology, ya que, sin sus espacios y el generoso apoyo de sus miembros hubiera sido imposible desarrollar los estudios de caso presentados. A Jan Meyer y Ana María Blanco, que con sus agudas y siempre oportunas observaciones me ayudaron comprender mejor varios de los aspectos acá tratados.

Resumen

Título en Español: Localización de Perturbaciones Estacionarias de Calidad de Potencia en Redes de Distribución.

El origen de las perturbaciones estacionarias es un problema que ha sido abordado desde múltiples perspectivas. Se han desarrollado varios métodos para determinar fuentes de perturbación, dispositivos que inyectan armónicos, la contribución de los elementos al desarrollo de una perturbación, asignación de responsabilidades y una larga lista de términos utilizados para referirse a lo mismo, el problema de Causalidad. Este problema en el contexto de calidad de potencia parte de la propia definición de Causa y, con ella, la clarificación de otros términos como Fuente y Responsabilidad. Una vez claros los conceptos elementales, la identificación y desarrollo de técnicas matemáticas que permitan su análisis es una tarea que involucra múltiples esfuerzos encaminados no sólo al desarrollo matemático, sino también, a la identificación y construcción de escenarios que permitan contrastar cada propuesta teórica.

Este trabajo aborda el problema de la Causalidad en calidad de potencia desde diferentes disciplinas matemáticas. Además, cada propuesta es evaluada a través de casos de estudio, algunos implementados en el laboratorio y otros medidos directamente en sistemas reales. Finalmente, todos los elementos matemáticos explorados se complementan, determinando así la Causa de la distorsión de forma de onda en sistemas eléctricos de baja tensión.

Palabras Clave: Causalidad, Sistemas de Distribución, Distorsión Armónica, Fuente Armónica, Perturbaciones Estacionarias de Calidad de Potencia, Problema de Asignación de Responsabilidades

Abstract

Título en Inglés: Location of Power Quality Stationary Disturbances Sources in Distribution Power Grids.

The origin of stationary disturbances is a problem that has been addressed from multiple perspectives. Several methods have been developed to determine sources of disturbance, devices that inject harmonics, the contribution of elements to the development of a disturbance, responsibilities assignment, and a long list of terms used to refer to the same thing,

the problem of Causality. This problem in the context of power quality starts from the very definition of Cause and, with it, the clarification of other terms such as Source and Responsibility. Once the elementary concepts are clear, the identification and development of mathematical techniques that allow their analysis is a task that involves multiple efforts aimed not only at mathematical development but also at the identification and construction of scenarios that will enable testing each theoretical proposal.

This work addresses the problem of Causality in power quality from different mathematical disciplines. In addition, each proposal is evaluated through study cases, some laboratory implementations, and others measured in real systems. Finally, all the mathematical elements explored are complementary, thus determining the Cause of the waveform distortion in low-voltage electrical systems.

Keywords: Causality, Distribution System, Harmonic Distortion, Harmonic Source, Power Quality Stationary Disturbances, Responsibility Assignment Problem

Contents

Figure List

Table List

1 Disturbance Source Location and Causality Problem in Power Quality

From the point of view of power quality, most regulatory policies and technical standards require that the voltage and current signals are within some established limits since the operation cost of the power system would be reduced [Bol00][Dug03]. However, the current growth of non-linear devices connected to the distribution system, like switched sources and inverters, commonly used in distributed generation, industrial, commercial, and residential applications, could represent a problem that should be faced by researchers in cooperation with industry [ANRR15][CSM17][MSS+17]. For this reason, it is essential to develop analysis methods to mitigate the harmful effects of power quality disturbances, particularly waveform distortion.

According to different standards, mainly two phenomena can be considered stationary disturbances: unbalance and waveform distortion [IEE09][ICO13][ICO00]. The waveform distortion includes phenomena like harmonics, notches, interharmonics, DC offset, and noise. Some other standards currently in development are looking for the inclusion the supraharmonics as a category inside the waveform distortion phenomena [MBA+14] [AMGP18]. However, the phase displacement is not taken into account as a power quality stationary disturbance in many standards, despite this is an abnormal condition (and undesirable in some cases) that affects the performance of power networks and equipment and whose effects on the development of others disturbances, as resonance effect, are well documented [DEP00][HAI17]. This work addresses the location of waveform distortion sources, understanding the phenomenon as the deviation of an optimal condition. Note that this approach, developed in the time domain, as will be seen, involves not only the harmonic distortion approach but also other distortion phenomena. In addition, the effect of phase displacement in the waveform distortion will be analyzed, too.

1.1. The Problem of Causality and Its Relationship with Waveform Distortion Source Location

The power quality stationary disturbances are mainly caused by the inherent behavior of some equipment, such as electronic devices (non-linear loads), electric machines (asymmetrical loads), and single-phase residential loads (that usually cause unbalance), among others, that need such disturbed state in the power network for a proper operation [Gar16][AMGP18]. Nevertheless, the interaction between non-linear loads can cause a compensation effect that could reduce the global THD in the measured PCC under some operative conditions. This phenomenon is called "harmonic cancellation" [HNB00] or "harmonic attenuation" [MGCS95]. In contrast, the interaction between different kinds of loads could amplify (or reduce in some cases) the disturbed effect inherent to the operation of each device, spreading the disturbances and, finally, impairing the power quality conditions of the power network. In this way, the work presented in [DEP00][CSM17][MPST04] shows how unbalance can affect the harmonic distortion assessment in power networks, and the work presented in [HAI17][HPLL16][WYAY$^+$04] shows how some reactive loads, such as capacitor banks, can amplify some harmonic components using the effect of resonance. Then, it is possible to say that waveform distortion is driven by the interaction between the devices connected to the system. Accordingly, finding the origin of disturbances implies, among other things, *fully identifying the set of conditions and elements that lead to the development of the disturbance*, in other words, determining the *causality*.

The magnitude and impact of the waveform distortion, on a certain moment, strongly depend on the electronic topology of the devices belonging to the system, the location of such devices, and the network configuration assessed [Bla18][ANRR15][EO12]. This implies that an adequate causality analysis must be carried out by simultaneously taking information from the network at multiple points. On the other hand, considering that networks are dynamic and their state constantly varies, either due to connection and disconnection of devices or network reconfiguration, a causality analysis done at one moment could no longer be valid at the next. Causality analysis requires extracting information from the system over considerable periods.

Nevertheless, most available methods for finding the origin of disturbances aim to calculate harmonic sharing or utility and load participation in the distortion's development. Thus, these run only in a system composed of an equivalent of the network and an equivalent of the load connected by a PCC with only one measure point in this boundary. Note that the equivalent models used for network and load are implemented with the information taken on the PCC and some operative information extracted from the utility as the short circuit impedance at the PCC [SBP$^+$17a] [GP19]. However, as was already mentioned, this information is valid for an instant of time, particularly the impedance; then, errors will be

introduced in the subsequent analysts along the time. On the other hand, available methods for finding harmonic sources are frequency-domain based and use the Norton equivalent in the Fast Fourier Transform approach for the analysis, neglecting the angle of harmonic components in many cases [GP19]. Thus, it is impossible to identify frequency bands without energy exchange or the effects of phase displacement in the system [AMGP18][MBA+14].

Considering the above, it is necessary to develop a causality assessment method for waveform distortion that considers all the variables that determine the system's dynamics, thus issuing a valid judgment for any instant of time and less susceptible to measurement errors. Said causality assessment would, in turn, lead to a qualitative and quantitative characterization of the devices belonging to the disturbance, thus identifying the role that each one plays in the development of the phenomenon (origin) and their contribution (responsibility), as will be discussed below.

1.1.1. Agents and their Roles in Responsibility Assessment

Power quality stationary disturbances harm the equipment and networks as excessive heating, overload, and malfunction of electronic equipment, among others [IEE14], some devices need these disturbances to work suitably. For example, an induction machine needs a phase displacement to create a magnetization process in its core. Thus, the presence of reactive power in the network is inherent to the connection of this machine. In the same way, waveform distortion in the system is intrinsic to the connection of non-linear loads, **these kinds of elements are called Causes in this work**; however, Cause is not necessarily the Source.

Causal relationships have been widely studied in different scientific fields. Many disciplines of knowledge have advanced studies in this regard due to the great importance of this topic in aspects such as system modeling, prediction, and forensic analysis, among others [Pea95] [AP08]. Almost all of these disciplines define the Cause as the action or set of actions that produce the Effect. However, note that this definition implicitly has a temporal notion, considered by almost all disciplines of knowledge as essential to establishing a causal relationship, namely, the Cause precedes the Effect [Bas65]. This condition of temporality supposes a couple of questions associated with the delay between the Cause and the Effect.

The first question would be, how far apart in time must two events be for one to be considered the Cause of the other? This issue has no universal rule, so it has usually been addressed experimentally since not all systems have the same response time. For example, causality studies in neuroscience assume that the Cause precedes the Effect by milliseconds. Conversely, in econometrics, the Cause can precede the Effect by months or even years. It would be challenging to know which precedes the other if we discuss measurable stationary

events in an indeterminate time horizon represented by a time series. Then, the temporary condition would be impossible to verify, or the analyses would lead to determining spurious causes.

The second question may be less obvious: Given two simultaneous events, or whose delay is so slight that it cannot be measured with current instrumentation, how would the Cause be identified? Once again, there would be no way to verify the temporality condition. Even if we are talking about a pair of stationary events represented by a time series, there would be no way to establish a causal relationship since the changes in said series would also be simultaneous [Bas65]. Nevertheless, these are precisely the scenarios that power quality causality analysis faces. On the one hand, stationary voltage and current signals present changes over time conditioned by the system's state. On the other hand, the delay between Cause and Effect is imperceptible since electromagnetic phenomena propagate at the speed of light.

1.1.1.1. Cause, Source, and Responsible

In the power quality literature, particularly about analyzing waveform distortion, it is common for terms such as Cause, Source, or responsible to be used interchangeably. Although it is true that, in some scenarios, the three things can be the same, it is necessary to differentiate them to avoid misjudgments. As in the rest of the literature, *Cause* will be defined as the condition or set of requirements that allows the development of a disturbance. On the other hand, the *Source* is the element from which the disturbance comes, in other words, the element that physically generates it. A simple and typical example in electrical systems is the tripping of a protection device in a distribution system that experiences a short circuit caused by the fall of a tree branch. The increase in current materialized in the protection tripping would be the *Effect*, while the *Cause* would be the branch's fall since the condition led to the phenomenon. On the other hand, the *Source* would be the network since it feeds the short circuit, in other words, the one that supplies the short circuit current. Note that, at least in this example, we cannot classify the network as the culprit of the disturbance despite this being the Source. It cannot blame the protection for the supply cut; these two elements only reacted to the conditions imposed by the Cause. In this way, it is possible to say that the Cause is an element that governs the system's behavior.

In many works as [GP17][MPST04] and [XLT04], it is intuitively shown that the Cause of waveform distortion is a device that demands such distortion or needs it for functioning, just as happens with the active power. Thus, any non-linear device, like certain types of loads or specific power sources that use power electronics to connect to the network, would be considered the Cause of waveform distortion. However, the state of the system can change depending on the dynamics of connection and disconnection of specific devices, and there-

fore, the mere presence of an element is not sufficient to determine the Cause or the set of components that governs the disturbance.

Regarding *Responsibility*, this can be defined as the degree of participation that a particular cause of a set of causes has on a disturbance. For example, assume a system composed of a public network with high background distortion, an ideally linear load, and two non-linear loads with different electronic architectures connected to a PCC. As was already mentioned, waveform distortion is inherent to the presence of non-linear devices in a system. In this sense, non-linear loads are part of the Cause, while the network would be a cause and the Source simultaneously since it supplies the current. However, since all the devices that constitute the Cause are different, it is necessary to evaluate which one has more impact on the development of the disturbance; in other words, to assess the Responsibility of each one.

To begin with, it is clear that the ideally linear load has no responsibility; in that order of ideas, all the Responsibility would be distributed among the non-linear loads and the network according to the impact that each one exerts or contributes, as it is called in many works [MPST04] [NO14] [PP11a] [SBP+17a]. A possible way to assess Responsibility under different distortion scenarios was widely discussed in [GP].

Assume the system shown in Figure **1-1** as another example. As discussed in [GPK+23], in this type of system, one of the inverters will respond to the kind of connected load so that if the load is linear (LIN), the portion of the total current converted in waveform distortion (Distorted Current i_D) would be minimal on current measure A_1. In contrast, if the load is non-linear (NLL), i_D in A_1 would be as high as the load demands it and the inverter components allow it, even if it has to reduce the active current generation, as shown in Figure **1-2**. However, the capacity of the inverter components is not the only restriction that this type of device would have to respond to the presence of a non-linear device; the system's operating conditions must also be considered. For example, the PV only operates during the day, meaning its inverter cannot respond to the load demands at night. In this order of ideas, this device would contribute to the development of the disturbance and its variations, not only due to being connected but also due to the different operating conditions it presents depending on the weather conditions. In this way, it is possible to say that the Cause of the distortion in the system is the interaction between all the devices connected to the system and the operating conditions along the time.

Finally, returning to the system depicted in **1-1**, the Responsibility would change according to operating conditions. Then, the Responsibility could be presented as a probability function as discussed in [PTSS12a].

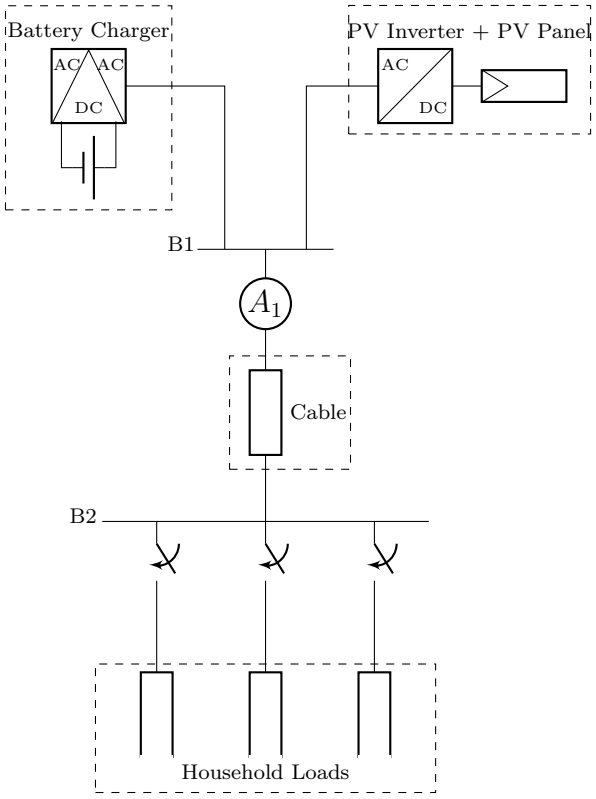

Figure 1-1: Dynamic System Depending on Weather Conditions

1.1.2. Standardization Framework in Power Quality

Many standardization efforts have been made in the world to guarantee optimum power quality conditions in the distribution networks; one of the most outstanding is the inclusion of the section "power quality" in the International Electrotechnical Commission Standards (IEC61000), which integrates the phenomena of power quality as an electromagnetic compatibility issue. In this way, several standards related to different power quality issues as emission limits (IEC61000-3-2 [IEC14], IEC61000-3-12 [IEC11]), immunity testing (IEC61000-4-13 [IEC02]), measurement (IEC61000-4-7 [IEC09b], IEC61000-4-30 [IEC15]) and compatibility levels (IEC61000-2-2 [IEC03b], IEC61000-2-12 [IEC03a]) have been published and applied in many countries. Another essential international advance in power quality standardization has been developed for power quality IEEE standards as IEEE 1159 [IEE09] and IEEE 519 [IEE14], which, in general terms, address the same issues that IEC61000 standards.

In the Colombian case, the Colombian Technical Committee of Power Quality and Electromagnetic Compatibility has addressed some issues by developing some own standards and adopting other international standards, aiming to unify concepts and apply these in the context of the Colombian power system. In this way, the NTC 5000 [ICO13] standard establishes fundamentals in power quality but also was adopted for NTC-EMC committee the

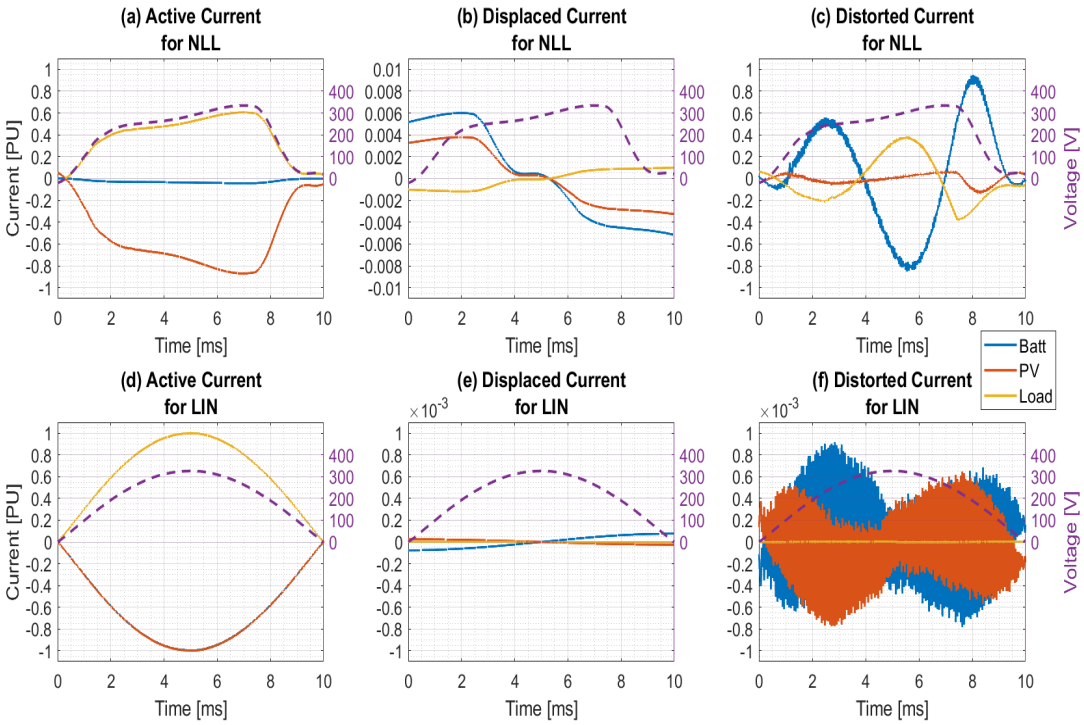

Figure 1-2: Active and Distorted Current Components Calculated from the system Depicted in Figure **1-1**

IEC61000-1-1 standard under the title *NTC-IEC-61000-1-1 Electromagnetic compatibility (EMC). Part 1. Generalities. Section 1: Application and Interpretation of definitions and fundamentals terms* [ICO00]. Other Colombian standards addressed issues such as measurement (NTC-IEC61000-4-7, NTC-IEC61000-4-15, NTC-IEC61000-4-30), permissible limits of disturbances in the MV/LV power networks and evaluation methods of such limitations (NTC 5001 [ICO08]). However, the location of the origin of disturbances is an issue that has not been addressed in NTC standards from the point of view of responsibility assignment or disturbance emission limits for appliances.

Furthermore, the location of the origin of disturbances is an issue that has not been addressed in many standardization frameworks worldwide, except for the technical report IEC TR 61000-3-6 [IEC08b] published in 2007, which provides a method to calculate the contribution limits, but not the responsibilities assignment. The problem of finding the origin of power quality disturbances has not been tackled mainly because no generally accepted methods exist to assess it [SBP+17b]. In contrast, some responsibility assignment methods have been proposed [XLL03] [PBP08] [PTSS12a] [SBP+17b] [IEC08b], and for some of these methods have been developed interesting improvements as presented in [AMGP18] [XLT04] [PP11b]. However, each method has limitations that can compromise the judgment about

the location and the contribution. In addition, works as presented in [MAFGF17] develops novel solutions to find the origin of disturbances in multi-point systems (systems composed of multiple PCCs as distribution power networks and microgrids).

1.2. Scope

As mentioned, solving the problem of locating sources of waveform distortion implies solving a broader issue, causality. As already discussed in previous sections, causality in the context of this work is defined as the set of conditions that govern the dynamics of a disturbance. Thus, to evaluate causality, it is necessary to make a correct identification, both qualitative and quantitative, of the role played by each of the agents connected to the system. However, in practice, providing a deterministic solution to the causality problem is impossible, given the constant variations in the network. That, eventually, can cause an agent to change its role from one moment to the next. In this sense, it is necessary to establish an adequate scope, which allows for defining the process of information acquisition, data processing, and subsequent analysis, as well as what is expected from the conclusions of the method that will be developed here.

1. **Data acquisition:** Given that, one of the motivations of this work is that those involved in a problem of assignment of responsibilities or location of sources of waveform distortion can apply the method while adhering to the current regulatory and normative framework. In this way, new a measurement method will not be proposed, because the existing technical standards, such as IEC 61000-4-30 [IEC08a] and IEC 61000-4-7 [IEC09a] suffice for responsibilities measurement purposes.

2. **Data Processing:** The initial data processing will be done following the provisions of the standards cited in the previous item. Subsequently, considering that a comprehensive analysis of the waveform distortion phenomenon is sought, which does not only address harmonic distortion, the information will be analyzed in the time domain, which implies having waveforms available instead of harmonic spectra. However, given the limitations often found in practice, these waveforms eventually could be reconstructed from the known spectra.

3. **Analysis:** The information analysis will be done in the time domain. Then, the potential of some decompositions based on Fryze power theory and the Method of Disturbances Interaction (MDI) will be analyzed first.

4. **Results:** Given the limitations in practice when it comes to providing a deterministic solution to the problem, the result of the decomposition will be analyzed from a probabilistic perspective to determine the cause. In this way, the results will show the

probability that a given agent is the cause of the waveform distortion.

In general terms, a method is sought that not only qualitatively (Origin) and quantitatively (Responsibility) identifies the role of each agent linked to a system with normatively unacceptable levels of waveform distortion. It also determines probabilistically which of the agents governs the system's dynamics regarding waveform distortion over a time window (Cause).

1.2.1. Objectives

1.2.1.1. General Objective

To develop a causality assessment method for harmonic distortion that allows characterizing the magnitude and direction of the contribution of all nodes belonging to the distribution system.

1.2.1.2. Specific Objectives

1 Characterize the agents in the distribution network according to their role in the current harmonic distortion state.

2 Calculating the contribution magnitude of each agent of the distribution system to the development of the specific state of harmonic distortion.

3 Assessing responsibilities according to the role and magnitude of the contributions, establishing a rank of sources and sinks that allows identifying the most harmful agents.

1.3. Methodology

As discussed in previous sections, the solution to the problem of locating sources of waveform distortion involves solving other issues, such as assigning responsibilities and causality. As previously mentioned, assigning responsibilities involves determining an agent's participation in developing a disturbance, making it a quantitative problem. On the other hand, the causality analysis seeks to determine the set of conditions that contribute to the development of a disturbance, which, in advance, classifies it as a problem with a qualitative solution. However, although the complete solution seeks a quantitative and qualitative assessment of the waveform distortion phenomenon, the methodology will be purely quantitative, given that the causality problem will be approached from a statistical framework.

Considering the above, the proposed methodology fragments the problem of locating sources of waveform distortion, called global problem in this section, into more minor issues called local problems. In that order of ideas, once the local problems have been resolved, the global problem is considered solved. The local problems identified and the solution methodology will be described below.

First, there are mainly two approaches to analyzing waveform distortion: the time and frequency domain approaches. Although the frequency domain approach is usually used more than the time domain approach, it is not because the latter is deficient or its implementation is more complex. For this reason, it is necessary to identify the advantages and disadvantages of each approach to determine which of the two is most appropriate for developing this work. In Chapter 2, a systematic review is made of some selected methods of harmonic distortion analysis and another assignment of responsibilities in the time domain, identifying their main advantages and disadvantages. Subsequently, all of them are compared, concluding that, under certain conditions, the results are comparable and even equal. However, the time domain approach is considered to be more versatile and provides more detailed insights into the waveform distortion phenomenon. With this as a start, local problems are defined:

- The first local problem involves identifying the propagation dynamics of the waveform distortion phenomenon. This is addressed experimentally in Chapter 3, through a system implemented in a laboratory that emulates different operating load conditions and two types of network: traditional distribution network and microgrid. Subsequently, the voltage and current signals measured under selected operating conditions are analyzed using three power theories based on the Fryze approach. This exercise concludes the advantages and disadvantages of each power theory. With this, a complementary analysis of the propagation dynamics of the waveform distortion is made, determining that said propagation fundamentally depends on the system's operating conditions and the network type. Therefore, the analyses currently applied to traditional distribution networks do not apply to microgrids.
- The problem of assigning responsibilities has been widely studied [GP19], which is why there are multiple methods of assigning or calculating participation, as already mentioned. In Chapter 2, several of them are studied, considering the time-domain appropriate for this work. Mainly, the Method of Disturbances Interaction (MDI) represents a good tool, but, in the opinion of the author of this thesis, it requires some improvements to make it even more conclusive and efficient in terms of calculation. Thus, Chapter 4 presents a proposal for improving the MDI based on Graph theory. This proposal includes the development of a centrality (importance) indicator called Laplacian Eigenvector Centrality, which allows optimizing calculations, inferring different characteristics of the system, such as the impact of distortion on the network, and concluding on the possible direction of propagation of the disturbance in traditional

distribution networks.

- The Causality problem is perhaps the most relevant in this work since, from this analysis, it is possible to determine whether the agents where the distortion is concentrated (who have been fully identified with the analysis of responsibilities) are sources or sinks. In Chapter 5, a solution proposal based on probabilities is presented, which uses the so-called Grager Causality to characterize the agents according to their role in the development of the disturbance. This approach is tested in a real microgrid, demonstrating its efficiency even in systems with complicated evaluation conditions, as also discussed in Chapter 3.

2 Commonly Used Methods to Assess Responsibilities in Waveform Distortion

In Chapter 1, the concept of responsibilities assignment was defined, and the existence of several analysis methods was mentioned. In this chapter, some methods considered relevant by the CIGRE C4.42 committee [SBP+17b] will be reviewed in addition to the Critical Impedance Method and the Method of Disturbances Interaction, which represents one of the bases of this work.

There are mainly two ways for assessing waveform distortion sources in single-point systems: the frequency domain methods (*FDM*) and the time domain methods (*TDM*). On the one hand, the *FDM* performs a Fast Fourier Transform (FFT) over the measured voltages and currents at the Point of Common Coupling. Then, a Thevenin (Fig. **2-1**) or Northon (Fig. **2-2**) model of the system is developed for each frequency component to establish the harmonic contribution corresponding to utility and the network. Finally, the overall participation is calculated using the superposition principle [XLL03][PBP08]. Usually, the implementation of *FDM* is easy, and the results are directly conclusive. However, these methods require information about the system that is not generally available and not simple to find, such as network equivalent impedance, utility impedance in the frequency domain, and background distortion.

On the other hand, the *TDM* uses signal analysis and disturbances definitions over the voltages and currents measured in the system analyzed. Then, correlations, interactions, or associations are performed to quantify the participation of a particular element connected to the PCC. The main advantage of *TDM* is the ability to assess waveform distortion and other power quality stationary phenomena such as unbalance, phase displacement, or other distortion phenomena like supraharmonics [AMGP18]. However, since power decomposition and signal analysis are required, *TDM* are hard to implement.

Next, three *FDM* and one *TDM* will be presented. Some aspects of each method, such as objectives, scope, measurement requirements, and mathematical formulation, will be briefly addressed. Additionally, some advantages and disadvantages of each approach will be men-

tioned.

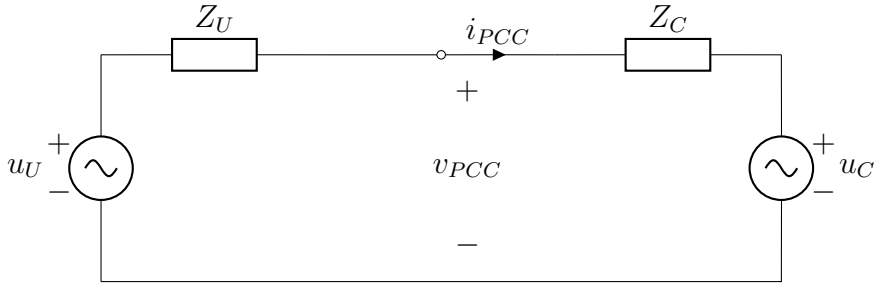

Figure 2-1: Thevenin Equivalent of the System

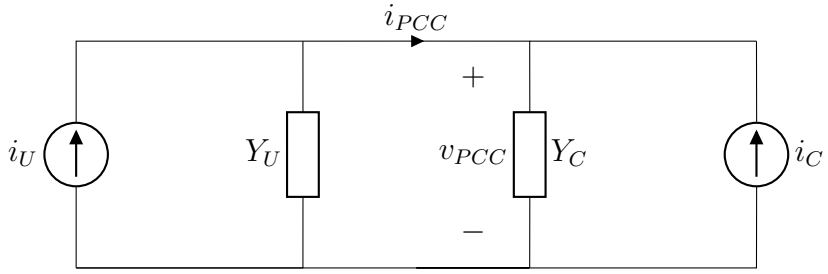

Figure 2-2: Northon Equivalent of the System

2.1. Methods to Assess Responsibilities on the PCC

According to [SBP+17a], the three most used harmonic evaluation methods are the Voltage Harmonic Vector Method (HVM) [PP11b], The IEC Voltage Phasor Method (IEC) [IEC08b] and the Harmonic Power Flow Method (HPF) [CF95]. However, *HPF* has been criticized, and its effectiveness seems questionable [SOPS11], mainly because the active frequency components have almost negligible magnitudes compared to the non-active frequency components [Pav12]. Furthermore, as discussed extensively in [XLT04], power calculation in the frequency domain ultimately results in a relationship between voltage and current phase angles, but not in the power flow direction.

On the other hand, considering that the HVM is a derivative simplifying the Critical Impedance Method [XLT04], it was decided to include the latter in the present analysis to establish the potential and deficiencies of the FDM.

Finally, only one TDM was considered in this analysis, the Method of Disturbances Interaction (MDI) [PTSS12b], not only because it represents one of the bases of this work but

because it is practically the only method that addresses the problem purely from the time domain.

2.1.1. Critical Impedance Method CIM

The *CIM* [XLT04] is a *FDM*, using the Critical Impedance index [XLL03] to find the *most significant harmonic source* in a system composed of two sides (utility and customer) connected to a PCC. *CIM* develops a Thevenin equivalent (for voltage harmonic analysis) or Northon equivalent (for current harmonic analysis), assuming Z_U as the sum of the transformer impedance and network equivalent impedance. Also, Z_C is modeled using a frequency sweep using the frequency components U_h and I_h of u_{PCC} and i_{PCC} respectively as depicted in Fig. **2-1**.

The evaluation procedure comprises four steps:

2.1.1.1. Measurement

CIM requires a measure in PCC of the magnitudes and angles of voltage and current frequency spectra. A particular standard for measurement is not recommended for the author to ensure accuracy; actually, an error analysis that shows the method's robustness even under bad impedance estimation is presented in [XLT04].

2.1.1.2. Modeling

A model for each frequency component should be developed, then, voltage and current measured at the PCC should be decomposed using FFT. Also, as mentioned, Z_U and Z_C should be measured or assumed. Since Z_U is known, the harmonics components U_{Uh} of u_U can be calculated as:

$$U_{Uh} = U_h - I_h Z_U \tag{2-1}$$

where U_h is the harmonic component h of u_{PCC}.

2.1.1.3. Index Calculation

Critical Impedance (CI) is an index that quantifies the customer's capability to affect the network. The equation (2-2) shows the CI for assessing the voltage harmonic h.

$$CI = 2\frac{U_{Uh}}{I_h} sin(\theta - \beta) \tag{2-2}$$

Where θ is the difference between the phase angles of U_{Uh} and I_h, and β should be calculated as it is shown in (2-3).

$$\beta = tg^{-1}\left(\frac{R_U + R_C}{X_U + X_C}\right) \tag{2-3}$$

Where $Z_U^2 = R_U^2 + X_U^2$ and $Z_C^2 = R_C^2 + X_C^2$.

2.1.1.4. Assessing

The CI should be interpreted as follows:

- If $CI > 0$, the customer side is the major voltage harmonic contributor.
- If $CI < 0$, the following must be applied:
  - If $|CI| > |Z_{max}|$, utility side is the major voltage harmonic contributor.
  - If $|CI| < |Z_{min}|$, customer side is the major voltage harmonic contributor.
  - If $|Z_{min}| < |CI| < |Z_{max}|$, there is no conclusion.

A general calculation process for current and voltage harmonic can be found in [XLT04].

CIM is a breakthrough in harmonic source assessment since it can find the major contributor, even if a bad estimation of system impedance was made [XLT04]. Also, its plausible mathematical formulation results in an easy and accurate indicator that addresses the concept of *Critical Impedance* like a *central* impedance between u_U and u_C. However, *CIM* implementation depends on many system information, sometimes hard to find, such as system impedance or utility impedance. This fact implies that the calculus must be made over suppositions, taking the risk of wrong conclusions or situations where the method does not conclude about contributions. Besides, the measurement scheme of this method makes it impossible to evaluate a system composed of more than two sides (two elements connected to the PCC). This fact makes it challenging to find the source of the disturbance when there is more than one customer connected to the PCC.

2.1.2. Harmonic Vector Method HVM

The *HVM* [PP11b] is a *FDM* similar to *CIM*. The main difference is that *HVM* also calculates u_C to perform a comparison between u_U and u_C (or i_U and i_C) then determining the *harmonic contribution of each side* (utility and customer) and consequently establish the *most significant harmonic source*.

The evaluation procedure can be summarized as follows:

2.1.2.1. Measurement

HVM requires a measure in PCC of the magnitudes and angles of voltage and current frequency spectra. A particular standard for measurement is not recommended for the author to ensure accuracy.

2.1.2.2. Modeling

HVM seeks to reduce system information requirements and facilitate calculation. This aim makes it possible to complete reasonable approximations for the customer and utility impedance. In this method, Z_U is assumed as only the transformer impedance, and Z_C is the fundamental customer resistance calculated as (2-4).

$$Z_C = R_C = \frac{|U_1|}{|I_1| * cos(\theta_1)} \tag{2-4}$$

Where U_1 and I_1 are the fundamental frequency components of u_{PCC} and i_{PCC} respectively, θ_1 is the phase angle difference between U_1 and I_1.

In the same manner as *CIM*, voltage and current measured at the PCC should be decomposed using FFT to develop a model for each frequency component. Then, the harmonic components U_{Uh} and U_{Ch} (or I_{Uh} and I_{Ch}) of u_U and u_C respectively should be calculated as it is shown in (2-5) and (2-6) for voltage contribution:

$$U_{Uh} = U_h + I_h Z_U \tag{2-5}$$

$$U_{Ch} = U_h - I_h Z_C \tag{2-6}$$

for current contributions I_{Ch} and I_{Uh} can be calculated as:

$$I_{Uh} = \frac{U_h}{Z_{Uh}} + I_h \tag{2-7}$$

$$I_{Ch} = \frac{U_h}{Z_{Ch}} - I_h \tag{2-8}$$

HVM assumes I_{Ch} and I_{Uh} are the harmonic source of customer and utility respectively. Thus, the contribution can be calculated using the superposition principle as:

$$I_U = I_{Uh} * \frac{Z_{Uh}}{Z_{Uh} + Z_{Ch}} \tag{2-9}$$

$$I_C = I_{Ch} * \frac{Z_{Ch}}{Z_{Uh} + Z_{Ch}} \tag{2-10}$$

2.1.2.3. Assessing

Once the contribution have been calculated, if $I_C > I_U$, the customer side is the major current harmonic contributor, and the utility side would be the major contributor if $I_{Ch} < I_{Uh}$. A general current and voltage harmonic evaluation method can be found in [PBP08].

As mentioned, *HVM* improves work presented in [XL00] that seeks to take advantage of its low susceptibility to impedance estimations to reduce its information requirements. This fact facilitates its implementation and also makes it easy to assess. Despite the above, *HVM* shares some disadvantages with *CIM*. First, the method can determine systems only with two sides (customer and utility). Second, its main advantage is also its main disadvantage since the approximations over the impedance could lead to wrong conclusions. Finally, *HVM* dispenses with the CI index that constitutes the central concept of the *CIM*.

2.1.3. IEC TR. 61000-3-6 IECM

IECM [IEC08b] is a *FDM* aimed to establish *planning levels in the network*. This method uses measurements at the PCC, before and after customer connection, to identify the background distortion, i.e., harmonic voltage contribution of the network seen from the PCC (background distortion) u_{back}. Finally, using a phasor subtraction, the approximated harmonic voltage contribution of customer u_{emi} is calculated from the value of u_{back} and u_{PCC}.

The assessment procedure comprises two steps:

2.1.3.1. Measurement

As it was already mentioned, *IECM* uses measurements before and after customer connection. Both sets of measurements should be taken at the PCC, following the recommendation of Std. IEC 61000-4-30. The measurement taken before the customer connection should be interpreted as the background distortion (u_{back}); on the other hand, the measurement taken after the customer connection should be interpreted as the effect of the new connection over PCC (u_{PCC}). It is worth noting that this measurement method is also used for assessing other power quality phenomena, such as phase displacement (Power Factor), unbalance, and voltage level deviations, among others, before connecting a new load to the network.

2.1.3.2. Calculation

Calculation process can be made directly from the two sets of measurements for each harmonic component as it is shown in (2-11):

$$U_{emi_h} = u_h - U_{back_h} \tag{2-11}$$

Where U_{emi_h}, U_h and U_{back_h} are the phasors of u_{emi}, u_{PCC} and u_{back} respectively, for the harmonic component h.

IECM has been widely used to assess the impact of connecting new loads to the system and estimate the customer contribution. However, the two sets of measurements (before and after the new load connection) reflect two different systems. This means the *IECM* does not consider interaction effects between utility and customer, such as harmonic compensation or resonance. Furthermore, the non-synchronized measurements could affect the accuracy of the estimation.

2.1.4. Method of Disturbances Interaction MDI

MDI [PTSS10a] is a *TDM* that uses FBD electric power theory to perform a current decomposition to assess *current distortion, phase displacement, and unbalance*. This method compares the decomposed current signal of each element with the decomposed current signal of each other, then, *MDI* establish *interaction groups and their contribution to the development of the analyzed disturbance*. This implies that *MDI* is capable of assessing contributions in a system composed of more than two agents (n elements connected to the PCC, including the network), as shown in Fig **2-3**.

The evaluation process has five stages:

2.1.4.1. Measurement and Ordering Currents

Given that *MDI* uses signals of all currents, it is necessary to know i_1, i_2, i_{PCC} and u_{PCC}, for this reason, a simultaneous multi-point measurement should be implemented. The synchronization of measurements is a critical issue since bad timing could generate wrong results in the subsequent stages, particularly in stage 3. The use of Std. IEC 61000-4-30 [IEC15] is suggested to ensure correct synchronization of measure equipment.

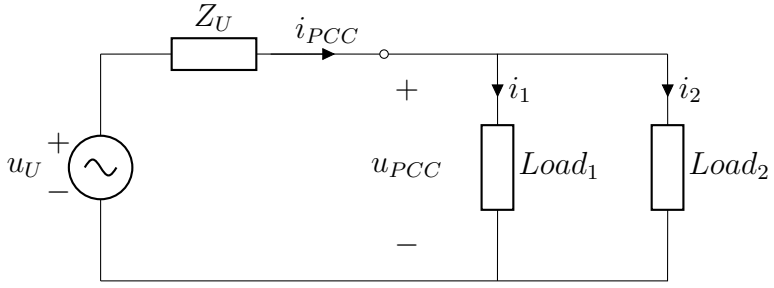

Figure 2-3: Basic *MDI* scheme

Once the measurement has been done, it is necessary to order currents. It means assuming a direction for each current (i_{PCC}, i_1 and i_2) ensuring the compliance of Kirchhoff's Laws, as it is shown in Fig. **2-3**. This allows the install $n-1$ to measure equipment and calculates the current of the rest, reducing implementation cost.

2.1.4.2. Decomposition of Currents

There are ways to decompose currents and voltages based on power theories such as FBD [Sta08] or Std. IEEE 1459 [IEE10a]. However, the orthogonal decomposition of currents FBD presented in [PTSS10a], could be the most suitable option if a comparison of signals is required since this theory establishes u_{PCC} as a reference to define the disturbances to compare the different current components resulting for each element connected to the PCC. Below, a brief description of the single-phase decomposition will be presented. A more detailed process can be found in [PTSS10a] and [Sta08].

FBD orthogonal decomposition proposes modeling a single-phase circuit like the one shown in Fig. **2-4** as a system composed of an ideal resistor parallel to a controlled current source. In this way, the current i_{PCC} delivered from PCC towards the load can be decomposed first into two components, active (i_a) and non-active (i_x). The active current component

i_a contains the current related to energy exchange throughout the system. In contrast, the non-active current component i_x contains information related to phenomena that do not have an average energy transmission.

$$\begin{aligned} i_{PCC} &= i_a + i_x \\ I_{PCC}^2 &= I_a^2 + I_x^2 \end{aligned} \tag{2-12}$$

Where I_{PCC}, I_a and I_x are the rms values of i_{PCC}, i_a and i_x respectively.

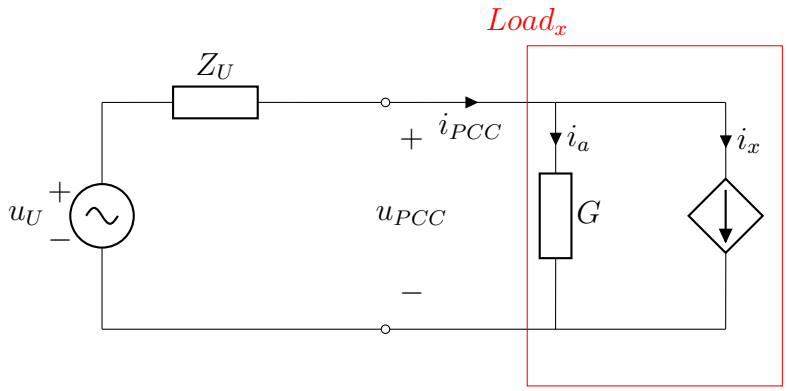

Figure 2-4: Equivalent circuit proposed by FBD power theory

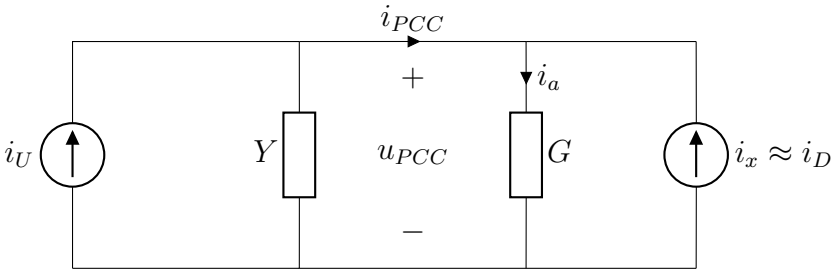

By definition, the inner product between the voltage and current signals equals the active power; the inner product between a signal and itself yields the squared rms value (2-13).

$$P = \langle u_{PCC}, i_{PCC} \rangle \qquad U^2 = \langle u_{PCC}, u_{PCC} \rangle \tag{2-13}$$

From (2-13), it is possible to define the equivalent active conductance G and the active current i_a as (2-14):

$$G = P/U^2 \qquad i_a = G u_{PCC} \tag{2-14}$$

Then, i_x can be calculated as (2-15):

$$i_x = i_{PCC} - i_a \tag{2-15}$$

Given that i_x contains the components related to phase displacement and current distortion, it can be split into two components, displaced (I_{Qd}) and distorted (I_D) current components. The displaced voltage is defined as (2-16):

$$u_d = u_{PCC}(t - T/4) \qquad U_d = U \tag{2-16}$$

The inner product between u_d and i_x yields a quantity named *displaced power* (Q_d). The displaced power represents the portion of power supplied by the source produced (or affected) by capacitances and inductances in the system. Analogous P and G, from Q_d it is possible to define the *displaced susceptance* B as (2-17):

$$Q_d = \langle u_d, i_x \rangle \ ; \qquad B = Q_d/U^2 \tag{2-17}$$

From (2-15) and (2-17) it is possible to calculate the displaced (i_{Qd}) and distorted (i_D) current components as (2-18):

$$i_{Qd} = Bu_d \qquad i_D = i_x - i_{Qd} \tag{2-18}$$

The displaced current component i_{Qd} should be interpreted as the portion of the current i_{PCC} associated with phase displacement. In the same way, the distorted waveform component i_{Qd} should be interpreted as the portion of the current i_{PCC} associated with current distortion. It is worth clarifying that i_D groups the distortion phenomena presented during the measurement process (notches, harmonics, interharmonics, etc.); I_D contains all frequency components not present in the voltage spectrum. Finally, i_{PCC} can be decomposed as (2-19):

$$\begin{aligned} i_{PCC} &= i_a + i_x = i_a + (i_{Qd} + i_D) \\ I_{PCC}^2 &= I_a^2 + I_x^2 = I_a^2 + (I_{Qd}^2 + I_D^2) \end{aligned} \tag{2-19}$$

This process should be performed the same way for each element connected to PCC to obtain three orthogonal components, i_a, i_{Qd}, and i_D for each current in the system. Note that in a system as depicted in Fig. **2-3**, the decomposition must be repeated for the currents flowing through the loads $Load_1$ and $Load_2$, changing i_{PCC} for i_1 and i_2 in the equations.

MDI can also assess unbalance in a three-phase system as shown in[PTSS10a]. However, these disturbances will not be addressed in this proposal. A complete decomposition process can be found in [PTSS10a][Sta08], and a wide analysis of this and other decompositions based on Fryze's power theory will be presented in Chapter 3.

2.1.4.3. Calculation of Interactions

Once the whole of currents flowing through PCC has been decomposed, these will be compared between them. The inner product reveals how similar the two signals are. Thus, it is possible to describe interactions between two agents resorting to their inner products. The interaction is calculated as (2-20):

$$\eta_{k_{1,2}} = \langle i_{k_1}, i_{k_2} \rangle \tag{2-20}$$

Where i_{k_1} and i_{k_2} are the current components k of loads $Load_1$ and $Load_2$, and $\eta_{k_{1,2}}$ is the non-normalized interaction index between loads $Load_1$ and $Load_2$ for the current component k. η must be calculated for each pair of elements connected to PCC, including the network that in this notation is represented for the current i_{PCC}, and the result gets ordered in a matrix for each current component called *interaction matrix*. Note that the interaction between different current components is zero by inner product definition because the above decomposition results in orthogonal current components. This proves the capability of *MDI* to assess distortion, phase displacement, and unbalance separately.

Results from inner products can be interpreted as follows:

- If the **inner product is zero** $\eta_{k_{1,2}} = 0$, **no interaction** between agents is observed. It means that there is no current interchange between the elements compared.
- If the **inner product is greater than zero** $\eta_{k_{1,2}} > 0$, **both elements interact with a third one** in such manner that **they balance the current component with the third element**.
- If **the inner product is less than zero** $\eta_{k_{1,2}} < 0$, **both elements interact** in such manner that **they interchange the current component** under analysis.

2.1.4.4. Establishing Interaction Groups

The sign in the interaction matrices implies that one group of elements interchange the current component k with another group of elements. The table **2-1** exemplifies a normalized interaction matrix for a supposed current component k. From the table **2-1**, it is easy to

understand that the interaction of an element with itself is 1, which means that the vectors compared are equal. On the other hand, the interaction between Utility and $Load_1$ is negative. According to stage 3, they interchange the current component k. However, the interaction between Utility and $Load_2$ is positive, which means that both elements interchange the current component k with a third element, that in this case is $Load_1$, fact that is checked with the negative interaction between $Load_1$ and $Load_2$.

Table 2-1: Example of an Interaction Matrix for Current Component k

η_k	Utility	Z_{C1}	Z_{C2}
Utility	1	-0,5	0,5
Z_{C1}	-0,5	1	-0,5
Z_{C2}	0,5	-0,5	1

Finally, it is possible to say that one group is composed of Utility and Z_{C2}, and the second group is composed of Z_{C1}. For differentiation effects in the analysis, these groups are called indistinctly α and β and represent *where the disturbance is concentrated*.

2.1.4.5. Assessment

In previous stages, the disturbances were separated using FBD orthogonal decomposition. Then, the interactions between pairs of agents, in terms of each disturbance, were calculated using inner products. Finally, the interaction matrices resulting from the process were analyzed to establish interaction groups α and β. This process must be repeated over time, which means there should be set interaction matrices and interaction groups for each integration period, following the suggestion of Std. IEC 61000-4-30 [IEC15].

The assessment using this method is based on the interpretation of results. Some work, as presented in [Pav12] has used probabilistic analysis on the interaction groups to establish the *most likely responsible*. The method presented in [PG14] uses epidemiological techniques to compare rms values of the current components along time and establish association and correlation between the disturbance and the presence of a load to discard the *non-responsible element* of the analysis. Some other methods, as presented in [GP15] [GP17] use graph theory indicators over the interaction matrices for establishing the direction of such interactions. This way, the method can prove the disturbance source and the elements that perceive such disturbance.

Despite the mathematical approach of *MDI* has been widely discussed and accepted [Sta08], it is clear to the reader that *MDI* is more complicated to implement than all *FDM*s presented above. Besides, the measurement scheme makes the implementation of this method expensive. However, this method can accurately assess the contribution of a system compo-

sed of n sides (n elements connected to the PCC) for current distortion, phase displacement, and unbalance, employing the interaction indexes. Besides, an improvement for this method is presented in [GP17] can establish the direction of the current components, allowing the identification of disturbance sources and demand.

2.2. Illustrations of Methods

The previously described methods were tested in a synthetic system implemented in the Power Quality Laboratory of the Institute of Electric Power Systems and High Voltage Engineering (IEEH) of the TUD Dresden University of Technology. Such a system allows the simulation of scenarios of voltage and current distortion generated on the utility side and current distortion generated on the customer side, as will be shown.

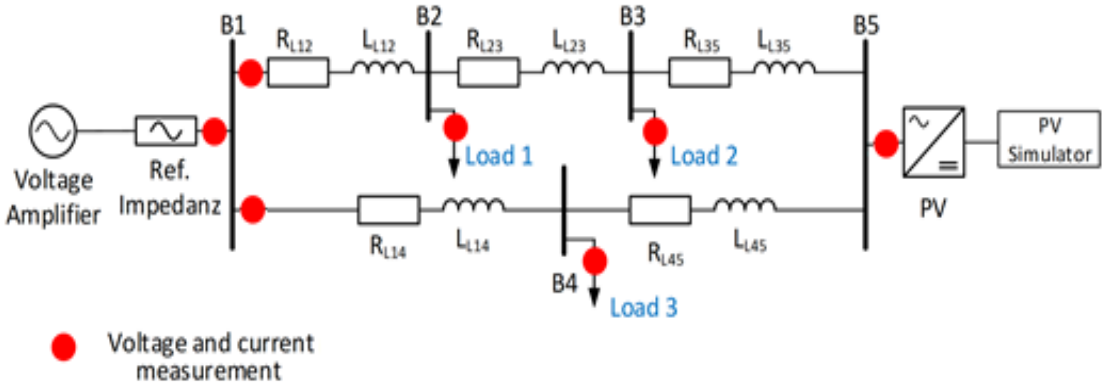

Figure 2-5: Synthetic system implemented in the Lab.

2.2.1. Setup of the System

A ring system was implemented in the laboratory, as shown in Fig. **2-5**. A voltage amplifier was connected to the busbar B1 to simulate the utility voltage, and a PV inverter was connected to the busbar B5 to emulate the presence of a non-linear power generation device at the utility network. In addition, three different kinds of load were connected to the buses B2, B3, and B4 to emulate different operative conditions in the utility and on the load side, as shown in Table **2-2**.

The main characteristics of the synthetic network will be presented below.

Table 2-2: Scenarios implemented in the Lab

Scenario	Current distortion at Utility	Voltage Distortion at Utility	Current Distortion at Customer
1			x
2		x	x
3	x		x
4	x	x	x
5	x		
6	x	x	

2.2.1.1. Voltage Amplifier

The S&S Voltage amplifier was used for the measurements, as it is the only amplifier with the ability to absorb power (In the operation manual of the Elgar amplifier, there is no information about this operation mode). The flicker reference impedance (0,4 Ω + j0,25 Ω) was used to represent the main grid more realistically. The main characteristics of the amplifier are shown in Table **2-3**.

2.2.1.2. PV-Inverter

The PV SMA was connected to the busbar B5. Aimed to generate a more significant impact in the system, this source was connected directly to the busbar B5 without any impedances, as shown in Fig. **2-5**. The main characteristics of the PV inverter are shown in Table **2-3**.

Table 2-3: Characteristics of the sources

Manufacturer	Spitzenberger&Spies	SMA Solar Technology AG
Model	**EP 2250/B**	**Wechselrichter Sunny Boy 5000TL**
Number of phases	1	1
U_{AC-nom} **in V**	135/270	230
$S_{out-nom}$ **in VA**	2250	5000
f in Hz	15 Hz to 1,5 kHz	50/60
Total Harmonic Factor	N,A	0,20 %
Amplifier Technology	Linear	Switched

2.2.1.3. Lines

The "Split network impedance" (Geteilte Netzimpedanz) was used as line impedance, which is the flicker reference impedance divided into five parts. This impedance contains five inductances of 0,12 mH, a series resistance of 0,06 Ω, five inductances of 0,08 mH, and a series resistance of 0,04 Ω.

It is important to mention that the impedances in the test stand represent in a better way the impedances of real cables in LV networks. Taking as reference a cable NAYY $4x35$ mm^2 (0,868 + j0,08 Ω/km), is possible to say that 0,12 mH and 0,06 Ω (0,06 Ω + j0,038 Ω) could represent a line NAYY $4x35$ mm^2 of 81 m, a cable length reasonable in distribution systems. In addition, neutral cable impedances were also implemented to get a more realistic test. Table **2-4** shows the impedances used in the system.

Table 2-4: Impedances used to emulate the lines of the system

Nodes		Line Name	Line			Neutral		
			R [Ω]	X [Ω]	Z [Ω]	R [Ω]	X [Ω]	Z [Ω]
Voltage AMP	B1	Network	0.4	0.25	0.472			
B1	B2	Line 1	0.06	0.038	0.071	0.040	0.025	0.047
B2	B3	Line 2	0.06	0.038	0.071	0.040	0.025	0.047
B3	B5	Line 3	0.06	0.038	0.071	0.040	0.025	0.047
B1	B4	Line 4	0.06	0.038	0.071	0.040	0.025	0.047
B4	B5	Line 5	0.06	0.038	0.071	0.040	0.025	0.047

2.2.1.4. Loads

Three kinds of load were connected to the system to simulate different operative scenarios: No Power factor correction load (NPFC), Active Power Factor Correction Load (APFC), and linear loads. All the loads are comparable in active power to simplify the analysis, as shown in Table **2-5**.

Table 2-5: Characteristics of the loads

Load	**CFL 30 W**	**LED Lamp**	**Incandecent Lamp**	**Resistor**
Total P_{out} W	241	240	211	240
PF	0,97	0,42	0,99	1
THDi in %	17,8	211,9		
Power Source Technology	Active PFC	No PFC	Linear	Linear

2.2.2. Measurement Setup

The Dewetron 2600 with HIS-HV and HIS-LV modules were used for the measurements. The main characteristics of the Dewetron modules related to this measurement setup are summarized in Table **2-6**. The voltages were measured directly with the modules Dewe HIS-HV. The currents of the loads and the network were measured using zero-flux transducers connected to the Dewe HIS-LV modules. The characteristics of the zero-flux transducers are summarized in Table **2-7**. Lines 1, 4, and PV currents were measured using the shunt resistances ATE RB50 available in the laboratory. The real values up to 60 kHz are 0,1016 Ω, 0,0991 Ω and 0,0995 Ω.

Table 2-6: Characteristics of the Dewetron

	Dewe HIS-HV	Dewe HIS-LV
Input ranges	20 V to 1400 V	12 ranges (10 mV to 50 V)
Bandwidth	2 MHz	2 MHz
Input resistance	10 mΩ —— 2.2 pF	1 MΩ
Input range	400 V	10 mV, 50 mV, 200 mV, 1 V
Filter type	Butterworth	Butterworth
Filter (lowpass)	300 kHz	300 kHz

Table 2-7: Characteristics of the zero-flux current transducer

Manufacturer	**Dewetron**
Reference	PM-CM-60
Current (max)	60 A
Ration	1:600
Bandwidth	800 kHz

2.2.3. Test

The six scenarios proposed were emulated using the setup presented in Table **2-8**, where busbar B2 is considered the PCC. In this way, Load 1 represents the *Customer Side*, and the rest of the system represents the *Utility Side*. Voltage, current, and harmonic impedance were measured at the PCC using the measurement setup previously commented on. Then, the CIM, HVM and MDI introduced were applied using the available information. The IECM was excluded from the analysis because its approach is limited to determining harmonic emission limits.

Table 2-8: Operative scenarios simulated

Scenario	Source Waveform	PV Generation Rate	Load 1	Load 2	Load 3
1	Sinus	0	NPFC 241 W	Linear 211 W	Linear 240 W
2	Flat top	0			
3	Sinus	0	NPFC 190 W	APFC 190 W	APFC 190 W
4	Flat top	358 W			
5	Sinus	0	Linear 240 W	APFC 240 W	NPFC 241 W
6	Flat top	358 W			

2.2.4. Current Contribution

Current contribution was calculated using each method considering the next:

- **HVM:** Note that the equation 2-4 can be rewrites as:

$$R_C = \frac{U_1^2}{P} \tag{2-21}$$

  Where P is the active power, in this way, R_C is a quantity that represents the active power flux from the utility to the customer in the same manner that the conductance G in the MDI (equation 2-14). Then, it is possible to say that the HVM directly makes Utility responsible for the active harmonic components.

- **CIM:** Although it is true that this method does not establish contributions but rather evaluates responsibilities according to the CI indicator, for comparison purposes, the contributions were calculated using a work by the same author presented in [XL00]. In general terms, the calculations are the same as in the HVM, but with the difference that the directly measured impedances are used and not estimates.

- **MDI:** As was already mentioned, the MDI quantifies the interactions between agents aimed to determine responsibilities. However, the contribution of each agent is unclear when the system comprises only two agents, given that the interaction matrix is symmetrical. In this way, the FBD currents I_a and I_D were directly taken as the utility and customer contribution, respectively. This supposition is supported in the analysis presented in Chapter 3. Although MDI is a TDM, for comparison purposes, I_a and I_D were decomposed using a Fast Fourier Transform.

2.2.4.1. Utility Contribution

The figure **2-6** shows, in absolute value, the utility contribution calculated with each method. At first glance, it is easy to see that the contributions follow the same pattern but not the same magnitude, particularly in the case of the CIM. This is because both HVM and MDI (FBD) use the same impedance to calculate the contributions in all harmonic components, namely R_C and $1/G$, respectively. On the other hand, the CIM uses the impedance of each harmonic component, which is individually smaller than $1/G$ or R_C, resulting in more significant contributions.

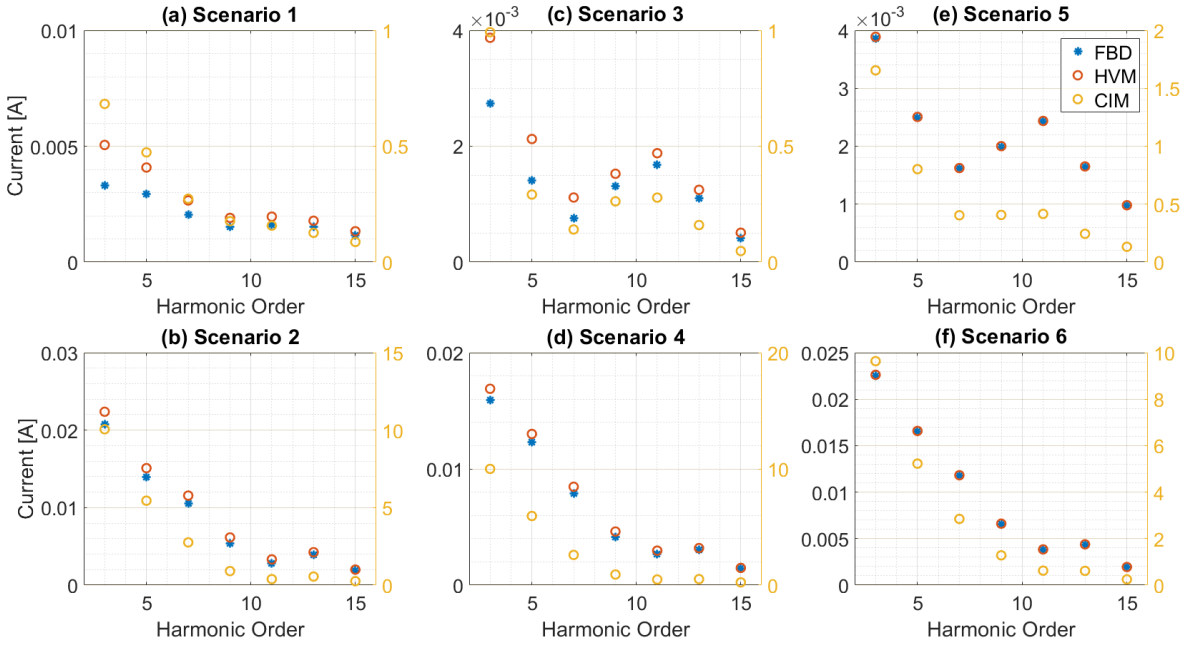

Figure 2-6: Utility contributions at the PCC

Note that in the scenarios without voltage distortion (scenarios 1, 3, and 5), the order of magnitude is significantly lower than in the others, almost twenty times lower. This makes sense given that voltage distortion is associated with Utility, at least in traditional distribution networks, as seen in Chapter 3. Additionally, without voltage distortion, the contributions calculated with HVM and MDI (FBD) are adjusted much better since the harmonic components have less presence and, consequently, the fundamental component is more present. Therefore, it is confirmed that I_U is a variable that explains the flow of active current from the Utility to the Customer.

Another important aspect worth highlighting is that in the scenarios with linear loading (scenarios 5 and 6), the contributions are equal when calculated with the HVM and the MDI (FBD). This is because the entire contribution of the Utility is the active current demanded

by the load. Then, given the nature of the said load, the current at the PCC will be composed mainly of the fundamental frequency component, which implies that $R_C \approx 1/G$. This shows that the MDI (FBD) is more sensitive and efficient in detecting active components other than the fundamental ones compared to the HVM.

2.2.4.2. Customer Contribution

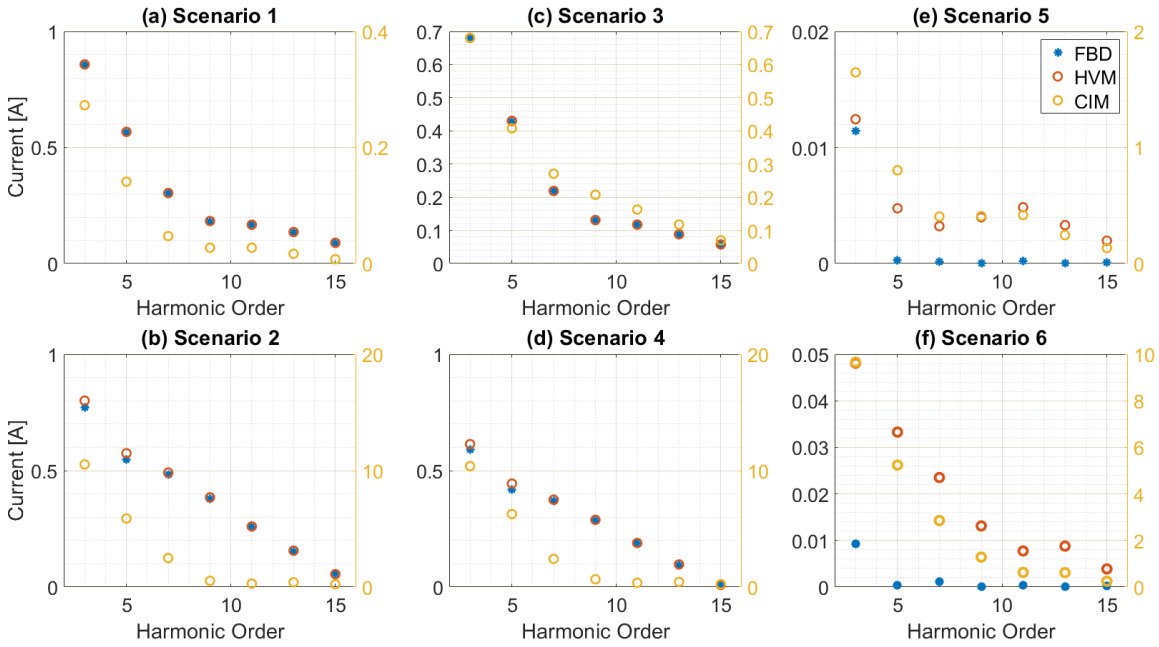

Figure 2-7: Customer contributions at the PCC

Figure **2-7** shows the Customer's contributions to the PCC. Unlike the previous figure, there is no significant difference in the orders of magnitude of the contributions with or without voltage distortion except in the CIM, which is more sensitive to voltage distortion. That confirms that the utility's contribution is associated with the background distortion in the system and Customer's contribution is mainly associated to current distortion.

Additionally, note that in the scenarios with current distortion in the Customer (scenarios 1, 2, 3, and 4), the contributions calculated using HVM and MDI (FBD) are almost the same regardless of whether or not there is voltage distortion or current distortion at the Utility. This means that the Customer contributions calculated with the HVM ultimately correspond to the distorted current, in other words, to harmonic current components that do not conform to a voltage component.

An important factor that provides more reliability to the MDI than to the HVM and CIM in this exercise can be seen in scenarios 5 and 6 (linear loading). By having no more than

a linear load connected on the customer side, it is clear that the Customer could not be responsible for the distortion or make a significant contribution. This is true in the MDI (FBD) case but not in the HVM and the CIM, which assign contributions to the Customer equal to or even higher than those of the Utility. This is due to its calculation method. Note that the way to calculate the distortion factors (equation 2-7) assumes that the contributions are proportional to the magnitude of the impedances used as reference, which disregards the nature or type of connected load. In this way, the three methods are comparable in calculating the Customer's contributions in scenario 3. This is due to two factors:

- The absence of voltage distortion causes the CIM to reduce the order of magnitude of the contributions until making them comparable with the MDI and the HVM.
- The load on the Customer side is non-linear, mitigating the error introduced in calculating the HMV and CIM sources, as previously mentioned.

2.2.5. Discussion

Table **2-9** shows the result of the current distortion responsibilities assignment obtained with each of the methods, as described in the previous section. In the Table, the sub-matrices represent the six scenarios analyzed, the column entitled h represents the harmonic components considered, and the letter C represents the cases in which it was determined that the primary responsible party was the Customer. The letter U represents the cases in which the utility was chosen as the main responsible.

Table 2-9: Comparison of the results for current distortion

		No Current Distortion at Utility			Current Distortion at Utility					
	h	CIM	HVM	MDI	CIM	HVM	MDI	CIM	HVM	MDI
No Voltage Distortion at Utility	3	C	C	C	C	C	C	C	C	C
	5	C	C	C	C	C	C	C	C	U
	7	C	C	C	C	C	C	C	C	U
	9	C	C	C	C	C	C	C	C	U
	11	C	C	C	C	C	C	C	C	U
	13	C	C	C	C	C	C	C	C	U
Voltage Distortion at Utility	3	U	C	C	U	C	C	U	C	U
	5	C	C	C	C	C	C	C	C	U
	7	C	C	C	C	C	C	C	C	U
	9	C	C	C	C	C	C	C	C	U
	11	C	C	C	C	C	C	C	C	U
	13	C	C	C	C	C	C	C	C	U
		Distorted Load						Clean Load		

At first glance, it is evident that the HVM holds the Customer responsible in all cases,

which is reliable in the scenarios with Distorted Load but not in the scenarios with Clean Load, as previously mentioned. On the other hand, the CIM blames the Utility for the 3rd harmonic in cases with voltage distortion, which makes sense considering that the waveform was flat top. However, it holds the Customer responsible in all other cases, even in those cases with Clean Load, resulting from an error introduced in calculating the sources of the equivalent model, as mentioned before. Finally, the MDI holds the Customer responsible in all cases except those with Clean Load.

Each method presents advantages over the others under different operating conditions of the system and the advantages associated with the implementation. For example, the HVM only requires voltage and current measurements at the PCC and the best available network impedance information. At the same time, the CIM also requires harmonic impedance measurements, which represents difficulties when implemented in a real system. It is impossible to measure voltage, current, and harmonic impedance simultaneously without introducing errors in the records. However, the results of the CIM are more reliable than those of the HVM.

On the other hand, MDI is not only easy to implement, even in real systems, but it also provides reliable results. However, its implementation in systems composed of only two agents is inconclusive; therefore, the results must be assumed directly from the FBD decomposition.

Finally, it is worth noting that there was no evidence of the influence of current distortion at the Utility side over the results. In this way, it is possible to say that distorted current on the utility side of a strong network does not directly affect the judgment of the methods. Therefore, waveform distortion at the PCC is associated only with the background distortion and the distorted current i_D coming from the load. In this order of ideas, it is not reasonable to talk about a contribution of distorted current from the network or a contribution of voltage distortion from the load in traditional distribution systems.

2.3. Chapter Summary

Three responsibility assessment methods were evaluated using a synthetic distribution network implemented in the laboratory. The system was designed to emulate different operating conditions by varying the type of load and network configuration.

All three methods make reliable judgments in nonlinear loading scenarios, even if background distortion exists. However, calculation errors in the HMV and the CIM lead to overestimating the impact of the Customer, assigning responsibility even when its load is linear. On the other hand, the MDI is not conclusive when the system is composed of only two agents, which implies the direct use of the FBD decomposition, assuming that the current

i_a flows from the Utility to the Customer and the current I_D flows in the wrong way. This assumption will be discussed in more detail in chapter 3.

2.3.1. Contributions of this Chapter

- The tests performed in this chapter show that FDMs and TDMs assign the same responsibility in traditional distribution systems; the utility is responsible for voltage distortion, and the customer is responsible for current distortion. However, in the case of HVM, this rule is satisfied if there is a high enough non-linear load on the Customer side; otherwise, this method returns erroneous results.
- The tests carried out in this chapter show that distorted current on the Utility side does not directly affect the assignment of responsibilities as voltage distortion does.

3 Waveform Distortion Assessment using Fryze's Approach-Based Power Theories

In Chapter 2, three responsibility assignment methods were analyzed, showing that MDI is easy to implement and provides reliable results. Nevertheless, although a PCC can connect many feeders, the responsibility assignment problem is usually reduced to two agents, the load and network sides. The MDI cannot conclude under such restriction; then, using the FBD decomposition directly under certain assumptions is necessary, as shown in Chapter 2.

This chapter approaches the problem of waveform distortion contribution from Fryze's power theory framework. The aim is to explore the potential of the more remarkable power theories derived from Fryze's proposal to assess responsibilities in a reduced system composed of a PCC and two agents, the load and the network. In this way, in section II, the mathematical definitions of voltage, current, active, and non-active power are presented using the Fourier series approach. These definitions are widely accepted and are the basis for developing this chapter.

Section III presents the power theories from a mathematical point of view, identifying their advantages, some limitations, and the main differences between them. In section IV, a study case was designed and implemented in the laboratory to test the power theories under different types of loads and voltage sources. Finally, the test results are analyzed and discussed in section V.

3.1. Remarkable Power Theories and Power Definitions

According to [AEET12], three schools currently dominate power theory definitions: Constantin I. Budeanu's school, Stanislaw Frize's school [Fry32] [Buc50], and the Pointing Vector-based power theory (IEEE Std. 1459 recommendation) [AEET12][IEE10b]. However, Budeanu's approach has been strongly criticized and abandoned by many researchers [Cza87][Pav12]. Four power theories are currently the most accepted but widely discussed by the remaining

two schools. One of them is the already mentioned IEEE Std. 1459 [IEE10b]. The other three are based on Fryze's work, namely, FBD power theory [Dep93][PTSS10b], Conservative Power Theory [Ten04][PTP10], and Current's Physical Components power theory [Cza88][Cza08]. They define reactive power to obtain and perform different orthogonal decomposition over the non-active powers. According to [Cza08], a power theory has to fulfill the following requirements:

1. *An explanation and physical interpretation of power phenomena that accompany energy delivery*
2. *A definition of power quantities which describe energy flow and its utilization, as well as can specify power ratings of the power equipment*
3. *Fundamentals for energy accounts between energy producers and customers*
4. *Fundamentals for studies on the effectiveness of energy delivery*
5. *Fundamentals for design and control of equipment for power factor improvement*
6. *Fundamentals for design and control of equipment for loading and supply quality improvement*

Indeed, the four theories agree on the first, the first part of the second, and the third requirement, understanding this as the formulation for power and energy calculations. The rest of the requirements are unclear to the authors, given that the fundamentals for studies and design, understanding "fundamentals" as the inputs, more than a requirement, is a natural result. In this way, it is possible to say that any power theory accomplishes the last three requirements.

Considering the agreement among power theories already commented, it is widely accepted that the concept of active power is a physical definition representing the energy exchange rate in a system. Particularly in electrical systems, such power is defined as (3-1):

$$P = \frac{1}{T}\int_{\tau}^{\tau+T} i(t)u(t)dt = \frac{1}{T}\int_{\tau}^{\tau+T} p(t)dt \tag{3-1}$$

Where $p(t)$ is the instantaneous power, T is the period, and $u(t)$ is the voltage, which can be defined for non-sinusoidal conditions as:

$$u(t) = U_0 + \sqrt{2}U_1\sin(\omega_1 t + \alpha_1) + \sqrt{2}\sum_{h=2}^{H} U_h \sin(h\omega_1 t + \alpha_h) \tag{3-2}$$

Where the first term is the DC component, this term must be considered only if the

DC level is observed in the measurement. The second term is the fundamental frequency component, and the third term could be considered as the voltage distortion reflected on the PCC. Finally, the current $i(t)$ can be expressed in the same manner as:

$$i(t) = I_0 + \sqrt{2}I_1 \sin(\omega_1 t + \beta_1) + \sqrt{2}\sum_{h=2}^{H} I_h \sin(h\omega_1 t + \beta_h) \tag{3-3}$$

According to 3-1, the components $u_h(t)$ that match with the components $i_h(t)$ and also are in phase shape the active power P. This implies that the voltage distortion of the network is reflected in the power P. In other words, voltage distortion is reflected in the active power. All the components $i_h(t)$ that match with the components $u_h(t)$ can be called *active harmonic components*, given that such components are involved in the energy exchange.

It is worth clarifying that each harmonic component h in the equations 3-2 and 3-3 is a phasor quantity composed by a magnitude U_h and a phase angle α_h for voltage case. Otherwise, the rms values of $u(t)$ and $i(t)$ can be calculated as:

$$U = \sqrt{\frac{1}{T}\int_{\tau}^{\tau+T} u^2(t)dt} \tag{3-4}$$

$$I = \sqrt{\frac{1}{T}\int_{\tau}^{\tau+T} i^2(t)dt} \tag{3-5}$$

Then, the apparent power, representing the maximum power rating of the equipment, can be defined as:

$$S = UI \tag{3-6}$$

From definitions 3-1 and 3-6, Non-active power is defined as:

$$N = \sqrt{S^2 - P^2} \tag{3-7}$$

Active power exchange is a desirable condition in the power system. As it was shown in [Pav12] that active harmonic components flow in the same direction as the fundamental harmonic component, feeding the loads even under non-sinusoidal conditions.

Non-active power contains all the information related to electric power with no-energy exchange; in other words, non-active power is related to all power quality disturbances except active harmonic powers. However, each power theory treatment of this amount can be

slightly different. This means that the first three requirements mentioned above are satisfied by each power theory in different ways; in fact, the results of each approach could change. Nevertheless, all the results obtained from each method can be helpful depending on the context and the objectives of the analysis in progress. At this point, it is worth mentioning that all power quality disturbances are not necessarily undesirable; some of them, like fundamental reactive power, are inherent to some equipment in the network and even necessary for the normal functioning of such equipment [GP17].

3.2. Power Theories Based on Fryze's Approach

This chapter is focused only on Fryze's approach. This school started with a time-domain power theory proposed by S. Fryze [Fry32], extended to multiconductor systems by F. Buchholz [Buc50], and generalized for nonsinusoidal systems by M. Depenbrock [Dep93] (FBD power theory) and L. Czarnecki [Cza88] (Current's Physical Components power theory). P. Tenti developed an additional improvement to Fryze's approach [Ten04] and aimed to describe nonactive powers in terms of conservative variables (Conservative power theory).

In Fryze's approach, it is assumed the existence of a fictitious equivalent conductance (Eq 3-8):

$$G = \frac{P}{U^2} \tag{3-8}$$

This quantity is suitable for modeling the active power flow from the voltage source to the loads, as shown in Fig. **3-2**. However, note that G not only represents the demanded fundamental active power, but it also represents the active harmonic power produced by the presence of voltage distortion, then, the quantity:

$$i_a(t) = Gu(t) = \frac{P}{U^2}u(t) \tag{3-9}$$

Known as active current, it forms along with the PCC voltage, the active power of the load. Since active power represents the energy exchange, all active harmonic components flow in the same direction as the fundamental component since energy generation is only possible in the power source [PTSS10b]. It means that the effects of voltage distortion in traditional distribution systems are reflected in the active current component. Thus, the following statements remain true for any distribution system:

- Active current, as defined in 3-9, can only flow from the power sources to the loads, given that loads cannot generate energy.

- It is possible that power sources share active current components. However, the active fundamental component always flows from power sources to loads.

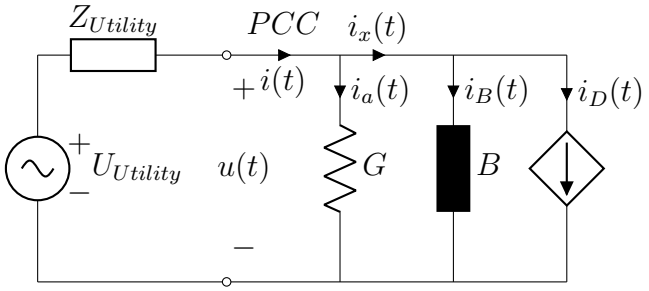

Figure 3-1: Extended Fryze's approach.

On the other hand, a decomposition over *non-active current* $i_x(t)$ is performed, splitting it into two orthogonal components represented in Fig. **3-1** by the susceptance B and the current source D. The definitions of B and D differ for each power theory mentioned; these variables and the associated powers can be interpreted differently. The equations of FBD power theory (FBD), Conservative power theory (CPT), and Current's Physical Components power theory (CPC) will be described below.

3.2.1. FBD Power Theory (FBD)

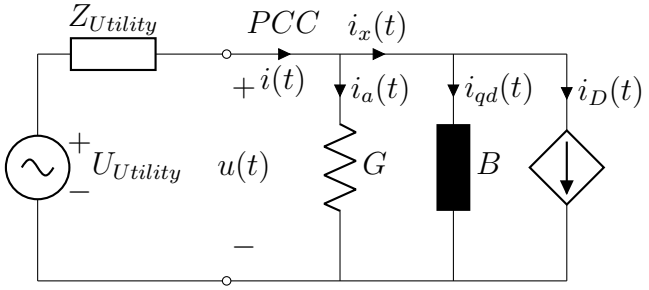

Figure 3-2: FBD Power Theory

In this power theory (Fig. **3-2** *displaced voltage* $u_d(t)$ is defined as the voltage of the source displaced a quarter of period ($u_d(t) = u(T - T/4)$). This definition allows to calculate the *displaced power*:

$$Q_d = \frac{1}{T}\int_{\tau}^{\tau\ +T} i_x(t)u_d(t)dt \tag{3-10}$$

Where the nonactive current is calculated as $i_x(t) = i(t) - i_a(t)$. Then, it is possible to define a *displaced current* $i_{qd}(t)$, associated with phase displacement, as:

$$i_{qd}(t) = Bu_d(t) = \frac{Q_d}{U^2}u_d(t) \tag{3-11}$$

Note that the voltage used as a reference for i_{qd} calculation has the same waveform of $u(t)$, which means that displaced current contains information related to phase displacement even in non-fundamental frequencies. Thus, voltage distortion is also reflected in the displaced current.

Finally, the *Distorted current* $i_D(t)$ is associated with waveform distortion unrelated to active and displaced components.

$$i_D(t) = i(t) - i_a(t) - i_{qd}(t) \tag{3-12}$$

In this chapter, the phase unbalance is neglected. However, a detailed description of the FBD decomposition process for single-phase and multi-phase systems is presented in [PTSS12b].

3.2.2. Conservative Power Theory (CPT)

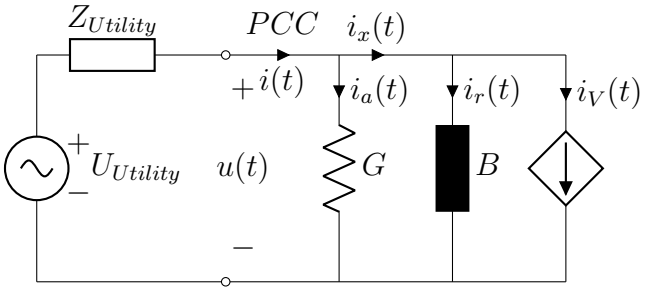

Figure 3-3: Conservative power theory approach

This theory resembles FBD (Fig. **3-3**). The main difference is the voltage reference to decompose $i_x(t)$. In this way, a quantity called *unbiased voltage* is defined as:

$$\hat{u}(t) = \int_0^t u(\tau)(d\tau) - \frac{1}{T}\int_0^T u(t)dt \tag{3-13}$$

Where the mean value of $u(t)$ is used as an unbiased estimator, note that the second term of 3-13 is zero without the DC level. On the other hand, the first term displaces the voltage a quarter of the period, as FBD, using the time-variable τ as a mathematical ploy to get the unbiased voltage as a function of t, avoiding the constant term resulting from

an indefinite integral. However, the difference in the mathematical procedure gives different results between FBD and CPT.

Let's suppose a system with voltage distortion and a negligibly DC level such that:

$$u(t) = \sqrt{2}\sum_{h=1}^{H} U_h \sin(h\omega_1 t + \alpha_h) \tag{3-14}$$

Then, the unbiased integral of $u(t)$ would be:

$$\hat{u}(t) = \int_0^t u(\tau)(d\tau) = \sqrt{2}\sum_{h=1}^{H} -\frac{U_h}{h\omega_1}\cos(h\omega_1 t + \alpha_h) \tag{3-15}$$

In fact, the voltage was displaced a quarter of the period. However, each harmonic component is divided by its frequency. This implies that the higher the harmonic order, the lower its impact on $\hat{u}(t)$. Even in a system without voltage distortion, $\hat{u}(t)$ is ω_1 times lower than $u(t)$. This filtering to displaced harmonic components matches the widely accepted criteria that reactive power is only defined for the fundamental frequency [IEE10a]. Figure **3-4** shows the displaced and unbiased voltages calculated from a measure from a system implemented in the lab. The voltage signal at the PCC has a flat-top waveform, which is the typical waveform seen in distribution systems [YM15].

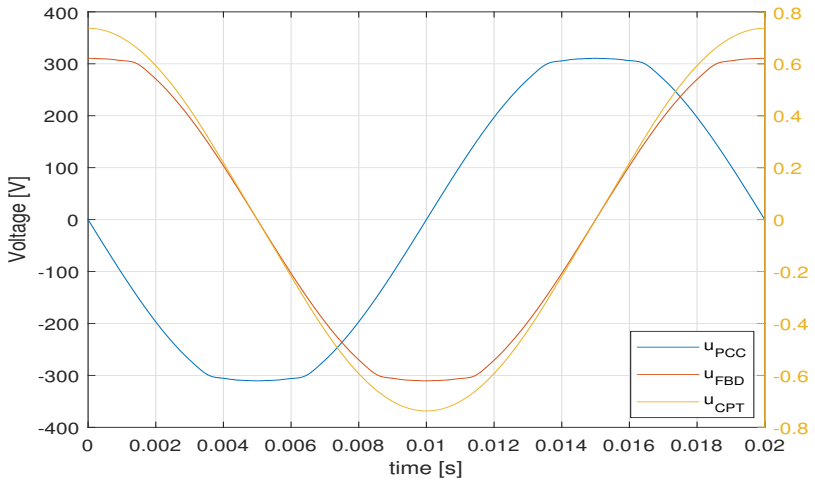

Figure 3-4: Displaced voltage (u_{FBD}) and unbiased voltage (u_{CPT}) were calculated from u_{PCC} measured. Note that u_{CPT} is 340 times smaller than the other voltages.

As mentioned, $u(t)$ and $u_d(t)$ have the same waveform but displaced 1/4 of a period. Otherwise, $\hat{u}(t)$ is almost sinusoidal, confirming that unbiased integral tends to reduce the harmonic voltage components with a phase displacement.

Nevertheless, from $\hat{u}(t)$ the quantity W is calculated and it is related to the presence of reactive power in the system:

$$W = \frac{1}{T}\int_{\tau}^{\tau+T} i(t)\hat{u}(t)dt \tag{3-16}$$

which in turn defines the *reactive current* i_r similar to FBD.

$$i_r(t) = B\hat{u}(t) = \frac{W}{\hat{U}^2}\hat{u}(t) \tag{3-17}$$

Finally, the *void current* $i_V(t)$ is defined as shown in Eq. 3-18. This component is associated with current distortion non-related to voltage, meaning that no harmonic of $i_V(t)$ should match the harmonics of $u(t)$.

$$i_V(t) = i(t) - i_a(t) - i_r(t) \tag{3-18}$$

An important advantage of this approach that shares with FBD is that W is a conservative quantity derived from a linear decomposition, which implies the accomplishment of Tellegen's Theorem [PSD70], a generalization of Kirchhoff Laws. In addition, CPT clearly describes reactive power usage in the system.

3.2.3. Current's Physical Components Power Theory (CPC)

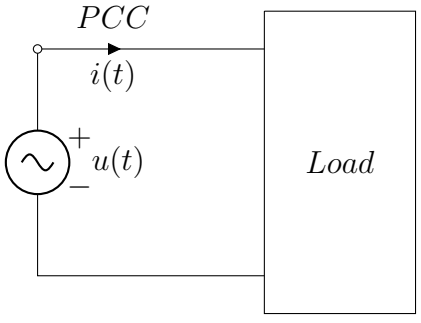

Figure 3-5: CPC Power theory

This power theory was developed from a hybrid time-domain and frequency-domain approach. The load depicted in Fig. **3-5** is modeled using the admittance Y in the frequency domain such that:

$$Y_h = G_h + jB_h \tag{3-19}$$

Y_h is not a theoretical admittance and has to be measured, which implies an additional challenge for the measurement campaign and data processing.

As the other power theories presented above, the active power is defined from the supposition of the conductance (G) presented in equation 3-8. In this way, the *active current* can be calculated as:

$$i_a(t) = Gu(t) = \sqrt{2}Re\sum_{h=1}^{H} GU_h e^{jhw_1 t} \tag{3-20}$$

Then, the *non-active current* is calculated as:

$$i(t) - i_a(t) = \sqrt{2}Re\sum_{h=1}^{H} (G_h + jB_h - G)U_h e^{jhw_1 t} \tag{3-21}$$

In turn, this quantity can be decomposed into two new currents called *reactive current* i_r and *scattered current* i_s:

$$i_r(t) = \sqrt{2}Re\sum_{h=1}^{H} jB_h U_h e^{jhw_1 t} \tag{3-22}$$

$$i_s(t) = \sqrt{2}Re\sum_{h=2}^{H} (G_h - G)U_h e^{jhw_1 t} \tag{3-23}$$

As the active current, these quantities can be rewritten as:

$$i_r(t) = \sqrt{2}\sum_{h=1}^{H} -B_h U_h sin(hw_1 t) \tag{3-24}$$

$$i_s(t) = \sqrt{2}\sum_{h=2}^{H} (G_h - G)U_h cos(hw_1 t) \tag{3-25}$$

Note that $i_r(t)$ contains phase displacement information in the frequency spectrum. On the other hand, $i_s(t)$ contains information related to harmonic components produced by the difference between a reference active power (calculated by means G) and the active harmonic components present in the system, represented by G_h. Despite CPC being well thought out in terms of circuit theory, the amount and quality of information needed for calculation could eventually lead to misinterpretations or mathematical errors; in other words, CPC

application could not be pretty practical in real systems. A detailed process description is presented in [Cza08].

3.3. Study Case and Comparison Among Power Theories

A microgrid was implemented in the Power Quality Laboratory of the Institute of Electric Power Systems and High Voltage Engineering (IEEH) of the TUD Dresden University of Technology, as shown in Fig. **3-6**. This system explores the advantages and disadvantages of the previously presented power theories. It is also used to test some methods of harmonic contribution assessment [KBG+21].

3.3.1. Measurement Setup

The system comprises 1 PV inverter, 1 Battery converter, and several household loads connected considerably away from the voltage source using a standard 20 m cable (Fig. **3-6**). The following subsections describe each of the components in more detail.

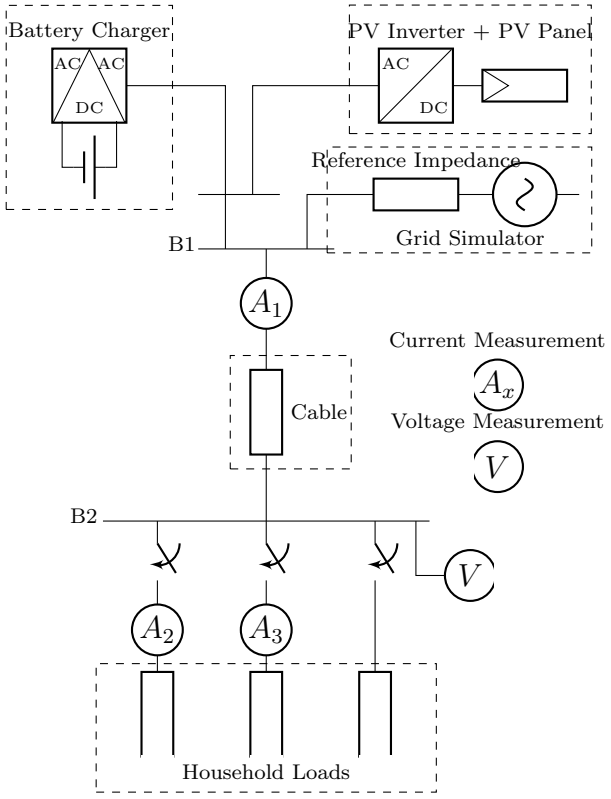

Figure 3-6: General scheme of the system implemented in Lab.

3.3.1.1. PV Inverter

The PV Inverter is an SMA Sunny Boy 5000TL. The characteristics of the PV are summarized in table **3-1**. This equipment is fed using a PV-Simulator, which can simulate the power generated by the solar panels. The PV-simulator can be programmed to give any desired active power [KBG+21].

Table 3-1: Characteristics of the sources

	PV Inverter	**Battery Converter**
Manufacturer	SMA Solar Technology AG	SMA
Product name	Inverter Sunny Boy 5000TL	Battery-Inverter Sunny Island
Model number	SB 5000TL-21	SI3.0M-11
$P_{out-nom}$	4600 W	2300 W
$S_{out-nom}$	5000 VA	
U_{AC-nom}	230 V	
$I_{out-nom}$	20 A	10 A
f	50/60 Hz	$45 - 65$ Hz

3.3.1.2. Battery Converter

The Battery converter is an SMA Sunny Island. The technical characteristics of the device are summarized in table **3-1**. A programmable DC-voltage source was connected to the DC side of the battery converter instead of genuine batteries to guarantee a flexible operation during the measurements.

3.3.1.3. Household Loads

Three types of household appliances with different electronic topologies were selected for the measurements: linear load (Linear), non-linear loads composed of single-phase switch mode power supplies with active power factor correction (APFC), and non-linear loads without power factor corrector (NPFC). Only loads with a constant operating mode or that can be fixed to have a continuous power demand were selected. Table **3-2** lists the household appliances and their rated powers.

Table 3-2: Characteristics of the household loads

Appliances	**Available Devices**	**Topology and Rated Power per Device [W]**		
		Linear	**NPFC**	**APFC**
Water heater	2	2000		
Desktop computer	2			100
Laptop	2		100	
Incandescent lamps	2	60		
CFL ≤ 25 W			400	
CFL > 25 W				100
Total Available Load		4120	600	300

3.3.1.4. Measurement Device

The Dewetron 2600 with HIS-HV and HIS-LV modules was used for the measurements as shown in Fig. **3-6**. The voltage is measured directly with the modules Dewe HIS-HV, and the currents are measured using zero-flux transducers connected to the Dewe HIS-LV modules. The ratio of the transducers is 1:600 with a maximum current of $60A$ and bandwidth of $800kHz$. The voltage and the currents were measured for 10 s per load scenario at a sample rate of 1 MS/s following the procedure presented in subsection 3.3.2. The voltage uncertainty is in the range of [1 % - 15 %] $\pm$ 7 mV for [1 – 0.06 V] as the input range for the frequency range of interest. Similarly, for the current measurement, the uncertainty lies in the range of [1 % - 15 %] in magnitude and [0 - 20^o] in phase angle for [1000 – 2 mA] as the input. More information on the measurement device can be found in [KBG$^+$21].

3.3.2. Measurement Procedure

Two connection modes were tested: islanded (ISM) and interconnected (ICM). In ISM, the PV inverter and the battery converter supply power to the busbar B1. In this mode, the battery converter operates as a voltage reference for the PV inverter. However, note that if the network impedance is much lower than the load impedance, the load can influence the voltage waveform. A complete analysis of the impact of harmonic impedance over voltage and current harmonics can be found in [KBG$^+$21]. In ICM, the battery converter and the

PV are disconnected, and a grid simulator feeds the loads. Finally, different combinations of loads were connected to different power generation. Table **3-3** summarizes the apparent powers of the performed tests. Note that the combination of loads emulates different harmonic pollution scenarios. The linear load is a non-polluting case, the non-power factor correction load (NPFC) represents the high pollution case, and the MIX load, composed of a combination of all appliances available, is an intermediate pollution scenario. Finally, active power factor correction load (APFC) represents a case where a compensation scheme is introduced in the system.

Table 3-3: Summary of apparent powers for each test

	ISM [VA]			**ICM [VA]**
	Battery	**PV**	**Load**	**Bus bar**
NPFC	599.94	535.29	794.70	1061.22
APFC	339.18	0.53	338.65	336.41
Linear	1030.62	1174.50	2204.84	2143.82
MIX	2128.11	1188.49	3257.11	3174.35

3.3.3. Impedance Characteristic of the Load Scenarios

The impedance characteristic for each loading scenario was measured over node B2 using a discrete frequency sweep. Currents with frequencies close to the harmonics were injected into the system, and the resulting voltage and the currents injected were computed to calculate the impedance characteristic. A more detailed description of the process and an analysis of the harmonic impedance and its impact on harmonic emission on the microgrid implemented in Fig. **3-6** can be found in [KBG+21].

3.3.4. Results

3.3.4.1. RMS Values and Scale Factor

The four scenarios were performed, and the original quantities were scaled using as reference the RMS value of the total current measured over each element as follows. From equations presented in section 3.2.1, it is possible to say that:

$$\begin{aligned} i(t) &= i_a(t) + i_{qd}(t) + i_D(t) \\ i(t) &= i_a(t) + i_r(t) + i_V(t) \\ i(t) &= i_a(t) + i_r(t) + i_s(t) \end{aligned} \tag{3-26}$$

Given that FBD, CPT, and CPC currents are orthogonal quantities, 3-26 can be rewritten in terms of RMS values as:

$$\begin{aligned} I^2 &= I_a^2 + I_{qd}^2 + I_D^2 \\ I^2 &= I_a^2 + I_r^2 + i_V^2 \\ I^2 &= I_a^2 + I_r^2 + I_s^2 \end{aligned} \tag{3-27}$$

Then, the quantities derived from 3-27 represent the size of each current component depending on the total RMS current measured in the PCC. These quantities allow the comparison between the different load scenarios:

$$\begin{aligned} 1 &= \frac{I_a^2}{I^2} + \frac{I_{qd}^2}{I^2} + \frac{I_D^2}{I^2} \\ 1 &= \frac{I_a^2}{I^2} + \frac{I_r^2}{I^2} + \frac{i_V^2}{I^2} \\ 1 &= \frac{I_a^2}{I^2} + \frac{I_r^2}{I^2} + \frac{I_s^2}{I^2} \end{aligned} \tag{3-28}$$

Note that equation 3-28 can also be used as an estimator of the error as follows:

$$e_{FBD} = \left| 1 - \frac{I_a^2}{I^2} + \frac{I_{qd}^2}{I^2} + \frac{I_D^2}{I^2} \right| \tag{3-29}$$

Table **3-4** shows the RMS scaled currents and errors calculated for each loading scenario in ISM and ICM. The first thing worth mentioning is that the higher the distorted current (distortion) in the system, the higher the error in the three power theories. This fact can be explained by noise in high harmonic pollution scenarios and numerical calculation issues. Errors for FBD and CPT are very low, and FBD has the highest performance. On the other hand, errors in CPC make evident the issues associated with the information requirements for this power theory implementation, like impedance measurement itself and the impossibility of making such measurements simultaneously with the voltage and current, situations that could derive misleading conclusions.

Another important thing is that the current components of FBD and CPT are very similar. As it was discussed in section3.2, the difference between these two theories lies in the definition of phase displacement, actually, in the absence of voltage distortion $i_r = i_{qd}$ and $i_V = i_D$. On the other hand, in the absence of phase displacement, $i_r = i_{qd} = 0$ and $i_V = i_D$.

Table 3-4: RMS values of the current components using the total current as the scale factor.

Load	**NPFC**		**APFC**		**MIX**		**LINEAR**	
Source	**ICM**	**ISM**	**ICM**	**ISM**	**ICM**	**ISM**	**ICM**	**ISM**
U	228,525	233,791	229,738	230,815	217,452	226,854	221,317	227,790
I	4,602	3,391	1,460	1,103	13,837	14,088	9,328	9,560
I_a	2,855	2,640	1,400	0,982	13,446	13,771	9,326	9,560
I_a/I	0,385	0,606	0,920	0,792	0,944	0,956	1,000	1,000
I_{qd}/I	0,085	0,010	0,059	0,155	0,008	0,003	0,000	0,000
I_D/I	0,530	0,384	0,021	0,053	0,047	0,042	0,000	0,000
e_{FBD}	0,001 %	0,000 %	0,001 %	0,004 %	0,000 %	0,000 %	0,000 %	0,000 %
I_r/I	0,085	0,004	0,061	0,152	0,014	0,002	0,000	0,000
i_V/I	0,535	0,393	0,023	0,054	0,049	0,041	0,000	0,000
e_{CPT}	0,516 %	0,235 %	0,399 %	0,197 %	0,715 %	0,206 %	0,003 %	0,001 %
I_r/I	0,047	0,042	0,042	0,023	0,000	0,000	0,000	0,000
I_s/I	0,841	0,009	0,218	0,073	0,000	0,001	0,001	0,000
e_{CPC}	49,336 %	60,200 %	5,126 %	1,603 %	0,002 %	0,027 %	0,44 %	0,56 %

3.3.4.2. Linear Load Scenario

As is shown in table **3-4**, there is an match among the three power theories for the Linear load scenario. This is a trivial result given that active power is calculated similarly and an important presence of other power quality phenomena is not expected. Figure **3-7** shows the current components associated with each power quality phenomenon analyzed using each theory. Once again, it is clear that, for definition, active current is an image of the voltage waveform, no matter the calculus method used, as it was explained in section 3.1. Figure **3-7** also shows the current components associated with phase displacement and distortion. Here are some remarks about it:

- **Phase Displacement in ISM:** The waveform is quite similar calculated by the three power theories and, in the absence of voltage distortion, can be considered a displaced image of the voltage waveform.
- **Distortion in ISM:** The signals follow a pattern. However, its magnitude is too small to be considered an issue, as shown in Table **3-4**.
- **Phase Displacement in ICM:** FBD and CPC are higher than CPT, given the voltage distortion. Here, the definition of phase displacement for FBD and CPC includes all displaced harmonic components. Otherwise, CPT includes in the definition only the fundamental harmonic component.

- **Distortion in ICM:** In contrast with phase displacement, the void current of CPT is higher than the distorted current of FBD. This is due to void current containing all frequency components that do not have a voltage reference but also frequency components with a displaced voltage reference.

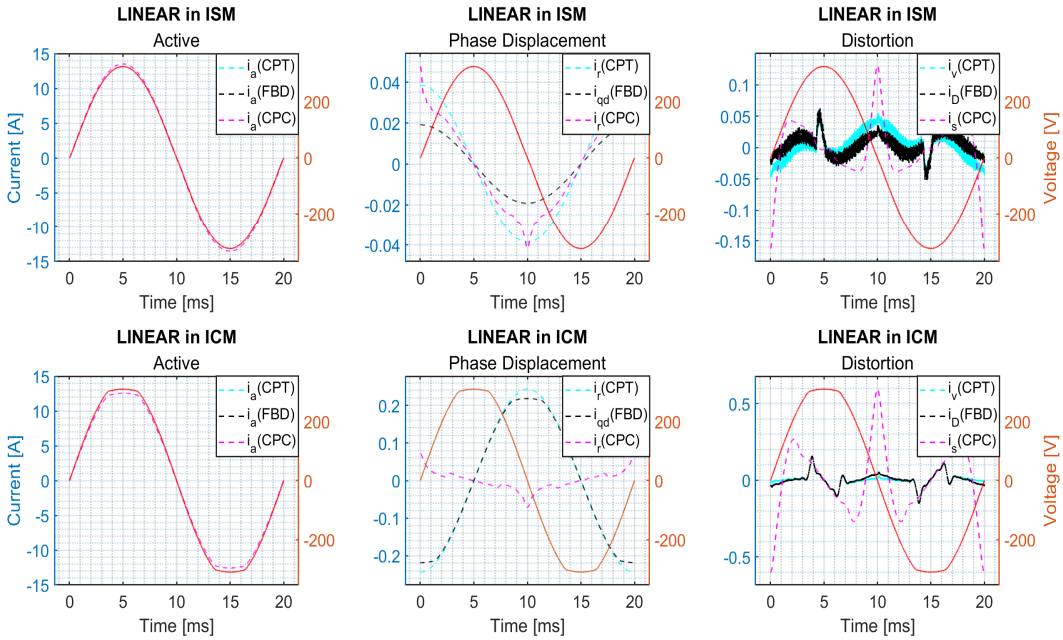

Figure 3-7: Current decomposition for the Linear scenario in both operation modes. The voltage was plotted in red as a visual reference.

3.3.4.3. MIX Load

The load for this scenario is composed of the NPFC load (700 W), the linear load (2000 W), and the APFC load (300 W). Then, a high distortion is expected, given the 1 kW of non-linear load composition. However, as also seen in table **3-2**, linear appliances in the experiment constitute the main part of the MIX. Therefore, this scenario's distorted current (also void and scattered currents) is very low compared to the total load, as seen in Table **3-4**. Because of the load composition, in this scenario, the results are similar to the Linear load scenario. In this way, previous remarks can be extrapolated to this scenario.

3.3.4.4. Non-linear Load (NPFC)

From table **3-4**, it is possible to see that CPC results are unreliable in the presence of distortion. On the other hand, in Fig. **3-8**, it is possible to see that FBD and CPT currents

match very well, given that there is a low phase displacement compared to the total current. Here are some remarks about it:

- **Phase Displacement in ISM:** In this case, the i_r and i_{qd} signals differ in shape since, as discussed before, the displaced current calculated using the FBD takes the form of the voltage waveform, while the reactive current calculated using the CPT takes the form of the fundamental component. However, the magnitudes of these two quantities are similar, as can be seen in Table **3-4**. This is not only because the phase displacement in the system is slight but also because the distortion in the voltage is not high enough for a significant difference between i_r and i_{qd}.
- **Distortion in ISM:** Since the phase displacement is low compared to the total signal size (1 %), there is a good fit between i_D and i_V.
- **Phase Displacement in ICM:** The voltage waveform is similar to the fundamental one; therefore, i_r and i_{qd} are almost identical as shown in Table **3-4**.
- **Distortion in ICM:** Although the phase displacement is high, as is the distortion, I_D and I_V are almost equal since the voltage distortion is low.

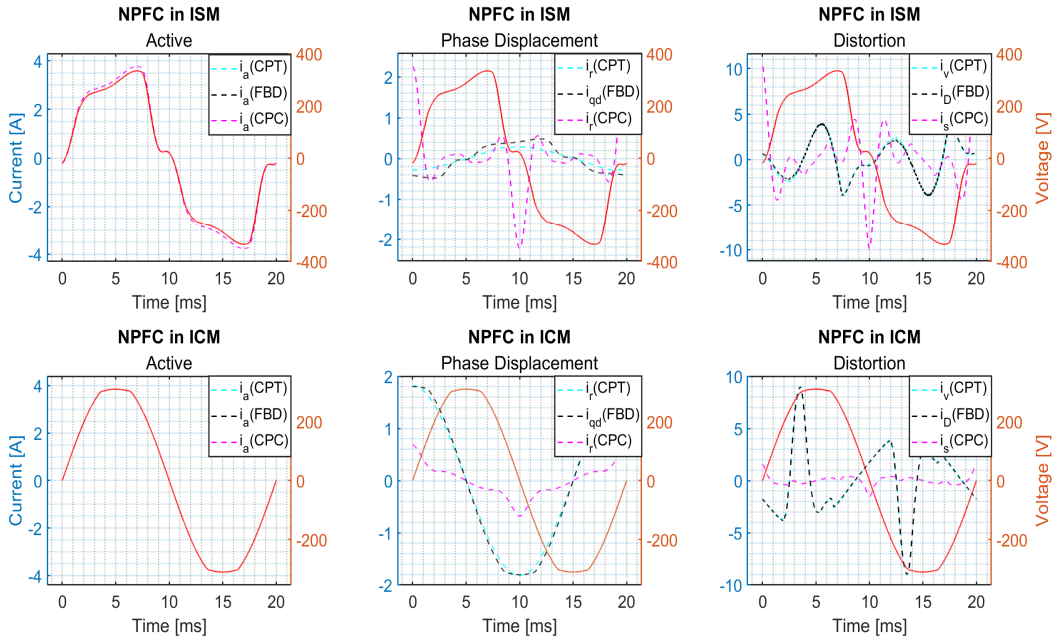

Figure 3-8: Current decomposition for NPFC scenario in both operation modes. The voltage was plotted in red as a visual reference.

3.3.4.5. Non-linear Load with compensation scheme (APFC)

The calculation results of this scenario are similar to the previous case. However, it could be more interesting, both in this scenario and in the others, to analyze the changes in the current components according to the type of load and source, as will be seen in the next section.

3.4. Power Quality Phenomena Assessment From FBD and CPT Power Theories

Up to this point, it is clear that CPC has no reliable results in high-distortion scenarios. In addition, some issues associated with information acquisition, like the impossibility of making impedance measurements simultaneously with the voltage and current, can lead to wrong conclusions. On the other hand, FBD and CPT present similar (or even equal) results in some particular conditions, namely: 1. Low voltage distortion, 2. Low phase displacement. As was already mentioned, the difference lies in the phase displacement definition. FBD gives a broader description of this phenomenon, including the fundamental displaced component and all displaced harmonic currents. CPT excludes such displaced harmonic, approaching the reactive power definition. Figure **3-9** shows the scaled RMS value of I_{qd} and I_r. In all load scenarios, the current is almost the same. However, I_{qd} is slightly higher for the reasons previously exposed. The highest difference can be found in the NPFC load scenario, given that this has the higher distortion.

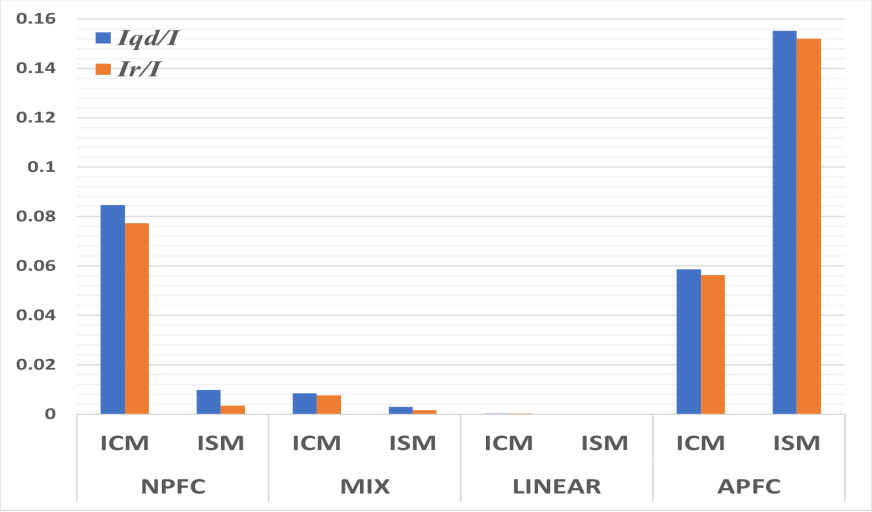

Figure 3-9: RMS scaled values of the current components I_{qd} and I_r calculated from CPT

In traditional power systems, namely, those with a high short-circuit ratio, voltage dis-

tortion is not a problem compared with the distortion caused by some non-linear loads. In other words, If the short-circuit ratio is high enough, the voltage waveform is stiff and barely influenced by the load. This way, CPT or FBD could be indifferent, given that the results should be almost identical. However, in nontraditional, novel and isolated power systems, like microgrids, the distortion caused by the loads can change the voltage waveform. As was already mentioned, the four load compositions implemented in the microgrid emulate different distortion conditions in the system. In addition, the interconnection mode simulates the two possible scenarios in a system; ICM represents a robust network whose voltage waveform can hardly be disturbed by the load. In addition, the network has a characteristic voltage distortion, as shown in Fig. **3-7**. Otherwise, ISM represents a weak network that the load can easily disturb. In addition, the inverter voltage output is usually a perfectly sinusoidal waveform (Fig. **3-7**).

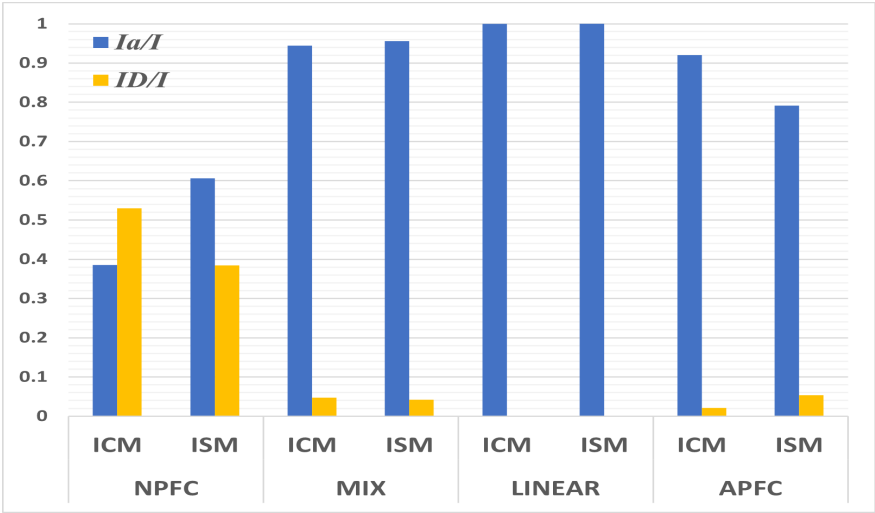

Figure 3-10: RMS scaled values of the current components I_a and I_D

Figure **3-10** shows the RMS scaled values of I_a and I_D. In the linear load scenario, it is clear that almost all power delivered from source to load is active, even in the presence of voltage distortion (ICM), I_D is not an issue for the system. The same conclusion applies to the MIX load scenario; a distorted current is less than 5 % of the total current. In addition, the difference in distortion between ICM and ISM is barely observable. In the NPFC load scenario, the situation is entirely different. In ICM, there is a high distortion, and less than the 40 % of the current delivered is active. However, it is worth highlighting the following:

- Given that the network is strong, and consequently, the load cannot modify the voltage waveform, it is possible to say that the load causes the distorted current.
- As mentioned, the active current contains the effect of voltage distortion. On the other hand, the active component can only flow from source to load. In this way, the source is

responsible for the active current component, including the voltage distortion reflected on it.

- Weakness or strength of the network, regarding short circuit ratio and circuit topology (structure) affects the interaction of agents and, consequently, the responsibilities to be assigned for the existence of undesirable power quality disturbances and conditions.

These highlights give it the key to asses responsibilities in strong networks (traditional distribution systems), namely: *The network is responsible for the active distortion and the load is responsible for non-active distortion.* Table **3-5** shows the contribution of the network and the load to the total current measured in the PCC. I_D is the same value shown in table **3-4**. On the other hand, $I_{Background}$ was extracted from the active current using a Fast Fourier Transform. In these cases, it is possible to say that the main contributor (or main responsible) is the load.

Table 3-5: Contribution of the Network ($I_{Background}$) and the load (I_D) to the Waveform Distortion in ICM.

Type of Load	**NPFC**	**APFC**
$I_{Background}$	0,04 %	0,09 %
I_D	53,03 %	2,11 %

This rule can be practical but valuable only in traditional and strong networks. In ISM, there is a highly distorted current and an even higher active current that also contains voltage distortion, as seen in Fig. **3-8**. However, as was already mentioned, the voltage waveform was set as a perfect sinusoid. This means that the load has modified the voltage waveform, causing the appearance of voltage distortion. Differences between FBD current components in ICM and ISM sum zero. This fact explains the increase in the active current compared to the ICM. In other words, a part of the distorted current is converted into the active current, more precisely in voltage distortion. Finally, it is possible to say that the load is responsible for the active and non-active distortion as long as the voltage waveform before the connection of the load is known. Table **3-6** shows the voltage distortion reflected on I_a and the distorted current I_D in the percentage of the total current measured on the PCC. As mentioned, the load is responsible for active and non-active distortion in these cases.

Table 3-6: Contribution of the Load to the Waveform Distortion in ISM.

Type of Load	**NPFC**	**APFC**
$I_{Background}$	1,89 %	0,71 %
I_D	38,41 %	5,31 %

3.5. Chapter Summary

In this chapter, FBD, CPT, and CPC power theories were reviewed and tested in a system implemented in the laboratory. The decomposition of current that each of them proposes was used to assess waveform distortion contribution on the PCC, and some conclusions were derived from this exercise:

- The three power theories have a plausible mathematical development. However, the simplicity of FBD makes it easy to understand and implement. On the other hand, CPC is more complicated, and its implementation requires harmonic impedance measurement.
- An indicator to calculate errors in the power theories was applied. The results of FBD and CPT were similar, while CPC results were unreliable in this exercise, particularly in scenarios with high waveform distortion.
- The current components derived from CPT and FBD are almost the same. As mentioned, the main difference lies in the reactive (CPT) and displaced (FBD) current components. However, there are two conditions under which the current components of these power theories should be equal: Low voltage distortion in the network and low reactive power in the system.
- Two types of networks were defined: strong and weak. Assessing waveform distortion contribution in strong networks is trivial, considering that the network is responsible for voltage distortion in the PCC, and the load is responsible for distorted (or void) current. However, assessing contributions in weak networks is more complex and requires knowing the voltage waveform before the loading.
- Under a hypothetical scenario with high distortion (or even distortion levels over the regulatory limit) and the possibility of changing the connection mode between the interconnected and the islanded, a part of the distorted (void) current generated in interconnected mode turns into active current (voltage distortion) in islanded mode. This implies that the load could be responsible for the distorted (void) current and a part of the active current in weak networks. Therefore, it is possible to state that the type of network partially influences the responsibility assigned to a load. In that sense, it is worth commenting that in a scenario of high distortion at the PCC due to the load connection in a weak network, it would not be possible to release the Utility from its responsibility, given that it is in charge of designing and operating said networks.

3.5.1. Contributions of this Chapter

This chapter describes the propagation dynamics of waveform distortion. In this way, the analyses of the two types of networks (strong and weak) show that in weak networks, part of the distorted current generated on the customer side is transformed into voltage distortion and, consequently, into active distortion when the load is connected. Therefore, knowing the voltage waveform at the PCC before interconnection is required to make a correct assignment of responsibilities. On the other hand, it is confirmed that the Utility is responsible for active distortion in strong networks or traditional distribution systems. At the same time, the Customer is responsible for non-active distortion.

4 Method of Disturbance Interaction From the Graph Theory Framework

In Chapter 2, the Method of Disturbance Interaction (MDI) was introduced as one of the existing proposals developed to assess stationary power quality disturbances. Its advantages are the ability to evaluate more than two agents simultaneously and the precision with which it divides them into two interaction groups (α and β), where the disturbance is concentrated [Pav12]. Then, consequently, MDI assigns them the same responsibility to both groups. An additional advantage of the MDI, not discussed in depth in Chapter 2, is the ability to discard agents that do not intervene in the development of the disturbance, that is, those that do not interact positively or negatively with the others (group *gamma*). This virtue was explored in more detail in [PG14], reinforcing the method using statistical techniques.

On the other hand, the main limitation of the MDI is that it cannot determine which of the two interaction groups linked in the development of the disturbance generates it (source) and which dissipates it (sink). It is clear that the cause of a disturbance understood as the set of conditions that facilitates the development of the disturbance and not only as the source, can be attributed to both groups since it needs both to appear in the system. However, without identifying sources and sinks, a complete view of the cause is unavailable, making the MDI an appropriate method to assess and quantify responsibility but not to determine causality.

The previously mentioned limitation of the MDI are addressed in [GP15] and [GP17], using basic graph theory analysis techniques such as centrality measures. Within these, a modification to the *Eigenvector Centrality Index* called *Laplacian Eigenvector Centrality* is developed and is presented as an alternative improvement to the MDI that allows not only a more efficient separation of the interaction groups but also determines the flow direction of all FBD current components using the active current flow as a reference. Next, the development of this improvement to the MDI will be presented, as well as its advantages and limitations, but first, some graph theory basics.

4.1. MDI and Its Interpretation in Graph Theory Context

Graph theory is a mathematical discipline that has boomed significantly since many applications have been successfully represented, modeled, and analyzed. Between these applications, we can find information, social networks, and electrical networks, among others. Many problems are being studied from a graph theoretical framework within these and other knowledge areas, significantly impacting the scientific field. From issues as complex and decisive for the development and preservation of life as the spread of epidemics to problems whose objective is only to make easy domestic tasks, such as the interaction between sensors, are some of the topics that are currently being studied. While it is true that this is a broad discipline in issues, this chapter only mentioned the most relevant aspects for developing power quality analysis methods.

In its simplest form, a graph represents a network or a complex system modeled from the interaction between interconnected agents. It can be defined as a collection of points called vertices joined by lines called edges [New18] **4-1**. Then, a random system is represented by the graph $G = (V, E)$ where V is the set of vertices and E the edges such that:

$$V = \{v_1, v_2 ... v_n\} \quad E = \{e_1, e_2 ... e_m\} \tag{4-1}$$

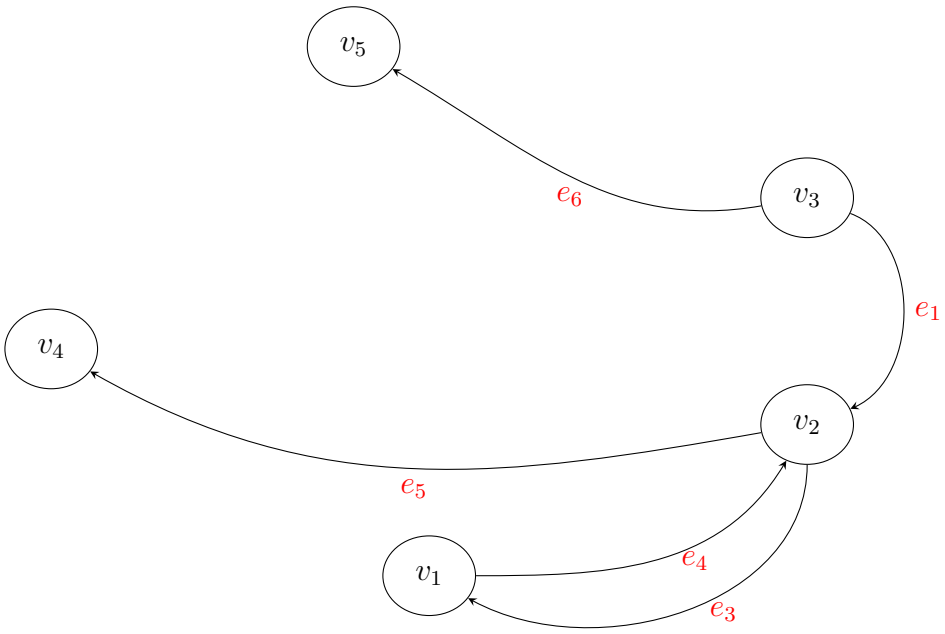

Figure 4-1: Graph Representation of a Random System

In general terms, a system is composed of two fundamental elements [New18]:

1. Dynamic units (Agents) are the system's actors endowed with the will and ability to communicate and interpret the environment.

2. Information Exchange Network (Network) is how agents communicate between them.

It is worth mentioning that, in the power quality context, the Dynamic Units are the devices connected to the system (loads and sources), and the Information Exchange Network can be understood as electrical current flux instead of information. This composition implies that a system can be analyzed from two approaches [New18]:

1. From the point of view of the Dynamic Units: It focuses on identifying the agent's behavior under different performance scenarios on the system.

2. From the point of view of the Exchange Network: It focuses on the interactions and their impact on the system performance.

The work presented in this chapter is based on the second approach. In the MDI context, V represents the devices, and the interaction matrices represent the Exchange Network for an FBD current component analyzed, as shown in Figure **4-2**. In this way, and taking into account that mathematically, there should be an interaction between each pair of agents, a system composed of n devices connected to the same PCC can be represented by a graph of n vertices and $m = \frac{1}{2}n(n-1)$ edges, which means that each agent is connected to the others, this kind of system is called *full information system*. Note that interactions could be different magnitudes. Then, a weighted graph $G_W = (V, E, W)$ is defined. In this representation, W is a vector containing the weights applied to each interaction represented by E and extracted from η in the MDI context. However, such weights can be any parameter helpful to analyze the system, for instance, the nominal current capacity, line length, or the current flowing through the lines.

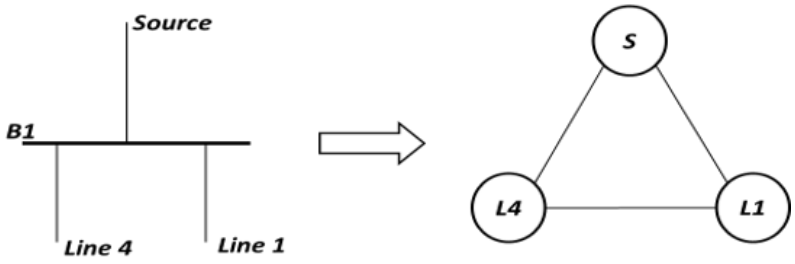

Figure 4-2: System Represented like a Graph

In some applications, event power systems, agents could be linked using directed interactions; power flux is an example. Digraph $D(G)$ is defined as a graph whose edges have a direction represented by arrows as shown in **4-1**. It is worth mentioning that such edges can also be bidirectional.

Finally, two more definitions could be helpful and will be used in this work: **Neighborhood** N_i is the set of agents directly connected to vertex i. For instance, refer to Figure **4-1** where the Neighborhood of the agent v_3 is composed of agents v_2 and v_5 such that $N_3 = \{2, 5\}$. In addition, a vertex's **Degree** is defined as the size of its Neighborhood; Thus, the Degree of v_2 is 4.

4.2. Graph and Matrices

As seen above, graphs represent the interactions between multiple agents linked to a system. Aimed at performing different analyses and taking an advance on the natural composition of graphs, multiple matrix representations have been developed and widely used. As mentioned in the previous section, electric power systems at any scale can be modeled using graphs. However, the way and variables used for the model determine the phenomenon to analyze. This section will explore some graph tools useful in some power quality assessments.

4.2.1. Degree Matrix and Disturbance Propagation

One of the most elementary representations is the *Degree Matrix*, a square array of zeros containing the Degree of each agent on its diagonal. Equation 4-2 shows the degree matrix of the system depicted in **4-1**.

$$\Delta(G) = \begin{bmatrix} d(v_1) & 0 & 0 & 0 & 0 \\ 0 & d(v_2) & 0 & 0 & 0 \\ 0 & 0 & d(v_3) & 0 & 0 \\ 0 & 0 & 0 & d(v_4) & 0 \\ 0 & 0 & 0 & 0 & d(v_5) \end{bmatrix} \tag{4-2}$$

$$\Delta(G) = \begin{bmatrix} 2 & 0 & 0 & 0 & 0 \\ 0 & 4 & 0 & 0 & 0 \\ 0 & 0 & 2 & 0 & 0 \\ 0 & 0 & 0 & 1 & 0 \\ 0 & 0 & 0 & 0 & 1 \end{bmatrix}$$

It is common to use the degree as an index of influence or importance of an agent. For instance, the most critical vertex in the figure **4-1** is the v_2. In that case, a disconnection of that vertex would isolate almost all the agents, spoiling network reliability. In this way, the higher the degree, the higher the influence. On the other hand, many vertex with high

degrees would result in a more liable network, guaranteeing the current flux through the system in case of any contingency, in other words, *ensuring the current propagation.*

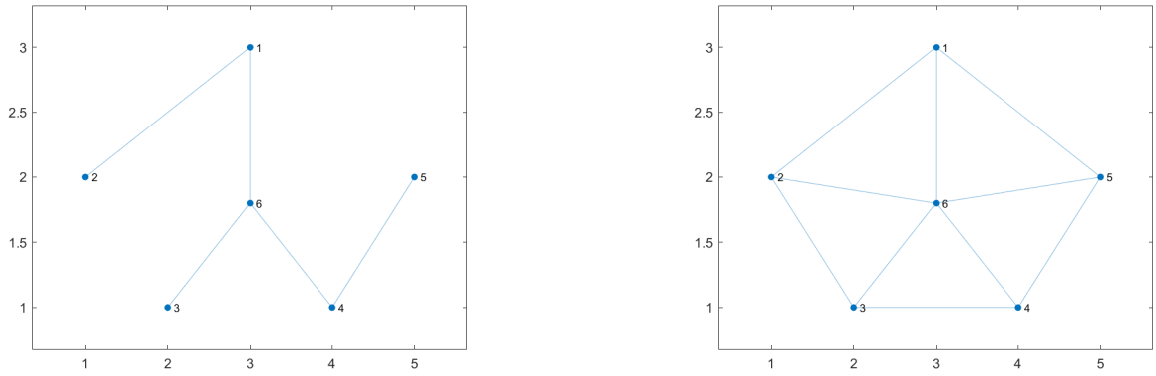

(a) Weakly interconnected graph

(b) Strongly interconnected graph

Figure 4-3: Graph representation of a random power system under different interconnection scenarios

Figure **4-3** shows the same system under two interconnection scenarios, scenario **4-3**a with a weak interconnection and **4-3**a representing a strong interconnection. It is easy to derive that the higher degree nodes, the easier the propagation. Consequently, the calculation of the trace of the degree matrix could be a good index of *propagation capability of a network.* However, it depends on the weights used for the model, as will be seen. The trace Tr is defined as the sum of the main diagonal of a square matrix, such that:

$$\begin{aligned} Tr(a) = \sum_{i=1} d(i) = 3+3+3+3+3+5 = 20 \\ Tr(b) = 2+1+1+2+1+3 = 10 \end{aligned} \tag{4-3}$$

Where $Tr(a)$ and $Tr(b)$ are the trace of the interconnection scenarios **4-3**a and **4-3**b respectively, to summarize, a strongly interconnected system makes easy the propagation and a simple indicator of this is Tr, the higher Tr the easier the propagation.

However, imagine a low-voltage system operating in weak and robust connection scenarios, as shown in **4-4** and **4-5**, respectively. Note that it is possible to use as weight the length of the lines, the impedance, or the current flowing through the lines. Whatever the case, the degree of a vertex i may be calculated as the weighted sum of the edges belonging i, such that:

$$d_w(i) = \sum_{j \subset N_i} e_{ij} w_{ij} \tag{4-4}$$

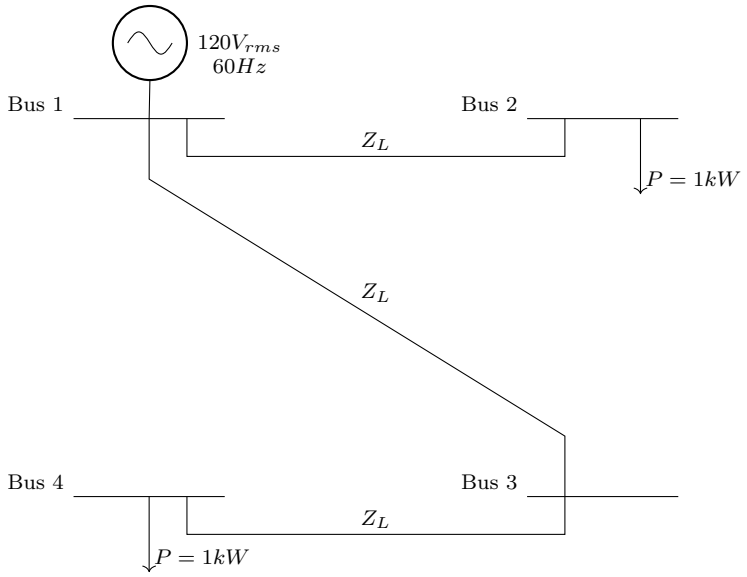

Figure 4-4: Low voltage system weakly connected. All lines have the same impedance $Z_L = 0{,}06 + 1 * 10^{-}6\ \Omega$, representing a typical low voltage distribution line.

Where w_{ij} is the weight of edge e_{ij} and j are the nodes that belong to the neighborhood of i.

Note that the variable used as weight defines the information extracted. For the case of power quality analysis, the use of line length could be irrelevant, but not the use of the line impedance. However, care must be taken when that variable is used, given that calculating $\Delta(G)$ as shown in 4-4 could lead to wrong interpretations. For a definition, the degree tries to identify the influence of a node in the network. However, $d_z(i)$ is just the neighborhood impedance as shown in Eq. 4-5 for the system depicted in Figure **4-4**, then, a better way to calculate the global impact could be to estimate the equivalent impedance of the network viewed from node i.

$$\Delta(G_{Z_L}) = \begin{bmatrix} 2Z_L & 0 & 0 & 0 \\ 0 & Z_L & 0 & 0 \\ 0 & 0 & 2Z_L & 0 \\ 0 & 0 & 0 & Z_L \end{bmatrix} \tag{4-5}$$

In that case, network impedance could be a kind of degree. Nevertheless, calculating the equivalent impedance at each node can be difficult. For this reason, it is reasonable to use currents instead of impedances as weights (Eq. 4-6).

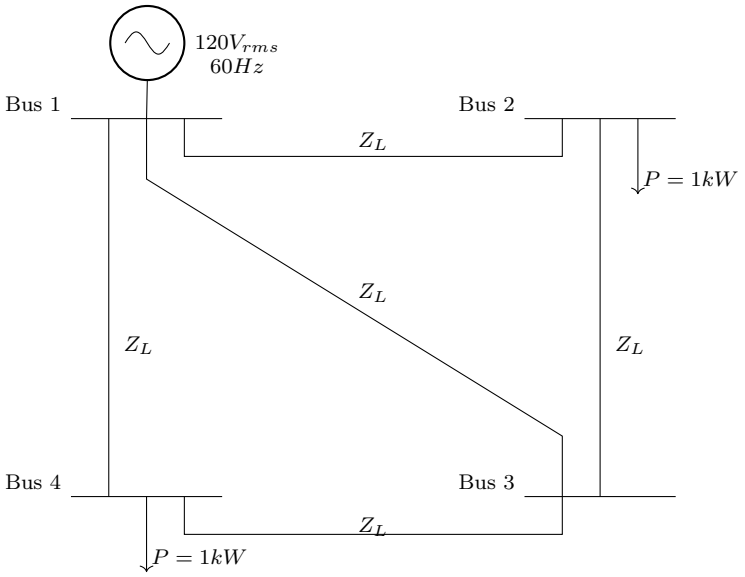

Figure 4-5: Low voltage system strongly connected. All lines have the same impedance $Z_L = 0{,}06 + 1 * 10^{-}6\ \Omega$, representing a typical low voltage distribution line.

$$\Delta(G_I) = \begin{bmatrix} -2I_L & 0 & 0 & 0 \\ 0 & I_L & 0 & 0 \\ 0 & 0 & 0 & 0 \\ 0 & 0 & 0 & I_L \end{bmatrix} \tag{4-6}$$

The sum of currents at each node must equal zero; however, by not including the current flowing to the loads or from the sources, $\Delta(G_w)$ would be just the equivalent currents entering or leaving each node. If a sign representing the direction of currents is assigned to the elements of $\Delta(G_w)$, the trace may be zero to accomplish Kirchhoff's current law. Note that without the direction in the currents, the degree matrix trace would not make sense regarding power balance, but it would make sense regarding system size. However, it must be considered that the size of the system in this approach refers to the total exchange of current in it but not to its infrastructure. This becomes evident in the fact that $\Delta(G_w)$ is the same for the systems of figures **4-4** and **4-5**.

In conclusion, we can say the following:

- The best way to calculate the degree matrix in the context of power quality is by using the currents between agents as weights. Estimating the directions of the currents is essential so that the trace complies with Kirchhoff's current law.
- When using signs to denote the direction of the currents, the trace of the degree matrix must be zero. Otherwise, the trace must be twice the total current exchange in the

system. This ultimately represents the size of the system in terms of its interactions.

4.2.2. Adjacency Matrix

The adjacency matrix is a symmetric array that represents the connections between vertices as follows:

$$[A(G)]_{ij} = \begin{cases} 1 & \text{if } v_i, v_j \in E \\ 0 & \text{any other case} \end{cases} \tag{4-7}$$

In other words, if there exists an edge between the vertices v_i, v_j, $A(G)$ takes a value of 1 in the positions (i, j) and (j, i). In this way, the matrix $A(G)$ for the systems presented in **4-4** and **4-5** are:

$$A(G) = \begin{bmatrix} 0 & 1 & 1 & 0 \\ 1 & 0 & 0 & 0 \\ 1 & 0 & 0 & 1 \\ 0 & 0 & 1 & 0 \end{bmatrix} \tag{4-8}$$

$$A(G) = \begin{bmatrix} 0 & 1 & 1 & 1 \\ 1 & 0 & 1 & 0 \\ 1 & 1 & 0 & 1 \\ 1 & 0 & 1 & 0 \end{bmatrix} \tag{4-9}$$

Unlike the degree matrix, the adjacency matrix provides information about the network's topology since it details the connections between the agents. However, these connections do not necessarily have to be physical, as seen with the degree matrix in the context of MDI, which can be the interactions extracted from the η matrix. This would imply that the lines where there is eventually no current flow would not be considered in constructing the matrix. In the same way, the connections through which low current values circulate would be represented by weak interconnections. Therefore, it is possible to define the so-called weighted adjacency matrix as $A_W(G) = (V, E, w)$, where w is the weight of the edges. Thus, $A_W(G)$ for the systems shown in figures **4-4** and **4-5**, using RMS currents as weights, would be:

$$A_W(G) = \begin{bmatrix} 0 & I & I & 0 \\ I & 0 & 0 & 0 \\ I & 0 & 0 & I \\ 0 & 0 & I & 0 \end{bmatrix} \tag{4-10}$$

$$A_W(G) = \begin{bmatrix} 0 & \frac{3}{4}I & \frac{2}{4}I & \frac{3}{4}I \\ \frac{3}{4}I & 0 & \frac{1}{4}I & 0 \\ \frac{2}{4}I & \frac{1}{4}I & 0 & \frac{1}{4}I \\ \frac{3}{4}I & 0 & \frac{1}{4}I & 0 \end{bmatrix} \tag{4-11}$$

While the degree matrix allows for identifying important nodes, the adjacency matrix identifies important connections. However, as explained in the previous section, these two things are related. Note that, with an adequate current ordering, the sum of each row (or column) of $A(G)$ must be equal in absolute value to the diagonal of $\Delta(G)$ accomplishing Kirchhoff's Law, as follows:

$$\Delta_W(G) + A_W(G) = 0 \tag{4-12}$$

4.2.3. Incidence Matrix

The two matrices seen above describe the importance of the nodes, the interconnections of the system, and, with them, the size of the system. Additionally, the sign assigned to the weights gave a notion of direction in the flow of interactions. However, with the use of the sign, it is not completely clear whether the currents enter or leave each node. The incidence matrix is an array of mxn that describes the m edges e_i of a digraph D composed by n nodes v_j such that:

$$[D(G^0)]_{ij} = \begin{cases} -1 & \text{if } v_j \text{ is the arrow tail} \\ 1 & \text{if } v_j \text{ is the arrow head} \\ 0 & \text{any other case} \end{cases} \tag{4-13}$$

Figures **4-6** and **4-7** show the system's current flux under the two interconnection scenarios. Likewise, equations 4-14 and 4-15 show the incidence matrix for each case. Here, it is evident that each matrix column can only be assigned one position with 1 and another -1. Although this information is enough to build all the system connections represented by a digraph, it is not enough to identify the size of the nodes, interactions, or the system per se.

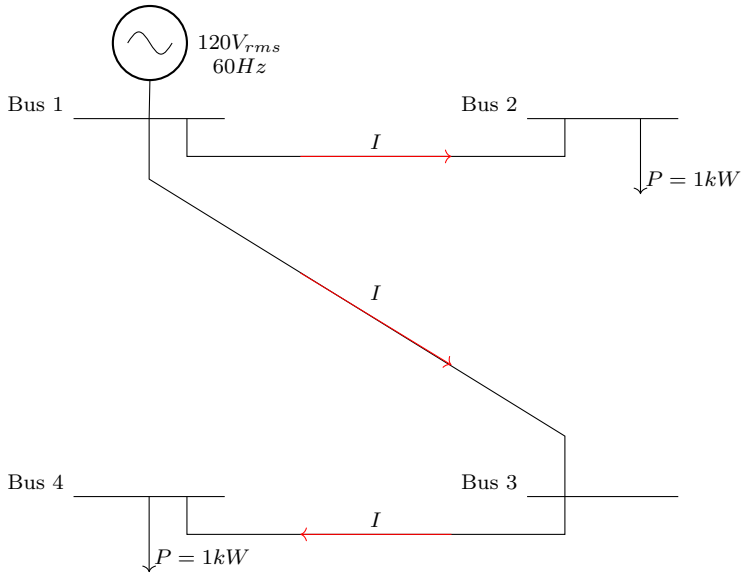

Figure 4-6: Current flow in the low voltage system weakly connected. $I = 4,17A_{RMS}$

$$\begin{array}{c} \\ Bus_1 \\ Bus_2 \\ Bus_3 \\ Bus_4 \end{array} \begin{array}{c} \begin{array}{ccc} L_{12} & L_{13} & L_{34} \end{array} \\ \begin{bmatrix} -1 & 1 & 0 \\ 1 & 0 & 0 \\ 0 & 1 & -1 \\ 0 & 0 & 1 \end{bmatrix} \end{array} = D(G^o) \tag{4-14}$$

$$\begin{array}{c} \\ Bus_1 \\ Bus_2 \\ Bus_3 \\ Bus_4 \end{array} \begin{array}{c} \begin{array}{ccccc} L_{12} & L_{13} & L_{34} & L_{14} & L_{23} \end{array} \\ \begin{bmatrix} -1 & 1 & 0 & -1 & 0 \\ 1 & 0 & 0 & 0 & 1 \\ 0 & 1 & -1 & 0 & -1 \\ 0 & 0 & 1 & 1 & 0 \end{bmatrix} \end{array} = D(G^o) \tag{4-15}$$

4.2.4. Laplacian Matrix

Up to this point, three different matrices help to identify the importance of the nodes, the size of the interactions, and the direction of the flows. In this section, a matrix representation will be seen that brings together all these qualities, thus allowing the development of different techniques for analyzing electrical systems, particularly power quality.

Laplacian Matrix is defined as the difference between Degree and Adjacency Matrices, such that:

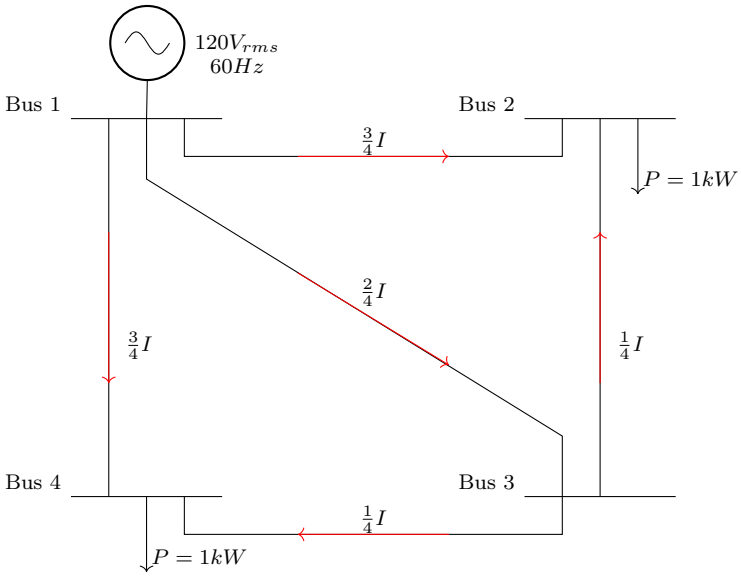

Figure 4-7: Current flow in the low voltage system strongly connected. $I = 4,17A_{RMS}$

$$L(G) = \Delta(G) - A(G) \tag{4-16}$$

This is more useful in many applications since it contains more information about the graph and directly presents the interactions between agents and their degrees. Equation 4-17 shows the Laplacian matrix of the system depicted in Figure **4-7**.

$$L(G) = \begin{bmatrix} 3 & 0 & 0 & 0 \\ 0 & 2 & 0 & 0 \\ 0 & 0 & 3 & 0 \\ 0 & 0 & 0 & 2 \end{bmatrix} - \begin{bmatrix} 0 & 1 & 1 & 1 \\ 1 & 0 & 1 & 0 \\ 1 & 1 & 0 & 1 \\ 1 & 0 & 1 & 0 \end{bmatrix} = \begin{bmatrix} 2 & -1 & -1 & -1 \\ -1 & 2 & -1 & 0 \\ -1 & -1 & 3 & -1 \\ -1 & 0 & -1 & 2 \end{bmatrix} \tag{4-17}$$

This representation was built just using the number of links, but weights can be used too, as shown in 4-18 shows the Laplacian matrix of the system presented in **4-7** using RMS currents as wights.

$$L(G_w) = \begin{bmatrix} 2 & 0 & 0 & 0 \\ 0 & 1 & 0 & 0 \\ 0 & 0 & 2 & 0 \\ 0 & 0 & 0 & 1 \end{bmatrix} - \begin{bmatrix} 0 & \frac{3}{4}I & \frac{2}{4}I & \frac{3}{4}I \\ \frac{3}{4}I & 0 & \frac{1}{4}I & 0 \\ \frac{2}{4}I & \frac{1}{4}I & 0 & \frac{1}{4}I \\ \frac{3}{4}I & 0 & \frac{1}{4}I & 0 \end{bmatrix} = \begin{bmatrix} 2 & -\frac{3}{4}I & -\frac{2}{4}I & -\frac{3}{4}I \\ -\frac{3}{4}I & 1 & -\frac{1}{4}I & 0 \\ -\frac{2}{4}I & -\frac{1}{4}I & 2 & -\frac{1}{4}I \\ -\frac{3}{4}I & 0 & -\frac{1}{4}I & 1 \end{bmatrix} \tag{4-18}$$

Note that the Laplacian matrix itself cannot give information about the direction of the interactions. Nevertheless, it is possible to define the Laplacian using the incidence matrix such that:

$$L(G) = D(G^0)D(G^0)^T \tag{4-19}$$

$$L(G) = D(G^0)WD(G^0)^T \tag{4-20}$$

This representation allows associating the interaction's direction with the Laplacian, giving a complete view of the system analyzed. In addition, the sum of each Laplacian matrix and weighted Laplacian matrix row (or column) is zero, accomplishing Tellegen's theorem for interconnected systems[PSD70].

4.2.5. MDI Interaction Matrix η in the Context of Graph Theory

In the Method of Disturbance Interaction presented in chapter 2, two groups are intuitively defined, α and β, to represent where the interaction is concentrated, but, as was already mentioned, it is not clear which group is the source of the analyzed disturbance. This means that in one of the two groups, be it α or β, all the sources should remain, while in the other, there would be all those agents that demand. The interaction groups are selected from the elements calculated in the η interaction matrix, defined as:

$$\eta = \begin{bmatrix} \langle i_{k_1}, i_{k_1} \rangle & \langle i_{k_1}, i_{k_2} \rangle & \langle i_{k_1}, i_{k_3} \rangle & \langle i_{k_1}, i_{k_4} \rangle \\ \langle i_{k_2}, i_{k_1} \rangle & \langle i_{k_2}, i_{k_2} \rangle & \langle i_{k_2}, i_{k_3} \rangle & \langle i_{k_2}, i_{k_4} \rangle \\ \langle i_{k_3}, i_{k_1} \rangle & \langle i_{k_3}, i_{k_2} \rangle & \langle i_{k_3}, i_{k_3} \rangle & \langle i_{k_3}, i_{k_4} \rangle \\ \langle i_{k_4}, i_{k_1} \rangle & \langle i_{k_4}, i_{k_2} \rangle & \langle i_{k_4}, i_{k_3} \rangle & \langle i_{k_4}, i_{k_4} \rangle \end{bmatrix} \tag{4-21}$$

Where i_{k_1} is the FBD current component k (active, non-active, displaced, or distorted) for agent 1. By definition, the square root of the inner product of a variable with itself is equal to the rms value of said variable such that:

$$I_1^2 = \langle i_1, i_1 \rangle \tag{4-22}$$

In which case, it is possible to state that the diagonal of the η matrix contains the squared rms value of the FBD current component that enters or leaves each agent [PTSS12a]. In other words, the diagonal contains information on the total contribution of each agent to the development of the analyzed disturbance. This information is directly associated with the

importance of each agent, or its degree, in terms of graph theory. In that sense, it is possible to say that the diagonal of the η matrix represents the same as the degree matrix, such that:

$$\Delta(\eta) = \begin{bmatrix} I_{k_1}^2 & 0 & 0 & 0 \\ 0 & I_{k_2}^2 & 0 & 0 \\ 0 & 0 & I_{k_3}^2 & 0 \\ 0 & 0 & 0 & I_{k_4}^2 \end{bmatrix} \tag{4-23}$$

On the other hand, interactions, which are also squared currents, represent the current exchange between each pair of agents. Thus, each value $\eta_{i,j}$ can be represented graphically as a weighted edge, as shown in Figure **4-2**. Thus, it is possible to say that the interactions calculated in the η matrix contain the same information usually recorded in the adjacency matrix. In this way, we have to:

$$A(\eta) = \begin{bmatrix} 0 & \langle i_{k_1}, i_{k_2} \rangle & \langle i_{k_1}, i_{k_3} \rangle & \langle i_{k_1}, i_{k_4} \rangle \\ \langle i_{k_2}, i_{k_1} \rangle & 0 & \langle i_{k_2}, i_{k_3} \rangle & \langle i_{k_2}, i_{k_4} \rangle \\ \langle i_{k_3}, i_{k_1} \rangle & \langle i_{k_3}, i_{k_2} \rangle & 0 & \langle i_{k_3}, i_{k_4} \rangle \\ \langle i_{k_4}, i_{k_1} \rangle & \langle i_{k_4}, i_{k_2} \rangle & \langle i_{k_4}, i_{k_3} \rangle & 0 \end{bmatrix} \tag{4-24}$$

Despite the above, it is impossible to affirm that the Laplacian matrix equals the eta matrix since not all inner products are negative. However, they have the same shape, and for this work, we will assume that $\eta = L$ under the next considerations:

- A graph must be defined for each FBD current component. In this way, the set of graphs G_k is defined such that G_a, G_x, G_{Qd}, and G_D, with a, x, Qd, and D being the active, non-active, displaced and distorted current components.
- Each agent is considered a homogeneous vertex of the graph. Consequently, all agents are equal, allowing them to analyze from the point of view of the interactions and not from the agents. This allows establishing a causality verdict even when the elements connected to each circuit are unknown, representing a significant advantage in logistical terms and eliminating possible biases in the analysis.
- There must be an interaction between all agents. Since all the agents are connected to the system through a PCC, there must be an edge for each pair of agents representing the interaction between them, resulting in a full information system.
- Each graph of G_k corresponds to a weighted graph, where the weights of the interactions are given by the interaction matrix η resulting from the MDI. In this way, the weight matrix $W_k = \eta_{ij} \forall i \neq j$ is defined.
- Given that the diagonal of the matrix η corresponds to the total rms current that each

agent supplies or receives from the system and that the sum of all the elements of any row of the same matrix is equal to zero, we can consider as the degree of each agent the total rms value supplied by it.

4.3. Laplacian Eigenvector Centrality

Laplacian Eigenvector Centrality (LEC) is a method derived from Eigenvector Centrality [MM10] that allows not only to identify the interaction groups quickly but also to define the source and the demand. Eigenvector Centrality (EC) is a centrality measure that seeks to determine the most critical agent based on the idea that one agent can be more critical than another if its neighbors have high degrees[New18] [Bon07]. In other words, an agent increases its importance if it interacts with other important agents.

In its canonical form, EC is written as the linear combination of the centralities of the neighborhood of an agent j (equation 4-25), Where x_i is the centrality of the analyzed agent, A_{ij} is the adjacency matrix and d_j is the degree of each agent in the neighborhood.

$$x_i = \sum_j A_{ij} d_j \tag{4-25}$$

Note that to achieve convergence of this equation from an initial estimate, it must be represented as a time series with t steps from 1 to ∞ as shown below in its matrix form.

$$x(t) = A^t x(0) \tag{4-26}$$

By rewriting $x(0)$ as the linear combination of the eigenvectors of A, Equation (4-26) becomes:

$$x(t) = A^t \sum_i c_i v_i = \sum_i c_i \lambda_i^t v_i = \lambda_1^t \sum_i c_i [\frac{\lambda_i}{\lambda_1}]^t v_i \tag{4-27}$$

Where λ_i are the eigenvalues of A. Note that when $t \to \infty$, $x \to c_i \lambda_1 v_i$ where λ_1 is the highest eigenvalues of A. In this way, it can be said that the centrality of the agent i is proportional to the eigenvector corresponding to the largest eigenvalue of the adjacency matrix, and therefore it holds that:

$$\mathbf{Ax} = \lambda_1 \mathbf{x} \tag{4-28}$$

An essential property of this method is that it can be applied to signed networks. In this way, it can divide the network into cliques (that can be α and β) and establish the centrality ranking of each clique [Bon07].

Although, indeed, the EC and the definition of the degree of an agent represent two valuable tools to evaluate the centrality or importance of an agent, understanding this in the context of power quality as its contribution to a disturbance, it is clear that its benefits do not represent anything different from what the MDI does on its own. Additionally, the application of these methods to a full information system such as the one described by η presents the following limitations:

- All elements of the system are interconnected. Therefore, the centrality would be equal.
- Definition of weights to mitigate the previous limitation. In other words, using the weighted adjacency matrix for the calculation, the results obtained would be the degree matrix.
- Calculating centrality from neighborhood influence excludes the influence inherent to the evaluated agent. This could lead to wrong conclusions when many *unimportant* agents were connected to a *high-ranking* agent.

However, it is possible to redefine the Equation (4-25) by replacing the matrix A of the system with the weighted Laplacian matrix L_W, resulting in the inclusion in the calculation of the importance inherent to each agent through the degree, in addition to the weight in the interactions. This modification would provide different degrees of importance for each agent and greater precision in the results. Note that the mathematical development to go from (4-25) to (4-28) would be the same for the matrix L_W, so that the resulting equation would be:

$$L\mathbf{x} = \lambda_1 \mathbf{x} \tag{4-29}$$

Then, the centrality of an agent in a full information system is proportional to the eigenvector corresponding to the largest eigenvalue of the Laplacian matrix with weights of the system L_W. This modification, called Laplacian Eigenvector Centrality (LEC), does not change the mathematical properties of the preceding method since L_W remains a symmetric matrix real and signed just like A. Therefore, the following very useful theorems remain valid:

- Any real nxn symmetric matrix has n linearly independent eigenvectors [Gro08].
- The real symmetric matrix eigenvectors corresponding to the different eigenvalues are orthogonal [Gro08].

- Let L_W be a real symmetric nxn matrix, then L_W has n orthonormal real eigenvectors [Gro08].

These properties, particularly the last one, guarantee that the centrality indices calculated with this method will be a set of normalized numbers. This makes more straightforward the analysis of the results and the procedure in general.

4.3.1. Application of LEC to a Simulated Distribution System

The MDI, including the improvement introduced by the LEC, was applied to the system presented in Figure **4-8**. This system, composed of a network equivalent and two loads connected by a PCC, is part of a more extensive distribution system implemented at the Power Quality Laboratory of the Institute of Electric Power Systems and High Voltage Engineering (IEEH) of the TUD Dresden University of Technology. Next, the most relevant characteristics of this system will be presented.

4.3.1.1. Grid Simulator and Reference Impedance Z_{Ref}

The S&S Voltage amplifier was used for the measurements as a grid simulator, given its ability to absorb power. The output was set as a flat top waveform at 230 V and 50 Hz. In addition, a flicker reference impedance (0.4 Ω + j0.25 Ω) was used to represent the main grid more realistically.

4.3.1.2. Loads

Each load comprises a mix of devices to simulate different harmonic pollution scenarios. Load composition was set as follows:

- Load 1: 193 W of No-PFC load and 174 W of linear load
- Load 2: 48 W of No-PFC load and 276 W of linear load

Note that both loads are comparable in magnitude to facilitate the analysis.

4.3.1.3. Measurement System

As in the system presented in Chapter 3, the Dewetron 2600 with HIS-HV and HIS-LV modules was used for the measurements. The voltage is measured directly with the modules Dewe HIS-HV, and the currents are measured using zero-flux transducers connected to the

Dewe HIS-LV modules. The ratio of the transducers is 1:600, with a maximum current of 60 A and a bandwidth of 800 kHz. The voltage and the currents were measured for 10 s per at a sample rate of 1 MS/s.

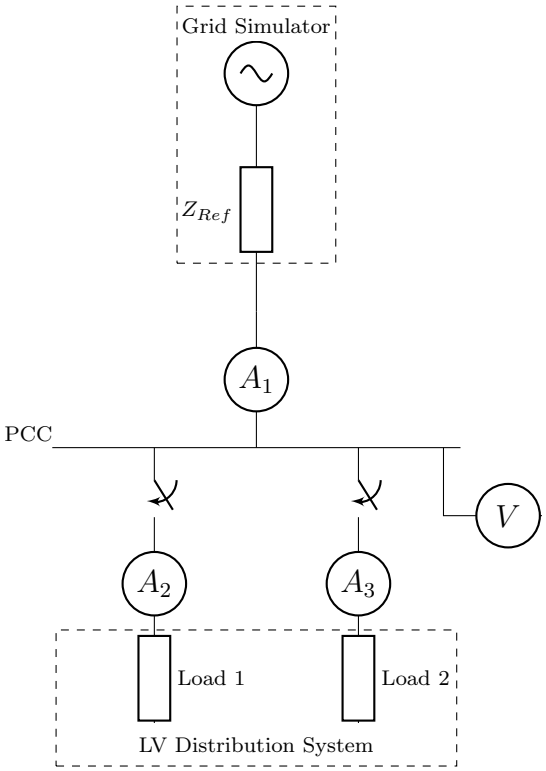

Figure 4-8: Measurement Setup

4.3.1.4. Results

The FBD current components were calculated as shown in Figure **4-9**. As was discussed in Chapter 3, the activated component has the same waveform as the voltage and, therefore, contains all of the active distortion in the system. On the other hand, ID represents the non-active distorted current.

From the current components, the interaction matrices were calculated for a single window of 200 ms, as shown in the equation 4-21. The matrices of active current η_a and distorted current η_D are shown in equations 4-30 and 4-31, respectively. The agents were ordered as network as agent 1, Load 1 as agent 2, and Load 2 as agent 3. In this way, $\eta(1,2)$ represents the interaction between the network and Load 1, $\eta(1,3)$ represents the interaction between the network and Load 2, and so on.

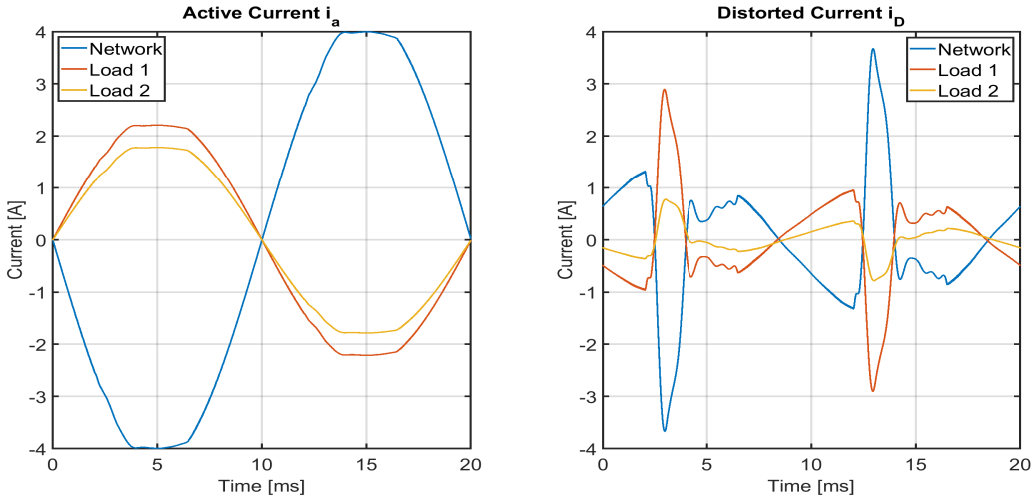

Figure 4-9: Active and Distorted Current Components Calculated from the Measurements

$$\eta_a = \begin{bmatrix} 8{,}7755 & -4{,}8572 & -3{,}9182 \\ -4{,}8572 & 2{,}6885 & 2{,}1687 \\ -3{,}9182 & 2{,}1687 & 1{,}7495 \end{bmatrix} \tag{4-30}$$

$$\eta_D = \begin{bmatrix} 1{,}4016 & -1{,}0723 & -0{,}3293 \\ -1{,}0723 & 0{,}8236 & 0{,}2488 \\ -0{,}3293 & 0{,}2488 & 0{,}0805 \end{bmatrix} \tag{4-31}$$

As mentioned above, we can evaluate which agents contribute most by directly taking the diagonal values of η. Furthermore, we can determine the groups α and β by observing the sign of the interactions. In the case of active current, it is clear that the agent that contributes the most is the network since it is the only one capable of generating energy. This is followed by loads 1 and 2 in that order, which agrees with the load composition. On the other hand, by observing the signs, it can be deduced that one of the interaction groups is composed of the network and the other of the loads since the interactions between charges are positive (the two agents interact against a third). In contrast, the interactions between the network and the loads are negative (both agents interact against each other).

This result may be trivial, but it illustrates the interpretation of the matrix η. In this way, we have that the performance of η_D is the same as that of η_a. The contribution is equally divided between the two interaction groups, the network on the one hand and the loads on the other. Note that, as in the previous case, the contribution of each load also corresponds to the composition, which highlights the effectiveness of the MDI for assessing responsibilities.

The results shown above only apply for a 200 ms window, implying that this analysis must be repeated for a more extended measurement campaign, such as a week, for each 200 ms

window recorded. Although it is true that, with good computing capacity, the entire process up to the calculation of η can be carried out without problems, separating the agents into interaction groups can be costly. This is where the LEC represents an improvement to the MDI. Taking η directly as the Laplacian matrix of the system, the highest eigenvalue and its associated eigenvector were calculated as shown in the equation 4-29. obtaining the results shown in Table **4-1**.

Table 4-1: Centrality index calculated by LEC

Agent	**Centrality** i_a $\lambda_1 = 13{,}2134$	**Centrality** i_D $\lambda_1 = 2{,}2999$
Network	-0.8149	-0.7806
Load 1	0.4511	0.5978
Load 2	0.3639	0.1828

In this result, the sign determines the interaction group directly. All the negatives belong to one group, and the positives belong to another. Thus, in both cases, the groups are formed as mentioned above, but they were determined in a more computationally efficient way. On the other hand, the magnitude of each eigenvector value represents the size of its contribution scaled based on the size of the system. From the equation 4-29:

$$\eta \mathbf{x} = \lambda_1 \mathbf{x} \tag{4-32}$$

Then, it is easy to demonstrate that:

$$x_i^2 = \frac{d(i)}{\lambda_1} \tag{4-33}$$

Where x_i is the $i_t h$ element of the eigenvector, $d(i)$ is the degree of the $i_t h$ agent, and λ_1 is the highest eigenvalue. By definition, in a real symmetric matrix, λ_1 is the Trace of such matrix such that:

$$\lambda_1 = Tr(\eta) = \sum_i d(i) \tag{4-34}$$

Then, the centrality can be alternatively calculated as:

$$x_i = \sqrt{\frac{d(i)}{Tr(\eta)}} \tag{4-35}$$

In this way, the result presented in the equation 4-35, which can be corroborated in Table

4-1, indicates that the normalized contribution of each agent is the degree of the agent divided by the size of the system.

Finally, to determine the nature or role of each interaction group in the development of the disturbance, it is enough to reference the centrality of the active current. In the case of the active current, the interaction groups comprised the network in the group that we will call α and the charges in the group that we will call β. In the group α, there is the only device capable of generating energy, in other words, the source. On the other hand, in the β group are the devices that demand said energy. However, even though the source supplies the active current component, we cannot say that it is the cause since it only responds to what determines the load. By applying the same group denomination for i_D, α the devices with negative centrality, and β the devices with positive centrality (as the active current component), the conclusion of the analysis for distortion would be the following:

- **Cause:** The presence of probably non-linear elements in loads 1 and 2.
- **Responsibility:** The responsibility lies with the group β with the participation of 0.5978 depending on the size of the disturbance in the system for load 1 and 0.1828 for load 2.
- **Source:** The source is estimated to be the α group, which is not the cause in this case.

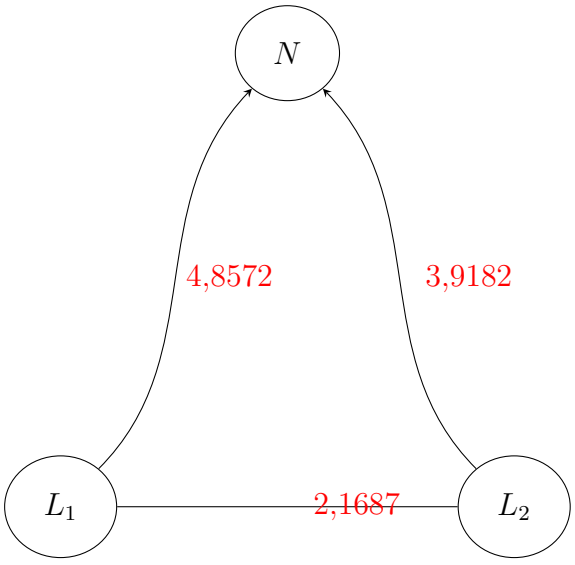

Figure 4-10: Graph of The System

To check the result, it is possible to use the equation 4-19. Considering that the cause is the group β, it is possible to represent the system as the graph shown in Figure **4-10**. In this scheme, positive interactions can be represented as an edge with two heads or two tails. In this way, the incidence matrix can be written as:

$$D_D = \begin{bmatrix} -1 & -1 & 0 \\ 1 & 0 & 1 \\ 0 & 1 & 1 \end{bmatrix} \tag{4-36}$$

Then:

$$D_D D_D^T = \begin{bmatrix} 2 & -1 & -1 \\ -1 & 2 & 1 \\ -1 & 1 & 2 \end{bmatrix} \tag{4-37}$$

Which corresponds to the weightless Laplacian of η_D.

4.4. Chapter Summary

This chapter addresses the Method of Disturbance Interaction from the graph theory perspective, and a study case was implemented and assessed for active and distorted FBD current components. Below are the most important points discussed:

- Due to its construction similar to that of the Laplacian matrix, the interaction matrix η allows different disturbances in the system to be modeled as a full information graph.
- The degree of an agent, recorded on the diagonal of η, represents the magnitude of its contribution to the development of the disturbance. In this way, it is possible to assess responsibilities from the direct observation of $d(i)$. However, it should be noted that this value is the square of the total effective current that passes through the feeder of such an agent, which limits the determination of its direction.
- The signs of the matrix elements η that result from calculating the interactions through inner products convert the system into a signed graph. This allows the development of indicators such as the LEC, which separates the agents into the interaction groups α and β, where the analyzed disturbance is concentrated.
- The largest eigenvalue of the interaction matrix λ_1 is associated with the size or magnitude of the disturbance in the system. This can be alternatively calculated as the trace of $Tr(\eta)$. This value additionally functions as a scaling factor to present the size of each agent's contribution to the disturbance or, in other words, its centrality.
- The eigenvector associated with λ_1 contains a collection of values related to each agent's centrality, interaction group, and nature. However, to determine this last characteristic in the non-activated current components, it is necessary to take the assessment in the

active current as a reference.

4.4.1. Contribution of this Chapter

In this Chapter, some tools from Graph theory are applied to power quality analysis. In this sense, the concepts of *Disturbance Size* and *Laplacian Eigenvector Centrality* are implemented as tools to calculate responsibilities and determine sources of disturbance in distribution systems.

5 Causality Assessment for Waveform Distortion Using Granger Causality and FBD Decomposition

This chapter addresses the problem of assessing causality in a system with waveform distortion through an innovative methodology in the context of power quality that mitigates the issues discussed in Chapter 1, Granger Causality. As in other works that address this problem, the system under study comprises a Point of Common Coupling (PCC) and various agents connected to it.

5.1. Causality and Granger Causality in the Context of Power Quality

In Chapter 1, Causality is defined as the set of conditions that govern the dynamics of a disturbance. However, as commented in Chapter 3, the dynamics of a disturbance can be influenced not only by the factor to which its appearance is attributed but also by factors inherent to the operation of the network, such as its impedance or use. This is how the connection and disconnection of devices with different electronic topologies, whether loads or power sources, convert networks into dynamic systems modeled through time series with often unpredictable behaviors. This makes some analyses such as those presented in chapters 2 and 4 efficient for analyzing responsibilities and sources of disturbances, but not for analyzing Causality, since a result obtained in an off-peak hour of the system can be reliable at that time of day but not at night when the typology of the network and its use have changed.

Another drawback raised in Chapter 1 is related to the fact that it is impossible to identify a single direction of causality when the relationship between the variables is strictly contemporary [Bas65]. This problem was addressed in Chapter 4 using graph theory, reaching the conclusion that it is necessary to incorporate additional information into the analysis; for example, the Laplacian Eigenvector Centrality Index organizes the interaction groups effec-

tively using time series or spot measurements but uses the direction of the active current source as a reference for the other current components. Thus, in specific scenarios, such as the connection of non-linear loads to weak networks analyzed in Chapter 3, the Laplacian Eigenvector Centrality provides reliable results regarding disturbance sources, but it leads to spurious conclusions if applied directly to evaluating Causality.

Given the above, the causality problem is addressed from a statistical point of view, using the well-known approach, but novel in this field, Granger Causality. This work combines Granger Causality with FBD power theory to find the cause of waveform distortion in a system composed of any number of agents connected to the same point of common coupling.

5.1.1. Granger Causality

Granger Causality is an assessment method that compares time series to establish the Cause of the other, but it is not based on the principle of temporality. Although the technique is better known as the Granger method, the idea was first proposed by Wiener [Wie56], and he described it as follows: *If the model of a time series can be improved by incorporating a second series, the latter has a causal influence on the former.* Note that this notion of Cause dispenses with the idea of displacement in time, allowing it to be applied to simultaneous time series (those that do not have a displacement between them). Although the idea made a lot of sense, Wiener did not have the mathematical and technical tools to implement it then, so 13 years later, Granger developed this proposal using linear regression models [Gra69]. In this context, Wiener-Granger Causality, or simply Granger, would be defined as follows:

Let A and B be two time series and let $\hat{A}^A$ be the autoregressive model (AR) of A and $\hat{A}_{AB}$ be the vector autoregressive model (VAR) of A using as inputs the past values of A and B such that:

$$\hat{A}_i^A = \alpha_0 + \sum_{j=1}^{lag} \alpha_j A_{i-j} + \epsilon_i^A \tag{5-1}$$

$$\hat{A}_i^{A,B} = \gamma_0 + \sum_{j=1}^{lag} \gamma_j A_{i-j} + \sum_{k=1}^{lag} \beta_k B_{i-k} + \epsilon_i^{A,B} \tag{5-2}$$

Where ϵ is the residual of each fitted value $\hat{A}_i$, lag is the number of past values of A and B taken into account to build the model, and α, β, and γ are constants optimized to reduce residual. *Then, if $\hat{A}_i^A$ has a worse fit than $\hat{A}_i^{A,B}$, B is said to explain A, and therefore, B causes A in the sense of Granger.*

In terms of GC, the mathematical expression of the previous definition would be:

$$\sigma^2(\epsilon^{A,B}) < \sigma^2(\epsilon^A) \tag{5-3}$$

Where $\sigma^2(\epsilon^A)$ is the variance of the optimized residuals for $\hat{A}^A$. In the same way, it can be verified that:

$$\sigma^2(\epsilon^{B,A}) < \sigma^2(\epsilon^B) \tag{5-4}$$

In this case, A is said to cause B in the Granger sense. In that order of ideas, when determining the relationships presented in 5-3 and 5-4, there would be three possible conclusions:

- If A causes B and B causes A: It is said there is feedback; both variables are explained (or affected) mutually.
- If A causes B and B does not cause A: A is an independent variable that explains B or helps explain it.
- If A does not cause B and B causes A: B is an independent variable that explains A or helps explain it.

The opposite case, i.e., $\sigma^2(\epsilon^{A,B}) > \sigma^2(\epsilon^A)$, is theoretically impossible. If B were not the cause of A, the coefficients β of the equation 5-2 would equal zero, in which case, $\alpha_j = \gamma_j$. Therefore:

$$\sigma^2(\epsilon^{A,B}) = \sigma^2(\epsilon^A) \tag{5-5}$$

Therefore, it is more accurate to say that B does not cause A if:

$$\sigma^2(\epsilon^{A,B}) \geq \sigma^2(\epsilon^A) \tag{5-6}$$

The previous result allows us to emphasize an essential fact of this method: GC determines unidirectional and bidirectional causality; that is, the results when evaluating the equations 5-3 and 5-4 are not the same, except if there is feedback. This is important since GC, being a statistical method, moves away from correlation and association analyses, which only makes it possible to determine whether the time series would eventually be linked. However, it has a disadvantage because it does not differentiate whether the time series belong to the same system and are cointegrated, sometimes determining spurious causalities. This implies that it is possible to compare two measurement records from two different electrical systems with the same characteristics and contrast that one is the cause of the other. For example, the current in two residential networks, but from different countries. This, of course, does not

imply a big problem in the case of power quality; an adequate measurement campaign is enough to reduce the risk of finding spurious causes.

5.1.2. Statistical Hypothesis Testing

One of the big questions that arise when applying GC is the following: When is $\sigma^2(\epsilon^{A,B})$ small enough to $\sigma^2(\epsilon^A)$ to consider that B causes A?. This is a question that not only applies to GC but to any statistical method, which is why the application of a hypothesis test is necessary. Since the widespread use of hypothesis tests, this work will not delve into its explanation. However, the four elementary steps of any hypothesis test will be discussed for this particular case.

5.1.2.1. Hypothesis Statement

Since we want to verify that the difference between $\sigma^2(\epsilon^{A,B})$ and $\sigma^2(\epsilon^A)$ is large enough to prove that B is or is not the cause of A, we can state as *Null Hypothesis* that all β_j values are zero. Therefore, the *Alternative Hypothesis* would be that at least one β_j value is different from zero, such that:

$$\begin{aligned} H_0 &: \beta_1 = \beta_2 = \beta_3 ... \beta_{lag} = 0 \\ H_1 &: \beta_1 \neq 0 \wedge \beta_2 \neq 0 ... \beta_{lag} \neq 0 \end{aligned} \tag{5-7}$$

5.1.2.2. Statistic Test

One way to test hypotheses is the F-test [Ham94]:

$$F = \frac{(RRSS - URSS)/P}{URSS/(N - 2P)} \tag{5-8}$$

Where P is the number of parameters β_j of the model, N is the length of the vector $\hat{A}$ or the number of model samples. Finally, $URSS$ and $RRSS$ are known as *Unrestricted Residual Square Sum* and *Restricted Residual Square Sum* respectively and are calculated as follows:

$$RRSS = \sum_{t=1}^{N} (\epsilon_t^A)^2 \tag{5-9}$$

$$URSS = \sum_{t=1}^{N} (\epsilon_t^{A,B})^2 \tag{5-10}$$

As can be deduced from the equations 5-9 and 5-10, the model $\hat{A}^A$ is known as the *Restricted Model*, while a $\hat{A}^{A,B}$ is known as *Unrestricted Model*.

5.1.2.3. Critical Value Calculation

Assuming that the time series $\hat{A}$ are stationary, which they are in the problem we are addressing in this work, we can state that the variances of their residuals would also be stationary. In this way, we have:

$$(\epsilon_t^A)^2, (\epsilon_t^{A,B})^2 \sim N(0, \sigma^2) \tag{5-11}$$

Therefore, the result of the equation 5-8 would follow a probability distribution $F_{P,N-2P}$. Assuming a significance level of 0.01 (the usual value in this type of test), we can calculate the distribution's critical value (CV) and compare it with the result of the F statistic. Another way consists of using the *p-values* of the F test and comparing it directly with the significance level.

5.1.2.4. Decision Rule

Finally, the rule consists of comparing if the result of F is greater or less than the critical value in such a way that:

- If $F > CV$, the difference between $\sigma^2(\epsilon^{A,B})$ and $\sigma^2(\epsilon^A)$ is large enough to consider that $\hat{A}^{A,B}$ has a better fit than $\hat{A}^A$. Therefore, B is indeed the cause of A.
- If $F < CV$, the difference between $\sigma^2(\epsilon^{A,B})$ and $\sigma^2(\epsilon^A)$ is not large enough. Therefore, $\hat{A}^{A,B}$ and $\hat{A}^A$ are considered to be equal, thus concluding that B is not the cause of A.

With the four steps discussed above, confirming or denying the results of 5-3 is possible. However, given the construction of the models and the optimization of the error, it is always possible to verify that the Unrestricted Model is better (or at least equal) to the Restricted Model, even in the presence of spurious variables. Therefore, when developing the method, it is mandatory to perform the test of hypotheses to confirm 5-3 or 5-4.

5.2. Causality Assessment over Multiple Agents Connected to the Same PCC

Until now, the possibility of comparing time series has been discussed, but the series per se has not been discussed. This work seeks to determine causal relationships between interconnected agents regarding stationary power quality disturbances. Three conditions are stationary in practice: phase displacement, unbalance, and waveform distortion. These conditions are inherent to the presence of certain elements in the system and, in fact, necessary for its proper functioning as discussed in [Gar16]. In this work, only waveform distortion will be addressed; therefore, it is necessary to separate this phenomenon from the previously mentioned. In this way, the FBD decomposition discussed in chapter 3 will extract the rms value of $i_D(t)$ for each integration interval and use them as a time series. In this work, the phase unbalance is neglected.

Next, the steps to evaluate the causality of waveform distortion in a system composed of multiple agents connected to the same PCC will be described:

1. Measurement: Although the method works with any time series, it is necessary to follow specific recommendations to guarantee the integrity of the results. Simultaneous measurement of the current and voltage signals in the time domain must be available in the feeders of each of the agents following the measurement interval consideration presented in [IEC15], one-week minimum assessment period for 10-minute samples of 10/12-cycle (10 cycles for 50 Hz and 12 cycles for 60 Hz). However, more than one week and a sampling frequency greater than 10 minutes are recommended for more accurate results.

2. Current decomposition using the FBD method: The second step consists of decomposing the registered currents for each agent using the FBD decomposition previously mentioned. This would result in three current 10/12-cycle signals $i_a(t)$, $i_{qd}(t)$ and $i_D(t)$ for each agent and each 10-minute value.

3. Construction of time series: Since we only want to assess the waveform distortion, the RMS value of the component $i_D(t)$ will be calculated for each 10-minute sample of 10/12-cycle and each agent. In this way, a time series will be obtained for each agent, comprising the RMS values of the distorted current with a resolution equivalent to 10 minutes.

4. Construction of autoregressive models of the time series: The AR model of each time series must be calculated as indicated by the equation 5-1. Additionally, VAR models must be computed using all possible pairs of agents as inputs. For example, in a system composed of agents A, B, and C, the VAR models $\hat{A}^{A,B}$, $\hat{A}^{A,C}$, $\hat{B}^{B,A}$, $\hat{B}^{B,C}$, $\hat{C}^{C,A}$,

and $\hat{C}^{C,B}$ must be calculated. Calculating models by hand can be time-consuming, so computational tools such as *R* or *Matlab* are recommended.

5. Comparison of models and hypothesis tests: Once the models have been built, the respective comparisons will be made as shown in the equations 5-3 and 5-4.

5.3. Study Case

GC was tested in a real system dependent on weather conditions to prove its efficiency and illustrate the correct interpretation of the results. Given that unbalance is out of the scope of this work, the system is assumed balanced, and in this study case, only one phase will be assessed.

5.3.1. Setup

Figure **5-1** shows an interconnected microgrid implemented in the Industrial Electrical Testing Laboratory of the Universidad Nacional de Colombia (LABE). This system comprises a PV array of LG photovoltaic panels of reference LG400N2W-A5 with a total installed power of 3 kW, connected to busbar B1 using APSystem micro inverters reference YC1000-3. A low voltage substation is also connected to bus B1, which has a 130 kVA, 440/220 V three-phase transformer connected to DY5. The load bus (B2) feeds office devices such as computers and LED lighting. The system frequency is 60 Hz. For the analysis, the substation will be called *Grid*, the PV array *PV*, and the loads *Load*

Two PSL-PQUBE class A power quality monitors were installed for 19 days at two places in the system, A_1 and A_2, as shown in Fig. **5-1**. Measurement equipment recorded the 12 cycles of current and voltage signals every 10 minutes with a sampling frequency of 128 spc (up to 64th harmonic).

5.3.1.1. Time Series and Models

Currents recorded were decomposed as explained in section 3, and the RMS values of the distorted current $i_D(t)$ were calculated, obtaining the time series shown in **5-2**. The Figure shows a clear high correlation between the three agents. However, it is necessary to complete the analysis to establish the cause, as was previously commented.

Using the time series shown in figure **5-2**, the AR model for each agent and the VAR models for the combination of two agents were calculated. The models were implemented

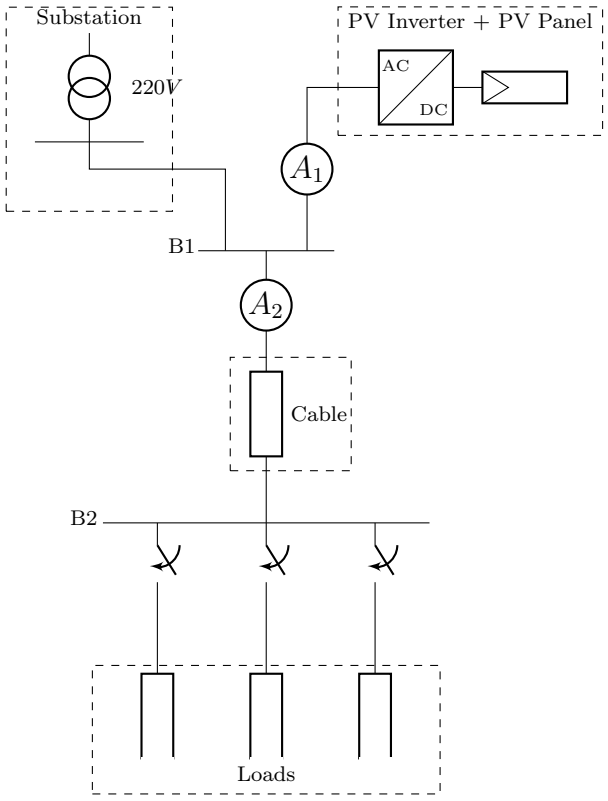

Figure 5-1: Real Interconnected Microgrid

using a lag vector [1 : 144] (one day), taking advance of the seasonality of the variables to improve the adjustment. Equation 5-12 shows the Lag Operator Representation of the model implemented.

$$(1 - \phi_1 L - \phi_2 L^2 - ... - \phi_{144} L^{144})\hat{A}_t = \epsilon_t \tag{5-12}$$

Where ϕ is the matrix of the coefficients γ, and β, ϵ is the error, and L is the Lag operator. This notation is equivalent to the notation of the equation 5-2.

At first glance, it is difficult to identify which model best approximates the original time series. However, the next section will show the results obtained from the F-test.

5.3.1.2. Results

F-test was performed, taking as reference the null and alternative hypotheses presented in 5-7. In this way, it is desirable to verify for every possible combination of agents that:

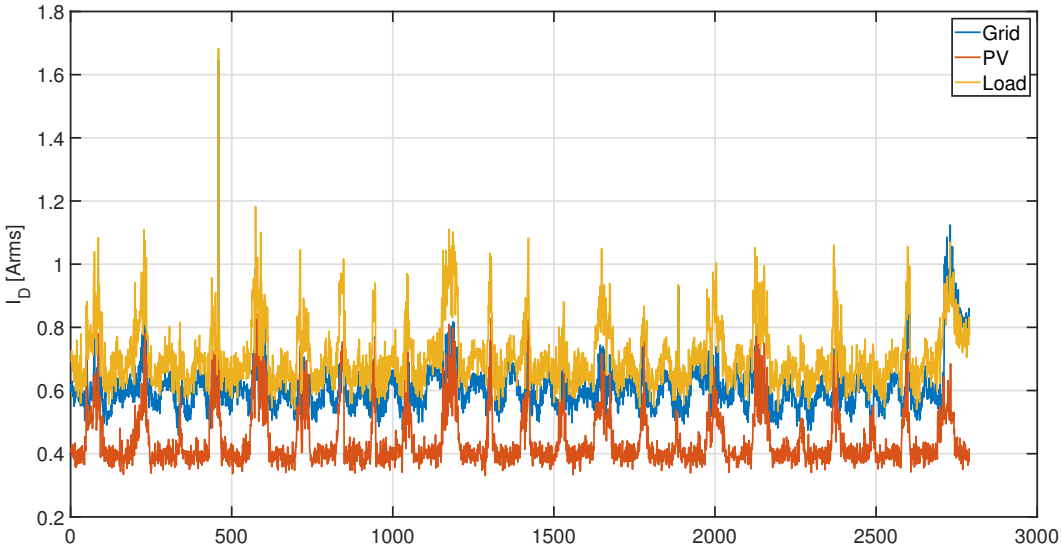

Figure 5-2: Time Series of the Distorted Current in the Agents

$$F = \frac{(RRSS - URSS)/144}{URSS/(2646 - 288)} < CV \tag{5-13}$$

$CV = 1,3065$ was extracted from the F probability distribution $F(144, 2646 - 288)$ with a significance level $\alpha = 0,01$. Then, the p-values were calculated from the f-rank for every test as shown in table **5-1**.

Table 5-1: GC for Distorted Current

Test	Probability	Conclusion
$Grid^{Grid,PV}$	1	$PV \rightarrow Grid$
$Grid^{Grid,Load}$	1	$Load \rightarrow Grid$
$PV^{PV,Grid}$	0.4879	$Grid \nrightarrow PV$
$PV^{PV,Load}$	0.9996	$Load \rightarrow PV$
$Load^{Load,Grid}$	0.1775	$Grid \nrightarrow Load$
$Load^{Load,PV}$	1	$PV \rightarrow Load$

5.3.2. Discussion

As mentioned above, the PV can only supply energy when there is sun, which makes the current components respond to the availability of the PV. On the other hand, the load

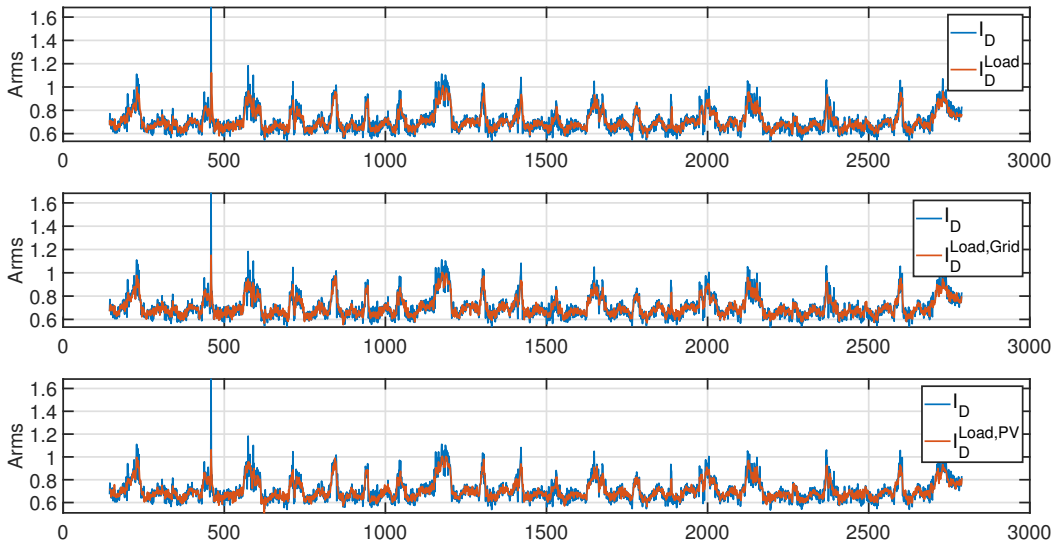

Figure 5-3: Models and Original Time series for Load

demands distorted current regardless of the operating conditions of the PV and the network; it only depends on the usage habits of the laboratory equipment. Finally, the network is always available and responds to the demands of the Load and availability of the PV.

In this order of ideas, unlike the MDI (LEC), GC does not determine the direction of the currents but rather the agent (or agents) that governs the dynamics of the disturbance. Figure **5-4** shows the centrality of agents to i_D as a function of time. It is possible to see that the interaction group α comprises Grid and PV, while the β contains Load. From this division, it is clear that no distorted current flows between the PV and Grid since they are in the same interaction group. However, we know that the PV can influence the behavior of the distorted current in the Grid, as can also be inferred from the evident evaluation between the centralities of Grid and PV.

5.4. Chapter Summary

This chapter proposes a methodology to assess causality in systems composed of multiple agents connected to the same PCC, which applies Granger Causality on a time series built from the RMS values of the current components obtained through FBD decomposition. The method was tested on a real system, getting the expected results.

Finally, from the perspective of GC and the proposed example, Cause is understood as the set of conditions that foster and govern the dynamics of a disturbance. This method is then

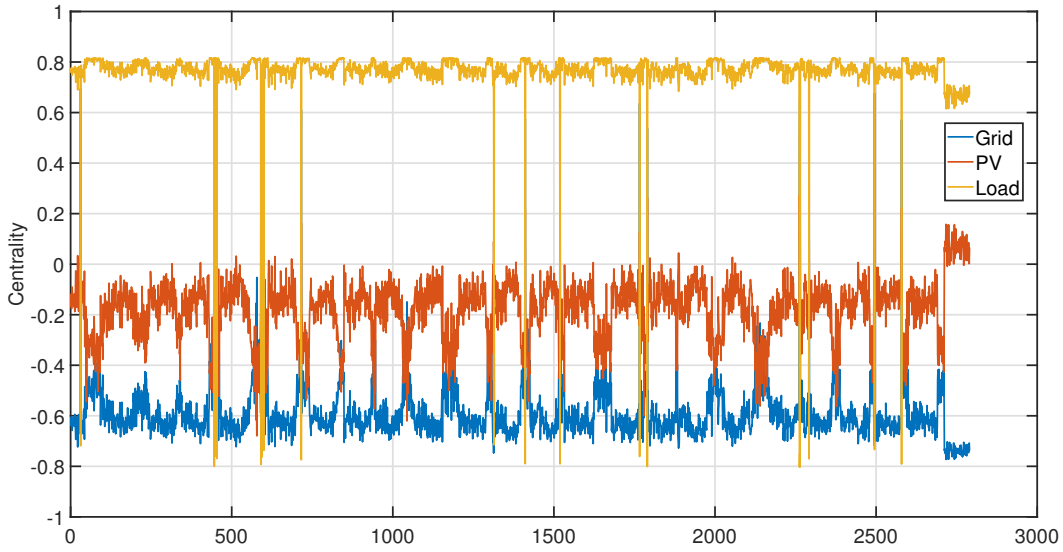

Figure 5-4: Centrality Calculated Using LEC

used as a complementary approach to the MDI (LEC), allowing them to identify sources, assign responsibilities, and evaluate causality in low-voltage distribution networks.

5.4.1. Contribution of this Chapter

This Chapter addresses the Causality problem from a novel perspective in the field of power quality, such as Granger Causality. Granger causality is applied under the premise that "the occurrence of the causes and effects of a power disturbance are appreciable simultaneously."With the application of the method, it is shown that the cause is associated with the set of conditions that govern the disturbance, such as the connection and disconnection of devices due to network use issues. Finally, the method is complementary to the MDI to determine responsibilities and sources of disturbance.

6 Conclusions and Future Work

As a result of the work developed in this thesis, some conclusions have been drawn, and motivation for future work has been proposed based on the findings discussed here.

6.1. Conclusions

1. In Chapter 1, the concepts of Cause, Source, and Responsibility were defined within the context of this work. The Source is the element (or elements) that supplies the analyzed current component. Responsibility is the contribution of each agent to the development of the disturbance, understanding agents as loads and power sources equally. Finally, Cause is defined as the set of conditions that govern the dynamics of the disturbance. In this way, Causality analysis was identified as an unsolved problem in power quality. Although it is true that several methods assign responsibilities or calculate the contributions of agents to the development of a disturbance, none of them can determine the role played by each agent, which reduces the analysis to the mere distribution of the disturbance among all potential participants as shown in Chapter 2.

2. In Chapter 2, some responsibility assignment methods were reviewed and compared through their application to a synthetic network that emulated a traditional distribution system or strong network. From the analysis, it was found that both the methods developed in the time domain and those developed in the frequency domain make the assignment in the same way; that is, they assign responsibility for the active harmonic current components to the network and for the non-active harmonic current components to the load. However, the difference in information requirements and signal processing means that the results differ, and in many cases, some of the methods lead to erroneous conclusions. On the other hand, From the analysis, it was possible to show that distorted current on the utility side of a strong network does not directly affect the judgment of the methods. Therefore, waveform distortion at the PCC is associated only with the background distortion and the distorted current i_D coming from the load. In this order of ideas, it is not reasonable to talk about a contribution of distorted current from the network or a contribution of voltage distortion from the load in traditional distribution systems or strong networks.

3. Chapter 3 analyzed the three main power theories developed from Fryze's postulates: CPT, CPC, and FBD. Within their capabilities, their usefulness was evaluated to analyze waveform distortion, finding in all of them the possibility of decomposing the current measured in the PCC to extract only the portion of the total current that is transformed into distortion. CPC theory is developed from an electrotechnical approach that defines non-active currents in the frequency domain as a function of the harmonic impedance of the load. This implies more complex measurement campaigns and slightly more time-consuming signal processing. On the other hand, FBD and CPT define non-active current based on the mathematical definition of disturbances, particularly phase displacement. Finally, remarkable similarity was found between FBD and CPT to the point that, under certain conditions, the results of the respective decomposition are the same. However, the definition of *displaced current* i_qd from the FBD theory also better explains the distortion phenomenon.

4. The case study in Chapter 3 allows determining how current components are usually distributed. It is concluded that, in robust networks such as traditional distribution systems or those in which the network impedance is much larger than the load impedance, the network is responsible for the distortion present in the active current component i_a, and the loads are responsible for the distorted current i_D. In contrast, weak networks such as microgrids have a more complex behavior since the distortion present in the active current component i_a is caused by the interaction between the power source and the non-linear loads, which, in turn, also modifies the distorted component i_D. In that sense, current international regulatory frameworks regarding power quality responsibilities must be reviewed to address the recent growth of distributed generation and power electronics in power systems.

5. Under a scenario of high distortion at the PCC due to the load connection in a weak network, it would be impossible to release the Utility from its responsibility, given that it is in charge of designing and operating said networks.

6. Chapter 4 explores graph theory as a valuable approach to assessing responsibilities. Notably, the MDI is interpreted from the graphics perspective, taking advantage of the mathematical development of the method. This allows not only the optimization of the technique but also the determination of the role of each agent (Source or Sink) through the development of the LEC centrality index. However, implementing the LEC shows that it is impossible to evaluate Causality using only the measurements taken at the PCC since the events analyzed in practice co-occur. Therefore, it is necessary to introduce additional criteria to determine the direction of Causality. In the case of the LEC, this criterion is to use the address of the active component as a reference for the others. However, this criterion can lead to erroneous conclusions in some scenarios, such as weak networks.

7. Granger Causality is proposed as a tool to assess causality in power quality, finding its effectiveness even in complex scenarios for analysis, such as the interconnected microgrid presented as a case study in Chapter 5. However, It is worth noting that this method exclusively evaluates causality, not responsibilities. It is also not able to find sources of distortion on the network. In that order of ideas, the complementary use of the LEC and GC constitutes a complete network analysis that can determine what should be taken to reduce the impact of waveform distortion on the system.

6.2. Future Work

- In this work, a mechanism that allows power quality problems to be evaluated accurately was found, addressing not only traditional electrical systems but also what constitutes their near future, microgrids and the inclusion of non-linear elements, as an interface for connecting Distributed Generators [GKB+21]. However, the methods developed here were applied only to waveform distortion analysis, discarding other phenomena such as unbalance and phase displacement. Although the proposed approach can be extrapolated to other stationary phenomena using the FBD or CPT decomposition of currents, this is out of the scope of this work. Thus, evaluating multiple stationary phenomena would constitute the next step in this research.
- A Graph Theory approach to analyze power quality phenomena was explored in this work. Several calculation tools and indexes were proposed but not deeply discussed and properly tested. Only the Laplacian Eigenvector Centrality was widely discussed and used as a possible solution to the Responsibilities Assignment Problem. However, a complete analytic framework can be developed as future work taking the tools proposed as a starting point.
- The assessment of Causality and Responsibility presented in this work was developed to be applied to the Point of Common Coupling (PCC). However, taking advantage of the potential of Graph Theory to analyze big networks, an extended disturbance source location method can be developed. This extended method should be capable of assessing systems composed of more than one PCC under certain assumptions like all the nodes have exactly the same voltage.
- In this work was demonstrated that the Utility is responsible for voltage distortion and Customer for current distortion only in networks with a high Short-Circuit Ratio (strong systems). However, in weak systems, a part of the current distortion is transformed into voltage distortion. In this way, a review of the international regulatory frameworks of power quality is necessary, aimed to address the high penetration of Distributed Generation and power electronics in the current power systems.

References

[AEET12] A. E. Emanuel, R. L. ; Testa, A.: Power definitions for circuits with nonlinear and unbalanced loads — The IEEE standard 1459-2010. In: *2012 IEEE Power and Energy Society General Meeting, San Diego, CA*, 2012, S. 1–6

[AMGP18] Agudelo-Martínez, D. ; Garzón, C. ; Pavas, A.: Interaction of power quality disturbances within 2–150 kHz (supraharmonics): Analytical framework. In: *2018 18th International Conference on Harmonics and Quality of Power (ICHQP)*, 2018. – ISSN 2164–0610, S. 1–7

[ANRR15] Aziz, T. ; Nandi, S. K. ; Rahman, M. S. ; Riadh, R. R.: Study of power quality with changing customer loads in an urban distribution network. In: *2015 3rd International Conference on Green Energy and Technology (ICGET)*, 2015, S. 1–6

[AP08] AY, NIHAT ; POLANI, DANIEL: INFORMATION FLOWS IN CAUSAL NETWORKS. In: *Advances in Complex Systems* 11 (2008), Nr. 01, 17-41. `http://dx.doi.org/10.1142/S0219525908001465`. – DOI 10.1142/S0219525908001465

[Bas65] Basmann, R. L.: A Note on the Statistical Testability of 'Explicit Causal Chains' Against the Class of 'Interdependent' Models. In: *Journal of the American Statistical Association* 60 (1965), Nr. 312, 1080–1093. `http://dx.doi.org/10.2307/2283407`. – DOI 10.2307/2283407. – ISSN 01621459

[Bla18] Blanco, A. M.: *Stochastic harmonic emission model of aggregate residential customers*, Technische Universität Dresden, Diss., 2018

[Bol00] *Kapitel* 1. In: Bollen, Math H.: *Overview of Power Quality and Power Quality Standards*. Wiley-IEEE Press, 2000. – ISBN 9780470546840, S. 1–34

[Bon07] Bonacich, Phillip: Some unique properties of eigenvector centrality. In: *Social Networks* 29 (2007), Nr. 4, 555-564. `http://dx.doi.org/10.1016/j.socnet.2007.04.002`. – DOI 10.1016/j.socnet.2007.04.002. – ISSN 0378–8733

[Buc50] Buchhokz, F.: Understanding the Correct Power Concept of Active and Reactive Power. In: *Selbsverlag, Munchen*, 1950

[CF95] Cristaldi, L. ; Ferrero, A.: Harmonic power flow analysis for the measurement of the electric power quality. In: *IEEE Transactions on Instrumentation and Measurement* 44 (1995), Nr. 3, S. 683–685. http://dx.doi.org/10.1109/19.387308. – DOI 10.1109/19.387308

[CSM17] Chidurala, A. ; Saha, T. K. ; Mithulananthan, N.: Harmonic impact of high penetration photovoltaic system on unbalanced distribution networks - Learning from an urban photovoltaic network. In: *IET Renewable Power Generation* 10 (2017), Nr. 4, S. 485–494. http://dx.doi.org/10.1049/iet-rpg.2015.0188. – DOI 10.1049/iet–rpg.2015.0188

[Cza87] Czarnecki, L. S.: What is wrong with the Budeanu concept of reactive and distortion power and why it should be abandoned. In: *IEEE Transactions on Instrumentation and Measurement*, 1987, S. 834–837

[Cza88] Czarnecki, L. S.: Orthogonal decomposition of the currents in a 3-phase nonlinear asymmetrical circuit with a nonsinusoidal voltage source. In: *IEEE Transactions on Instrumentation and Measurement*, 1988, S. 30–34

[Cza08] Czarnecki, L. S.: Currents' Physical Components (CPC) concept: A fundamental of power theory. In: *2008 International School on Nonsinusoidal Currents and Compensation, Lagow, Poland*, 2008, S. 1–11

[Dep93] Depenbrock, M.: The FBD-method, a generally applicable tool for analyzing power relations. In: *IEEE Transactions on Power Systems* 8 (1993), Nr. 2, S. 381–387. http://dx.doi.org/10.1109/59.260849. – DOI 10.1109/59.260849

[DEP00] Davis, E. J. ; Emanuel, A. E. ; Pileggi, D. J.: Evaluation of single-point measurements method for harmonic pollution cost allocation. In: *IEEE Transactions on Power Delivery* 15 (2000), Jan, Nr. 1, S. 14–18. http://dx.doi.org/10.1109/61.847222. – DOI 10.1109/61.847222. – ISSN 0885–8977

[Dug03] Dugan, Roger C.: *Electrical power systems quality.* Nueva York McGraw-Hill, 2003. – ISBN:9780071761550

[EO12] Emanuel, A. E. ; Orr, J. A.: Fryze's power definition: Some limitations. In: *2012 IEEE 15th International Conference on Harmonics and Quality of Power*, 2012. – ISSN 2164–0610, S. 518–522

[Fry32] Fryze, S.: Effective Reactive and Apparent Powers in Circuits with Nonsinusoidal Waveforms. In: *Electrotehn Zeitshrift* Bd. 53, 1932, S. 596–99, 625–27, 700–02

[Gar16] Garzón, C.: *Evaluación de Causalidad para Perturbaciones Estacionarias de*

Calidad de Energía, Universidad Nacional de Colombia, Facultad de Ingeniería, Diplomarbeit, 2016

[GKB+21] Garzón, Camilo A. ; Kannan, Shrinath ; Blanco, Ana M. ; Romero, Miguel ; Meyer, Jan ; Pavas, Andrés: Power Quality Issues in AC Islanded Microgrids: Mitigation and Commonly Used Control Strategies. In: *Simposio Internacional sobre la Calidad de la Energía Eléctrica - SICEL* 10 (2021), mar. https://revistas.unal.edu.co/index.php/SICEL/article/view/97132

[GP] Garzón, Camilo ; Pavas, Andrés: Potential Use of Fryze's Approach-Based Power Theories in Waveform Distortion Contribution Assessment. In: *Revista UIS Ingenierías*. http://dx.doi.org/Accepted. – DOI Accepted

[GP15] Garzón, C. ; Pavas, A.: Causality assessment for power quality stationary disturbances by means of centrality index. In: *2015 IEEE Workshop on Power Electronics and Power Quality Applications (PEPQA)*, 2015, S. 1–5

[GP17] Garzón, C. ; Pavas, A.: Laplacian eigenvector centrality as tool for assessing causality in power quality. In: *2017 IEEE Manchester PowerTech*, 2017, S. 1–6

[GP19] Garzón, Camilo ; Pavas, Andrés: Review of Responsibilities Assignment Methods for Harmonic Emission. In: *2019 IEEE Milan PowerTech*, 2019, S. 1–6

[GPK+23] Garzón, Camilo A. ; Pavas, Andres ; Kannan, Shrinath ; Blanco, Ana M. ; Romero, Miguel ; Quintero, Vanessa ; Meyer, Jan: Assignment of Responsibilities for Power Quality Stationary Disturbances in an Islanded Microgrids. In: *Simposio Internacional sobre la Calidad de la Energía Eléctrica - SICEL* 10 (2023), mar. https://revistas.unal.edu.co/index.php/SICEL/article/view/97104

[Gra69] Granger, C. W. J.: Investigating Causal Relations by Econometric Models and Cross-spectral Methods. In: *Econometrica* 37 (1969), Nr. 3, 424–438. http://www.jstor.org/stable/1912791. – ISSN 00129682, 14680262

[Gro08] Grossman, S.I.: *Álgebra Lineal*. McGraw-Hill Interamericana de España S.L., 2008 (Elibro Catedra). – ISBN 9789701065174

[HAI17] Hamouda, S. H. ; Aleem, S. H. E. A. ; Ibrahim, A. M.: Harmonic resonance index and resonance severity estimation for shunt capacitor applications in industrial power systems. In: *2017 Nineteenth International Middle East Power Systems Conference (MEPCON)*, 2017, S. 527–532

[Ham94] *Kapitel* 11. In: Hamilton, James D.: *Vector Autoregressions*. Princeton University Press, 1994. – ISBN 0–691–04289–6, S. 302–307

[HNB00] Hansen, S. ; Nielsen, P. ; Blaabjerg, F.: Harmonic cancellation by mixing nonlinear single-phase and three-phase loads. In: *IEEE Transactions on Industry Applications* 36 (2000), Jan, Nr. 1, S. 152–159. http://dx.doi.org/10.1109/28.821810. – DOI 10.1109/28.821810. – ISSN 0093–9994

[HPLL16] Heydt, G. T. ; Patil, H. U. ; Loehr, J. ; LaRose, T.: Harmonic resonance assessment for transmission class shunt capacitors. In: *2016 IEEE/PES Transmission and Distribution Conference and Exposition (T D)*, 2016. – ISSN 2160–8563, S. 1–5

[ICO00] ICONTEC: COMPATIBILIDAD ELECTROMAGNETICA (CEM). PARTE 1. GENERALIDADES. SECCION 1: APLICACION E INTERPRETACION DE DEFINICIONES Y TERMINOS FUNDAMENTALES. In: *ICONTEC NTC-IEC 61000-1-1* (2000), December, S. 1–29

[ICO08] ICONTEC: CALIDAD DE LA POTENCIA ELECTRICA. LIMITES Y METODOLOGIA DE EVALUACION EN PUNTO DE CONEXION COMUN. In: *ICONTEC NTC 5001* (2008), May, S. 1–51

[ICO13] ICONTEC: CALIDAD DE LA POTENCIA ELÉCTRICA (CPE). DEFINICIONES Y TÉRMINOS FUNDAMENTALE. In: *ICONTEC NTC 5000* (2013), June, S. 1–20

[IEC02] IEC: Part 4-13: Testing and measurement techniques - Harmonics and interharmonics including mains signalling at a.c. power port, low frequency immunity tests. In: *Electromagnetic compatibility (EMC) - IEC Std. 61000-4-13* (2002), June, S. 1–55

[IEC03a] IEC: Part 2-12: Environment - Compatibility levels for low-frequency conducted disturbances and signalling in public medium-voltage power supply systems. In: *Electromagnetic compatibility (EMC) - IEC Std. 61000-2-12* (2003), June, S. 1–55

[IEC03b] IEC: Pat 2-2: Environment - Compatibility levels for low-frequency conducted disturbances and signaling in public low-voltage power supply systems. In: *Electromagnetic compatibility (EMC) - IEC Std. 61000-2-2* (2003), June, S. 1–29

[IEC08a] *Testing and measurement techniques – Power quality measurement methods.* : *Testing and measurement techniques – Power quality measurement methods*, 2008. – 1–292 S.

[IEC08b] IEC: Part 3-6: Limits - Assessment of emission limits for the connection of distorting installations to MV, HV and EHV power systems. In: *Electromagnetic*

compatibility (EMC) - IEC TR Std. 61000-3-6 (2008), June, S. 1–29

[IEC09a] *General guide on harmonics, interharmonics measurements and instrumentation, for power supply systems and equipment connected thereto.* : *General guide on harmonics, interharmonics measurements and instrumentation, for power supply systems and equipment connected thereto*, 2009. – 1–41 S.

[IEC09b] Part 4-7: General guide on harmonics, interharmonics measurements and instrumentation, for power supply systems and equipment connected thereto. In: *Electromagnetic compatibility (EMC) - IEC Std. 61000-4-7* (2009), June, S. 1–29

[IEC11] IEC: Part 3-12: Limits - Limits for harmonic currents produced by equipment connected to public low-voltage systems with input current >16 A and ≤75 A per phase. In: *Electromagnetic compatibility (EMC) - IEC Std. 61000-3-12* (2011), June, S. 1–29

[IEC14] IEC: Part 3-2: Limits - Limits for harmonic current emissions (equipment input current 16 A per phase). In: *Electromagnetic compatibility (EMC) - IEC Std. 61000-3-2* (2014), June, S. 1–29

[IEC15] IEC: Part 4-30: Testing and measurement techniques – Power quality measurement methods. In: *Electromagnetic compatibility (EMC) - IEC Std. 61000-4-30* (2015), June, S. 1–29

[IEE09] IEEE: IEEE Recommended Practice for Monitoring Electric Power Quality. In: *IEEE Std 1159-2009 (Revision of IEEE Std 1159-1995)* (2009), June, S. c1–81. http://dx.doi.org/10.1109/IEEESTD.2009.5154067. – DOI 10.1109/IEEESTD.2009.5154067

[IEE10a] IEEE: IEEE Standard Definitions for the Measurement of Electric Power Quantities Under Sinusoidal, Nonsinusoidal, Balanced, or Unbalanced Conditions. In: *IEEE Std 1459-2010 (Revision of IEEE Std 1459-2000)* (2010), March, S. 1–50. http://dx.doi.org/10.1109/IEEESTD.2010.5439063. – DOI 10.1109/IEEESTD.2010.5439063

[IEE10b] IEEE: IEEE Standard Definitions for the Measurement of Electric Power Quantities Under Sinusoidal, Nonsinusoidal, Balanced, or Unbalanced Conditions. In: *IEEE Std 1459-2010 (Revision of IEEE Std 1459-2000)* (2010), March, S. 1–50. http://dx.doi.org/10.1109/IEEESTD.2010.5439063. – DOI 10.1109/IEEESTD.2010.5439063

[IEE14] IEEE: IEEE Recommended Practice and Requirements for Harmonic Control in Electric Power Systems. In: *IEEE Std 519-2014 (Revision of IEEE Std 519-*

1992) (2014), June, S. 1–29. http://dx.doi.org/10.1109/IEEESTD.2014.6826459. – DOI 10.1109/IEEESTD.2014.6826459

[KBG+21] Kannan, Shrinath ; Blanco, Ana M. ; Garzón, Camilo ; Pavas, Andrés ; Meyer, Jan: Harmonic Impedance Characteristics in an Islanded Microgrid and its Impact on Voltage and Current Harmonics. In: *2021 IEEE Madrid PowerTech*, 2021, S. 1–6

[MAFGF17] Moradifar, A. ; Akbari Foroud, A. ; Gorgani Firouzjah, K.: Comprehensive identification of multiple harmonic sources using fuzzy logic and adjusted probabilistic neural network. In: *Neural Computing and Applications* (2017), S. 1–14. http://dx.doi.org/10.1007/s00521-017-3022-8. – DOI 10.1007/s00521–017–3022–8

[MBA+14] Meyer, J. ; Bollen, M. ; Amaris, H. ; Blanco, A. M. ; Castro, A. G. ; Desmet, J. ; Klatt, M. ; Kocewiak, L. ; Ronnberg, S. ; Yang, K.: Future work on harmonics - some expert opinions Part II - supraharmonics, standards and measurements. In: *2014 16th International Conference on Harmonics and Quality of Power (ICHQP)*, 2014. – ISSN 2164–0610, S. 909–913

[MGCS95] Mansoor, A. ; Grady, W. M. ; Chowdhury, A. H. ; Samotyi, M. J.: An investigation of harmonics attenuation and diversity among distributed single-phase power electronic loads. In: *IEEE Transactions on Power Delivery* 10 (1995), Jan, Nr. 1, S. 467–473. http://dx.doi.org/10.1109/61.368365. – DOI 10.1109/61.368365. – ISSN 0885–8977

[MM10] Mehran Mesbahi, Magnus E.: *Graph Theoretic Methods in Multiagent Networks*. Princeton University Press, 2010. – ISBN 9781400835355

[MPST04] Muscas, C. ; Peretto, L. ; Sulis, S. ; Tinarelli, R.: Effects of load unbalance on multipoint measurement techniques for assessing the responsibility for PQ degradation. In: *2004 11th International Conference on Harmonics and Quality of Power*, 2004, S. 759–764

[MSS+17] Meyer, J. ; Stiegler, R. ; Schegner, P. ; Röder, I. ; Belger, A.: Harmonic resonances in residential low-voltage networks caused by consumer electronics. In: *CIRED - Open Access Proceedings Journal* 2017 (2017), Nr. 1, S. 672–676. http://dx.doi.org/10.1049/oap-cired.2017.0460. – DOI 10.1049/oap–cired.2017.0460. – ISSN 2515–0855

[New18] Newman, Mark: *Networks*. Oxford University Press, 2018. http://dx.doi.org/10.1093/oso/9780198805090.001.0001. http://dx.doi.org/10.1093/oso/9780198805090.001.0001. – ISBN 9780198805090

[NO14] Nunes, I. ; Oliveira, J. C.: A proposal of methodology for the assignment of responsibilities on harmonic distortions using the superposition principle. In: *IEEE Latin America Transactions* 12 (2014), Dec, Nr. 8, S. 1426–1431. http://dx.doi.org/10.1109/TLA.2014.7014510. – DOI 10.1109/TLA.2014.7014510. – ISSN 1548–0992

[Pav12] Pavas, A.: *Study of Responsibilities Assignment Methods in Power Quality (Summa Cum Laude)*, Universidad Nacional de Colombia, Facultad de Ingeniería, Diss., 2012

[PBP08] Pfajfar, T. ; Blazic, B. ; Papic, I.: Harmonic Contributions Evaluation With the Harmonic Current Vector Method. In: *IEEE Transactions on Power Delivery* 23 (2008), Jan, Nr. 1, S. 425–433. http://dx.doi.org/10.1109/TPWRD.2007.911165. – DOI 10.1109/TPWRD.2007.911165. – ISSN 0885–8977

[Pea95] Pearl, Judea: Causal Diagrams for Empirical Research. In: *Biometrika* 82 (1995), Nr. 4, 669–688. http://dx.doi.org/10.2307/2337329. – DOI 10.2307/2337329. – ISSN 00063444

[PG14] Pavas, A. ; Garzon, C.: Causality assessment for power quality stationary disturbances. In: *IEEE PES Innovative Smart Grid Technologies, Europe*, 2014. – ISSN 2165–4816, S. 1–7

[PP11a] Pfajfar, T. ; Papic, I.: Harmonic emission level estimation based on measurements at the point of evaluation. In: *2011 IEEE Power and Energy Society General Meeting*, 2011. – ISSN 1932–5517, S. 1–5

[PP11b] Pfajfar, T. ; Papic, I.: Harmonic emission level estimation based on measurements at the point of evaluation. In: *2011 IEEE Power and Energy Society General Meeting*, 2011. – ISSN 1932–5517, S. 1–5

[PSD70] Penfield, P. ; Spence, R. ; Duinker, S.: A generalized form of Tellegen's theorem. In: *IEEE Transactions on Circuit Theory* 17 (1970), Nr. 3, S. 302–305. http://dx.doi.org/10.1109/TCT.1970.1083145. – DOI 10.1109/TCT.1970.1083145

[PTP10] P. Tenti, P. M. ; Paredes, H. K. M.: Conservative Power Theory, sequence components and accountability in smart grids. In: *2010 International School on Nonsinusoidal Currents and Compensation, Lagow, Poland*, 2010, S. 37–45

[PTSS10a] Pavas, A. ; Torres-Sánchez, H. ; Staudt, V.: Method of Disturbances Interaction: Novel approach to assess responsibilities for steady state power quality disturbances among customers. In: *Proceedings of 14th International Conference on Harmonics and Quality of Power - ICHQP 2010*, 2010. – ISSN

1540–6008, S. 1–9

[PTSS10b] Pavas, Andrés ; Torres-Sánchez, Horacio ; Staudt, Volker: Method of Disturbances Interaction: Novel approach to assess responsibilities for steady state power quality disturbances among customers. In: *Proceedings of 14th International Conference on Harmonics and Quality of Power - ICHQP 2010*, 2010, S. 1–9

[PTSS12a] Pavas, A. ; Torres-Sanchez, H. ; Staudt, V.: Statistical analysis of power quality disturbances propagation by means of the Method of Disturbances Interaction. In: *2012 3rd IEEE PES Innovative Smart Grid Technologies Europe (ISGT Europe)*, 2012. – ISSN 2165–4816, S. 1–9

[PTSS12b] Pavas, Andrés ; Torres-S¡nchez, Horacio ; Staudt, Volker: Statistical analysis of power quality disturbances propagation by means of the Method of Disturbances Interaction. In: *2012 3rd IEEE PES Innovative Smart Grid Technologies Europe (ISGT Europe)*, 2012, S. 1–9

[SBP+17a] Spelko, A. ; Blazic, B. ; Papic, I. ; Pourarab, M. ; Meyer, J. ; Xu, X. ; Djokic, S. Z.: CIGRE/CIRED JWG C4.42: Overview of common methods for assessment of harmonic contribution from customer installation. In: *2017 IEEE Manchester PowerTech*, 2017, S. 1–6

[SBP+17b] Spelko, A. ; Blazic, B. ; Papic, I. ; Pourarab, M. ; Meyer, J. ; Xu, X. ; Djokic, S. Z.: CIGRE/CIRED JWG C4.42: Overview of common methods for assessment of harmonic contribution from customer installation. In: *2017 IEEE Manchester PowerTech*, 2017, S. 1–6

[SOPS11] Santos, I.N. ; Oliveira, J.C. ; Paula Silva, S.F.: Critical evaluation of the performance of the method of harmonic power flow to determine the dominant source of distortion. In: *IEEE Latin America Transactions* 9 (2011), Nr. 5, S. 740–746. `http://dx.doi.org/10.1109/TLA.2011.6030984`. – DOI 10.1109/TLA.2011.6030984

[Sta08] Staudt, V.: Fryze - Buchholz - Depenbrock: A time-domain power theory. In: *2008 International School on Nonsinusoidal Currents and Compensation*, 2008. – ISSN 2375–1428, S. 1–12

[Ten04] Tenti, Paolo: A Time-Domain Approach to Power Term Definitions under Non-Sinusoidal Conditions, 2004

[Wie56] Wiener, N.: The theory of prediction. In: *Modern mathematics for engineers* 1 (1956), S. 125–139. – ISSN 0486497461, 9780486497464

[WYAY+04] Wanik, M. Z. C. ; Yusuf, Y. ; Al-Yousif, S. N. ; Umeh, K. C. ; Mohamed,

A.: Simulation of harmonic resonance phenomena in industrial distribution system. In: *2004 IEEE Region 10 Conference TENCON 2004.* Bd. C, 2004, S. 240–243 Vol. 3

[XL00] Xu, Wilsun ; Liu, Yilu: A method for determining customer and utility harmonic contributions at the point of common coupling. In: *IEEE Transactions on Power Delivery* 15 (2000), Nr. 2, S. 804–811. http://dx.doi.org/10.1109/61.853023. – DOI 10.1109/61.853023

[XLL03] Xu, Wilsun ; Liu, Xian ; Liu, Yilu: An investigation on the validity of power-direction method for harmonic source determination. In: *IEEE Transactions on Power Delivery* 18 (2003), Jan, Nr. 1, S. 214–219. http://dx.doi.org/10.1109/TPWRD.2002.803842. – DOI 10.1109/TPWRD.2002.803842. – ISSN 0885–8977

[XLT04] Xu, Wilsun ; Li, Chun ; Tayjasanant, T.: A çritical impedance"based method for identifying harmonic sources. In: *IEEE Power Engineering Society General Meeting, 2004.*, 2004, S. 917 Vol.1–

[YM15] Yanchenko, Sergey ; Meyer, Jan: Harmonic emission of household devices in presence of typical voltage distortions. (2015), S. 1–6. http://dx.doi.org/10.1109/PTC.2015.7232518. – DOI 10.1109/PTC.2015.7232518